

A
TD
224
U8U85
no.156

DYNAMIC STREAM TEMPERATURE
MODEL FOR UNSTEADY FLOW

Final report to
National Oceanic and Atmospheric Administration
National Weather Service
Office of Hydrology
Silver Spring
Maryland

David S. Bowles
Larry E. Comer
William J. Grenney

PRWG156
Utah Water Research Laboratory
College of Engineering
Utah State University
Logan, Utah 84322

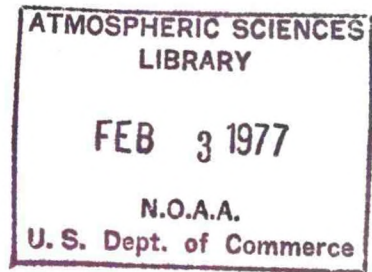
December 1975

A
TD
224
U8U85
no.156

DYNAMIC STREAM TEMPERATURE
//
MODEL FOR UNSTEADY FLOW ,

Final report to
National Oceanic and Atmospheric Administration
National Weather Service
Office of Hydrology
Silver Spring
Maryland

David S. Bowles
Larry E. Comer
William J. Grenney



PRWG156
Utah Water Research Laboratory
College of Engineering
Utah State University
Logan, Utah 84322

December 1975

77 0250

ACKNOWLEDGMENTS

The development of the Dynamic Stream Temperature Model (DSTEMP) and its application to the Brazos-Little Rivers, Texas, were accomplished under contract to the Hydrologic Research Laboratory, National Weather Service, National Oceanic and Atmospheric Administration. Field investigations leading to the development of a mathematical submodel for heat transfer processes in the bed of a small stream were carried out under the same contract and are described in a separate report. Special thanks are extended to Dr. Danny L. Fread, who supervised the work for NOAA, and provided guidance throughout the contract period, especially with the adaptation and calibration of the Implicit Dynamic Routing Program (DNRT).

Gratitude is also expressed to those individuals and organizations who provided data for the Brazos-Little application of DNRT-DSTEMP. Particular mention is made of the following: R. J. Pickering, Chief, Quality of Water Branch, USGS, Reston, Virginia; Leon S. Hughes, Chief, Quality of Water Unit, USGS, Austin, Texas; John F. Griffiths, Texas State Climatologist, College Station, Texas; and the National Climatic Center, Asheville, North Carolina. In addition, thanks are extended to Carl Relyea, Hydrologic in Charge, Ohio River Forecast Center, NOAA, Cincinnati, Ohio, who provided data for application of DNRT-DSTEMP to the Ohio River. Although it was not practical to

apply DNRT-DSTEMP to the Ohio during the contract period it is hoped that a future application may make use of the excellent data made available by Mr. Relyea and his colleagues.

TABLE OF CONTENTS

	Page
ACKNOWLEDGMENTS	ii
LIST OF FIGURES	vi
LIST OF TABLES	vii
ABSTRACT	
 Chapter	
1. INTRODUCTION	1
2. REVIEW OF LITERATURE	3
Stream temperature models	3
Meteorologic considerations	25
3. DYNAMIC STREAM TEMPERATURE MODEL DESCRIPTION	29
Introduction	29
Program Capabilities	30
Implicit Dynamic Routing Program (DNRT)	34
Model Formulation	35
Numerical Solution	46
Implicit four-point finite difference scheme	46
Numerical solution of advection equations	48
Point loads	54
Heat Exchange Components	55
General	55
Solar radiation	58
Vegetative radiation	77

TABLE OF CONTENTS (Continued)

Chapter	Page
Atmospheric radiation	78
Back radiation	80
Latent heat of vaporization associated with evaporation	81
Conduction	82
Latent heat of fusion associated with snowfall	83
Surface layer renewal	84
Solar radiation absorbed by streambed	84
Back radiation from streambed	85
Conductive flux across streambed	85
 4. APPLICATION OF DSTEMP TO BRAZOS-LITTLE RIVERS, TEXAS	 88
Introduction	88
Brazos-Little River System	89
Data Sources	91
Streamflow Modeling	91
DSTEMP Problem Set-Up	92
Results	95
 5. CONCLUSIONS AND FURTHER WORK	 100
DNRT	101
DSTEMP	101
 REFERENCES	 103
 APPENDIX A	 108
1. Overall flow chart	109
2. Input data and decision parameter description	110
3. Program listing	133
4. Examples of input and output	
a. Main stream only	143
b. Main stream and one tributary	146

LIST OF FIGURES

Figure	Page
3.1. Relationship between computation time intervals and meteorologic time intervals for the case where $IMDT=8$ and $DT(JJ)=3$, $JJ=J, (J+8)$	32
3.2. Sub-reach control volume	36
3.3. Network of points on (x,t) plane for the generalized implicit four-point finite difference method (adapted from Amein and Fang, 1970)	47
3.4. Parabolic distribution of observed daily solar radiation flux by technique 2 (adapted from Albertson et al., 1974)	68
3.5. Sensitivity of incident solar radiation to reflectivity of ground adjacent to stream (R_g)	73
3.6. Sensitivity of incident solar radiation to total dust depletion coefficient (d_p)	74
3.7. Comparison of solar radiation calculated by the three techniques	76
3.8. Atmospheric radiation factor, β (after Raphael, 1962)	79
3.9. Dissipation of incident solar radiation flux	86
4.1. Schematic of Brazos-Little River System	90
4.2. Partial listing of DSTEMP model input for the Brazos-Little River System (December 5-28, 1972)	93
4.3. Hydrographs and thermographs at upstream and downstream boundaries of Brazos-Little River System including model predictions (December 5-28, 1972)	96
4.4. Assumed lateral inflow thermograph	98

LIST OF TABLES

Table		Page
2.1.	Summary of stream water temperature models (notation explained on following pages)	5
3.1.	Definition of dummy variables used in DSTEMP and in Equations 3.25 through 3.29	52
3.2.	Total dust depletion coefficient, d_p	65
3.3.	Albedo of ground surface, R_g	67

ABSTRACT

Current interest in stream temperature prediction stems largely from concern for the possible deleterious environmental consequences of thermally polluted surface waters. Stream temperature is an important determinant of the solubility of dissolved gases, biological reaction kinetics, the distribution of fish and lower forms of aquatic life, and the efficiency of water treatment for domestic and industrial use. This report describes the Dynamic Stream Temperature Model (DSTEMP). The model is suitable for prediction of stream temperatures over a diurnal cycle or over extended periods of time. DSTEMP may be used for unsteady flow conditions by linkage with a dynamic streamflow routing model (DNRT). Alternatively steady flow conditions may be specified. Data requirements are realistic in terms of data types usually collected by the National Weather Service, NOAA, and the United States Geological Survey. A users manual for DSTEMP is included in Appendix A. In addition to describing the model an application of DSTEMP to the Brazos-Little Rivers, Texas, is included. The combined DNRT-DSTEMP models provide a powerful tool for streamflow-stream temperature forecasting in a wide variety of streams and river systems.

CHAPTER 1

INTRODUCTION

Temperature is perhaps the single most important parameter in stream water quality. Human activity generally raises natural stream-water temperatures due to impoundments, industrial uses, irrigation, and modifications of topographic features. As a result, higher temperatures reduce the solubility of dissolved oxygen, increase metabolism, respiration, and oxygen demand of aquatic life, intensify many types of toxicity, and promote "less desirable" fish species and aquatic organisms (McKee and Wolf, 1963).

Numerous mathematical models of the mechanisms of heat transfer in streams are now available. In contrast to most of the previous models, the stream temperature model described in this report is dynamic and can be used in conjunction with a dynamic streamflow model. The Dynamic Stream Temperature Model (DSTEMP) may be used for prediction of stream temperatures over a diurnal cycle or over extended periods of time. DSTEMP can be applied to small streams in which streambed heat exchange is important, or it can be applied to large river systems with first order tributaries, thermal discharges, and meteorologic conditions that vary spatially over the river basin. Data requirements are realistic in terms of data types usually collected by the National Weather Service, NOAA, and the United States Geological

Survey. A complete description of DSTEMP, its capabilities, and formulation is contained in Chapter 3. Appendix A includes a description and examples of the input requirements of DSTEMP.

In Chapter 4 an application of DSTEMP to the Brazos-Little River System, Texas, is presented. A 12 hour computational time interval is used for the simulation of a storm of 23 days duration. As part of the same research project DSTEMP was used to represent the diurnal variation of stream temperatures on a small mountain stream, Spawn Creek, Utah. Full details of this application are contained in Comer et al. (1975). An example of the DSTEMP input and output for the Spawn Creek study is contained in Appendix A. Another hypothetical example of a main river and tributary system is also included in Appendix A.

Chapter 3 contains a literature review of previous stream temperature models. Conclusions and suggestions for further work are presented in Chapter 5.

C represents the concentration of constituents and with regard to temperature modeling, can be replaced by T, water temperature.

Several assumptions are made with the use of the advection dispersion equation, one of which is one-dimensionality. One-dimensional simulations assume complete and total mixing so that temperature is uniform at any given cross-section. In a turbulent stream, total mixing is considered a reasonable assumption. The source-sink term for temperature is typically based on the thermal energy conservation or heat balance approach. Much of the thrust of past temperature modeling has been directed toward refinement or simplification of the thermal energy budget.

Further assumptions and simplifications are often made in model development to facilitate ease of use and solution, and to minimize the complexity of input data required. Additional variations are sometimes made to fit local situations or specific meteorologic conditions.

Summaries of several existing stream temperature models are presented in Table 2.1 with accompanying discussion focusing on the uniqueness of each model. The tabular format of the summary associates similarities in model components and reduces the erratic and conflicting notation found in literature into a common set of terms.

Table 2.1. Summary of stream water temperature models (notation explained on following pages).

Harper (1972)

General Equation	$\frac{\partial T}{\partial t} + U \frac{\partial T}{\partial x} = \frac{\partial^2 T}{\partial x^2} + \frac{\phi_T}{C_p \gamma h}$
Energy Budget (Heat Balance)	$\phi_T = \phi_R - (\phi_B + \phi_E + \phi_H)$
Solar Radiation, ϕ_R	$\phi_R = f(\alpha, L, C) \quad (\text{Raphael, 1962}) \text{ or Direct Observation}$
Evaporation, ϕ_E	$\phi_E = K_E U_a (e_s - e_a)$
Back Radiation, ϕ_B	$\phi_B = 0.79\sigma(T_w^4 - \beta T_a^4)$
Conduction, ϕ_H	$\phi_H = K_H U P (T - T_a)$
Streambed Heat Transfer, ϕ_{SB}	Assumed negligible
Other Terms	Tributaries-- $T_B = \frac{QT + Q_{in} T_{in}}{Q + Q_{in}}$

Steady flow, uniform cross-section, constant dispersion coefficient

Dailey and Harleman (1972)

General Equation	$\frac{\partial}{\partial t} (A T) + \frac{\partial}{\partial x} (QT) = \frac{\partial}{\partial x} \left(AE_L \frac{\partial T}{\partial x} \right) - K_T A \Delta T_E + S$
------------------	---

Nonuniform cross-sections, steady flow

Harleman et al. (1973)

General Equation	$\frac{\partial}{\partial t} (AT) + \frac{\partial}{\partial x} (QT) = \frac{\partial}{\partial x} \left(AE_L \frac{\partial T}{\partial x} \right) + \frac{b\phi_T}{\rho C_p} + \frac{WHD + THD}{\rho C_p}$
------------------	---

Energy Budget
(Heat Balance)

$$\phi_T = \phi_{RI} - \phi_{RR} + \phi_a - \phi_{ar} - \phi_E - \phi_H$$

$$\phi_T = \phi_R \{ 4 \times 10^8 (T_s + 460^4) + f(U) \{ (e_s - e_a) \} + 0.255 (T_s - T_a) \}$$

Table 2.1. Continued.

Harleman et al. (1973) Continued.

Energy Budget (Heat Balance) (Continued)	$\phi_T \approx -K (T_S - T_E)$
Solar Radiation, ϕ_R	$\phi_R = \phi_{RI} - \phi_{RR}$ (Same as Harper, 1973)
Evaporation, ϕ_E	$\phi_E = f(U) (e_s - e_a)$
Back Radiation, ϕ_B	$\phi_B = \phi_{bs} - \phi_a + \phi_{ar}$ WHERE $\phi_a = 1.2 \times 10^{-12} (T_a + 460)^6 (1 + kc^2)$ $\phi_{ar} = 0.03 \phi_a, \phi_{bs} = 4.0 \times 10^{-8} (T_s + 460)^4$
Conduction, ϕ_H	$\phi_H = R\phi_E$ WHERE $R = 0.255 \left \frac{T_s - T_a}{e_s - e_a} \right $
Streambed Heat Transfer, ϕ_{SB}	Neglected due to generally low thermal conductivity of earth and limited temperature gradients
Other Terms	Heat Discharges-- $\frac{WHD + THD}{\rho C}$ Nonuniform cross-sections, unsteady flow

Novotny and Krenkel (1971)	
General Equation	$\frac{\partial T}{\partial t} + U \frac{\partial T}{\partial x} = E_L \frac{\partial^2 T}{\partial x^2} + \frac{K_a}{hC_p \rho} (\Delta T_E)$
Energy Budget (Heat Balance)	$\phi_T = \phi_{RI} - \phi_{RR} - \phi_a - \phi_{ar} - \phi_{bs} - \phi_E - \phi_H - \phi_W$
Streambed Heat Transfer, ϕ_{SB}	Assumes all thermal input at the air water interface
Other Terms	$K_a = 11.42 + h_v (0.0166e^{.0625T_a} + \rho_a C_{pa})$ WHERE $h_v = 392 \times 10^{-1} U_s$ Uniform cross-sections, steady flow, surface temperature differs from bulk

Table 2.1. Continued.

Pailey et al.
(1974)

General Equation	$\frac{\partial T}{\partial t} + U \frac{\partial T}{\partial x} = E_L \frac{\partial^2 T}{\partial x^2} + \frac{f(T)}{h\rho C_p}$
Energy Budget (Heat Balance)	$\phi_T = \phi_R - (\phi_B + \phi_E + \phi_H + \phi_S)$ $\phi_T = -(\epsilon T + \eta)$
Solar Radiation, ϕ_R	$\phi_R = \phi_{RI} - \phi_{RR} \quad \text{WHERE}$ $\phi_{RI} = \phi_{CL} \{ .35 + 0.61(10 - C) \}$ $\phi_{RR} = 0.108 \phi_{RI} - 6.766/10^{-5} \phi_{RI}^2$
Evaporation, ϕ_E	$\phi_E = \frac{\phi_H}{R} \quad \text{WHERE } R = 6.1 \times 10^{-4} \rho \left(\frac{T_w - T_a}{e_s - e_a} \right)$
Back Radiation, ϕ_B	$\phi_B = \phi_{bs} - \phi_a + \phi_{ar} \quad \text{WHERE } \phi_{bs} = .97\phi T_w^4$ $\phi_a = (a + b e_a) \phi T_a^4, \quad \phi_{ar} = 0.03\phi_a$
Conduction, ϕ_H	$\phi_H = \{ 8 + 0.35(T_w - T_a) + 3.9U_a \} (T_w - T_a)$
Streambed Heat Transfer, ϕ_{SB}	Not mentioned
Other Terms	$\phi_{sm} = 7.85v^{2.375} \{ L + C_i (T_w - T_a) \}$ Complete mixing, uniform cross-sections, steady flow

Brown (1965)

General Equation	$\Delta T_{PR} = \frac{A_s \times \phi_T}{Q} \quad (0.000267)$
Energy Budget (Heat Balance)	$\phi_T = \phi_{NR} \pm \phi_E \pm \phi_C \pm \phi_H \pm \phi_A$
Solar Radiation, ϕ_R	Net Radiation: $\phi_{NR} = \phi_R - \phi_B$ (Measured directly)
Evaporation, ϕ_E	$\phi_E = K_E L U_a (e_s - e_a)$
Back Radiation, ϕ_B	Accounted for in ϕ_{NR}

Table 2.1. Continued.

Brown (1965)	
Conduction, ϕ_H	$\phi_H = 0.0002 U P(T - T_a)$
Streambed Heat Transfer, ϕ_{SB}	$\phi_{SB} = K_{SB} (dT/dz)$ Up to 25% ϕ_{NR} absorbed
	Steady flow, no tributary sources, no ground-water

Brown (1972)	
General Equation	$\Delta T_{PR} = \frac{A_s \times \phi_{NR}}{Q} (0.000267)$
Energy Budget (Heat Balance)	$\phi_T \approx \phi_{NR}$
Solar Radiation, ϕ_R	ϕ_{NR} Measured directly or obtained graphically
Streambed Heat Transfer, ϕ_{SB}	About 20% ϕ_{NR} transferred to streambed (bed-rock)
Other Terms	Non-flowing water not included in A_s
Assumptions	Steady flow, no tributaries, no groundwater $\phi_{NR} \approx 0.95 \phi_T$

Morse (1972a)	
General Equation	$\frac{\partial T}{\partial t} + U \frac{\partial T}{\partial x} = \frac{\phi_T}{C_p \rho h}$
Energy Budget (Heat Balance)	$\phi_T = A''T^2 + B''T + C''$ $A'', B'',$ and C'' from monthly averaged meteorologic data
Streambed Heat Transfer, ϕ_{SB}	Neglected
Other Terms	ϕ_T found as a function of statistical constants $A'', B'',$ and C'' . Dispersion neglected, variable cross-sections, meteorological records "typical"

Table 2.1. Continued.

QUAL-1 (Texas Water
Development Board)
(1971)

General Equation

$$A \frac{\partial T}{\partial t} = \frac{\partial \left(A E_L \frac{\partial T}{\partial x} \right)}{\partial x} - \frac{\partial (A U T)}{\partial x} \pm \frac{A \phi_T}{\gamma C_p h}$$

Energy Budget
(Heat Balance)

$$\phi_T = \phi_R + \phi_a - (\phi_B \pm \phi_H + \phi_E)$$

Solar Radiation, ϕ_R

$$\phi_R = \phi_{RI} a_t (1 - R) (1 - 0.65 C^2)$$

Evaporation, ϕ_E

$$\phi_E = \gamma L (a + bU) (e_s - e_a)$$

Back Radiation, ϕ_B

$$\phi_B = \sigma (T_s + 460)^4$$

Conduction, ϕ_H

$$\phi_C = \phi_E (0.01 R) \quad \text{WHERE} \quad R = \frac{P}{29.92} \frac{(T_s - T_a)}{(e_s - e_a)}$$

Streambed Heat Transfer,
 ϕ_{SB}

Considered groundwater heat input but conduction relatively insignificant compared to ϕ_T

Other Terms

$$\phi_a = (2.89 \times 10^{-6}) \sigma (T_a + 460)^6 (1 + 0.17 C^2) (1 - .03)$$

Complete mixing, variable cross-section,
variable dispersion coefficient

Bowles et al. (DSTEMP)

General Equation

$$\frac{\partial}{\partial t} (AT) + \frac{\partial}{\partial x} (QT) = \frac{\phi_{TS} W}{\rho c_p} + \frac{\phi_{SB} W}{\rho c_p} + Q_{\ell} T_{\ell}$$

$$+ q_g T_g W + q_r T_r W - q_e T_w$$

$$\phi_{TS} = C_1 + C_2 T$$

$$\phi_{SB} = C_3 + C_4 T$$

Energy Budget
(Heat Balance)

$$\phi_{TS} = (\phi_{RI} - \phi_{RR}) + (\phi_v - \phi_{rr}) (\phi_a - \phi_{ar})$$

$$- \phi_{bs} - \phi_E + \phi_H - \phi_s - \phi_W$$

$$\phi_{SB} = \phi_{sb} + \phi_{bb} + \phi_{cb}$$

Table 2.1. Continued.

Bowles et al. (DSTEMP)
(Continued)

Solar Radiation, ϕ_R	$\phi_R = f(\alpha, R_g, R, d_p, C)$ (Wunderlich, 1972) or by parabolic distribution of observed solar radiation between sunrise and sunset or by direct use of observed solar radiation
Vegetative Radiation, ϕ_v	$\phi_v = \sigma(T_a + 460)^4$ (Pluhowski (1970)) $\phi_{vr} = R_l \phi_v$
Atmospheric Radiation, ϕ_a	$\phi_a = \beta \sigma(T_a + 460)^4$ (Raphael (1962)) $\phi_{ar} = R_l \phi_a$
Back Radiation, ϕ_{bs}	$\phi_{bs} = 0.97 \sigma(T + 460)^4$ (Anderson (1954))
Evaporation, ϕ_E	$\phi_E = \rho L K_E U_a (e_s - e_a)$ (Wunderlich (1972))
Conduction, ϕ_H	$\phi_H = 0.217 (T - T_a) P \rho L K_H U_a$ (Bowen (1926))
Melting Snow, ϕ_s	$\phi_s = q_r \rho [L_f + c_s (T - T_r)]$
Surface Layout Renewal, ϕ_w	$\phi_w = 3.96 \times 10^4 K_w \left(\frac{U}{h}\right)^{0.33} (T_s - T)$ (Novotny and Krenkel (1971))
Streambed Solar Radiation, ϕ_{sb}	$\phi_{sb} = 0.4 (1 - R_b) \phi_R \exp(-zh)$
Streambed Back Radiation, ϕ_{bb}	$\phi_{bb} = \epsilon \sigma (T_b + 460)^4$
Streambed Conduction, ϕ_{cb}	$\phi_{cb} = \alpha_1 + \alpha_2 \phi_{sb} + \alpha_3 T_g + \alpha_4 T$ (Comer et al. (1975))
Other Terms	Point Loads $T_B = \frac{Q T + Q_{in} T_{in}}{Q + Q_{in}}$

Unsteady flow from Implicit Dynamic Routing Program (Fread, 1973), variable cross-sections, tributaries, point and diffuse thermal loads, variable meteorologic data across stream system, dynamic representation of temperature, dispersion neglected

NOTATION FOR TABLE 2.1.

(Units: H = heat, ℓ = length, m = mass, T = temperature, t = time)

A	=	Cross-sectional area of channel	ℓ^2
A''	=	Quadratic coefficient (Morse, 1972a)	
A _s	=	Surface area	ℓ^2
a, b	=	Long-wave radiation constants, a function of cloud height	
a _t	=	Atmospheric transmission	
B''	=	Linear coefficient (Morse, 1972a)	
C	=	Cloud cover in tenths	
C''	=	Constant (Morse, 1972a)	
C _{1, 2, 3, 4}	=	Coefficients (DSTEMP)	
c _i	=	Specific heat of ice	Hm ⁻¹ T ⁻¹
c _p	=	Specific heat of water	Hm ⁻¹ T ⁻¹
c _s	=	Specific heat of ice	Hm ⁻¹ T ⁻¹
d _p	=	Total dust depletion coefficient of atmosphere	
$\frac{dT}{dz}$	=	Streambed temperature gradient	T ℓ^{-1}
F _L	=	Longitudinal dispersion coefficient	

e_a	= Vapor pressure of ambient air	
e_s	= Saturation vapor pressure of air	
$f(U)$	= Wind speed function for heat flux (energy/ area·time·time·p)	
g_r	= Precipitation	ℓ
h	= Mean depth of flow	ℓ
k	= Coefficient of thermal diffusion	
K	= Overall heat transfer coefficient	ℓt^{-1}
K_a	= Vapor-transfer coefficient in boundary layer	ℓt^{-1}
K_E	= Evaporation heat-transfer coefficient	ℓt^{-1}
K_H	= Convection heat-transfer coefficient	
K_{SB}	= Thermal conductivity of streambed material	
K_w	= Coefficient of thermal conductivity of water	$H\ell^{-1}t^{-1}T^{-1}$
L	= Latent heat of vaporization	
L_f	= Latent heat of fusion	Hm^{-1}
P	= Atmospheric pressure	$m\ell^{-2}$
Q	= Mean stream discharge	$\ell^3 t^{-1}$
Q_{in}	= Discharge of tributary or point load	$\ell^3 t^{-1}$
Q_ℓ	= Rate of surface lateral inflow	$\ell^2 t^{-1}$

q_e	=	Evaporation	l
q_g	=	Rate of groundwater lateral inflow	lt^{-1}
R	=	Albedo of the water surface to short-wave radiation	
R_b	=	Albedo of streambed to solar radiation	
R_g	=	Albedo of ground adjacent to stream to short-wave radiation	
R_l	=	Albedo of water surface to long-wave radiation	
S	=	Thermal energy source-sink term	
T	=	Water bulk temperature	T
T_a	=	Air temperature	T
T_b	=	Temperature of streambed interface	T
T_B	=	Boundary temperature found by mass balance	T
T_E	=	Equilibrium	T
ΔT_E	=	$(T - T_E)$	T
T_g	=	Temperature of groundwater lateral inflow	T
T_l	=	Temperature of surface lateral inflow	T
ΔT_{PR}	=	Predicted temperature	T
T_r	=	Wet-bulb temperature	T

T_s	=	Water surface temperature	T
T_w	=	Water temperature	T
THD	=	Tributary heat discharge	
U	=	Mean stream velocity	lt^{-1}
U_a	=	Wind velocity	lt^{-1}
v	=	Visibility	l
w	=	Top width of stream	l
W	=	Wetted perimeter of stream	l
WHD	=	Waste heat discharge	
X	=	Distance downstream	l
Z	=	Bulk extinction coefficient	l^{-1}
α	=	Solar altitude	
$\alpha_{1,2,3,4}$	=	Regression coefficient (Comer et al., 1975) .	
β	=	Raphael's coefficient for long-wave radiation computation	
γ	=	Specific weight of water	
ρ	=	Density of water	ml^{-3}
ϵ	=	Heat exchange coefficient	
η	=	Base heat exchange rate	
σ	=	Stefan-Boltzman constant	
ϕ_a	=	Incoming long-wave radiation	$Hl^{-2}t^{-1}$
ϕ_{ar}	=	Reflected long-wave radiation	$Hl^{-2}t^{-1}$

ϕ_B	= Back radiation heat flux	$Hl^{-2}t^{-1}$
ϕ_{bb}	= Back radiation heat flux emitted by stream- bed	$Hl^{-2}t^{-1}$
ϕ_{bs}	= Long-wave radiation for water surface . .	$Hl^{-2}t^{-1}$
ϕ_{cb}	= Conductive heat flux across streambed . .	$Hl^{-2}t^{-1}$
ϕ_E	= Evaporation heat flux	$Hl^{-2}t^{-1}$
ϕ_H	= Conductive heat flux	$Hl^{-2}t^{-1}$
ϕ_r	= Heat flux by surface layout renewal . . .	$Hl^{-2}t^{-1}$
ϕ_R	= Short-wave radiation heat flux	$Hl^{-2}t^{-1}$
ϕ_{RI}	= Incident short-wave radiation	$Hl^{-2}t^{-1}$
ϕ_{RR}	= Reflected short-wave radiation.	$Hl^{-2}t^{-1}$
ϕ_s	= Heat transfer during melting snow . . .	$Hl^{-2}t^{-1}$
ϕ_{sb}	= Short-wave radiation heat flux absorbed by streambed	$Hl^{-2}t^{-1}$
ϕ_{SB}	= Streambed heat transfer	$Hl^{-2}t^{-1}$
ϕ_T	= Total heat flux	$Hl^{-2}t^{-1}$
ϕ_{TS}	= Total surface heat transfer	$Hl^{-2}t^{-1}$
v	= Vapor-transfer coefficient in air boundary layer	lt^{-1}

balance ratio was used to define a new boundary temperature and discharge. By dividing the modeled stream into reaches of constant physical and dynamic characteristics, such as cross-sectional area, discharge, and dispersion coefficients, and using these variables as new boundary conditions, the simulation equation may be further simplified. Harper assumed steady flow, uniform cross-sectional area, and a constant dispersion coefficient while employing these boundary condition techniques.

Other possible sources and sinks which are assumed negligible are heat transfer to the ground, internal heat generated by chemical and biological reactions, and friction losses.

A model developed by Dailey and Harleman (1972) is divided into two parts: a hydraulic submodel, and a water quality submodel which includes a temperature component (see Table 2.1). Due to several shortcomings, this model was later modified (Harleman et al., 1973). Apart from a deficient derivation of terms in the temperature equation, the 1972 model failed to allow for variations in flow characteristics and variability of meteorological conditions. Harleman et al. (1973) stated that the earlier model was valid for temperature only when lateral inflow was zero.

In terms of the developed equation, the new model of Harleman et al. differs from the Dailey and Harleman (1972) model by only a flux term ϕ_T . Rather than using the linearized simplification of the surface

heat flux, ϕ_T was calculated at each mesh point and time step by the following equation:

$$\phi_T = \phi_R - \{4 \times 10^8 T_s + 460\}^4 + f(U_a) [(e_s - e_a) + .255 (T_s - T_a)] \quad 1.3$$

Harleman et al. (1973) also used the equilibrium temperature concept, developed by Edinger and Geyer (1965). They defined the equilibrium temperature T_E as the temperature at which, under a given set of meteorological conditions, the net surface heat flux is equal to zero. Equilibrium temperature may be found by substituting T_E for T_S in Equation 2.3 and $\phi_T = 0$. Jobson and Yotsukura (1972) concluded that the introduction of the equilibrium temperature concept has been unnecessary and inconvenient due to its dependence on trial-and-error solution, error from the linearization effect of T_E , and inadequacy in predicting diurnal fluctuations.

Also included in this model are source terms allowing for waste heat discharge (WHD) and tributary heat discharges (THD). Development of net surface heat flux (Equation 2.3) was made under the assumption that radiation, convection, and evaporation are several orders of magnitude higher than other possible sources or sinks, such as heat fluxes via evaporated water and direct rainfall. Of particular interest is the rationale used for neglecting stream bed heat transfer:

Heat transfer between a body of water and the environment can occur through the free surface and through the bottom and sides. In the latter case, the heat flux is limited by conduction in the adjacent soil and remains very small because of generally low thermal conductivity of earth and because the temperature gradients are limited. (Harleman et al., 1973, p. 89)

A model by Novotny and Krenkel (1973) describes the dynamic nature of the air-water interface of a turbulent river (see Table 2.1). It is assumed that the primary mechanism of heat transfer is turbulent motion of the water surface. Also, it is stressed that the water surface temperature is different from the bulk temperature. Timofeyev and Malevskiy-Malevich (1967) report that the difference may be as great as several tenths of a degree Celsius.

Novotny and Krenkel (1973) develop a thermal energy budget under the assumption that all thermal energy acts on the air-water interface. Heat transfer across the stream bed-water interface is not considered. Pailey et al. (1974) developed a closed-form solution of the unsteady one-dimensional advection-diffusion equation for temperature distributions downstream from a thermal load input (see Table 2.1). Rigorous solution of the conservation of thermal energy equation was made by assuming complete mixing, uniformity of stream cross-section, discharge, and diffusion coefficient, and linearity of surface heat exchanges. Pailey et al. (1974) state that the surface heat exchange term ϕ_T can be expressed as a

linear function of the mixed temperature of the stream, without significant loss of accuracy. The linear relation is given as

$$\phi_T = -(\epsilon T + \eta) \dots \dots \dots 2.4$$

where η = the base heat exchange rate corresponding to a stream temperature of 0°C ; T = stream temperature in $^\circ\text{C}$; and ϵ = a heat exchange coefficient. Values for ϵ and η for various wind velocities, relative humidities, and air and stream temperatures are determined by approximate relations given by Dingman and Assur (1967). Correlation coefficients of at least 0.999 were found between the derived linear relation and the more involved energy budget.

Also presented are the linear relations of the equilibrium temperature model by Edinger and Geyer (1965) and an excess temperature model by Jobson and Yotsukura (1972).

Pailey et al. (1974) state that heat dispersed in a receiving water is eventually transferred to the atmosphere by evaporation, radiation, or by conduction as sensible heat. "There may be some transfer of heat at the soil-water interface due to infiltration of river water into the ground. The amount of heat transferred by diffusion and dispersion in the porous media, however, is generally very small and may be neglected." (p. 531)

The stream temperature submodel of QUAL-1 (Texas Water Development Board, 1971) is also based on the general heat budget equation (see Table 2.1). Net solar and atmospheric radiation are found

where ϕ_{SB} , the heat transfer through the streambed is equal to the product of K_{SB} , the streambed material thermal conductivity, and dT/dz , the streambed temperature gradient. The bed transfer term is a function of conduction only and did not consider heat transport due to groundwater inflow.

Brown (1969) measured temperature gradients in streambeds of gravel and bedrock materials by the use of copper-constantan thermocouples placed at 1 cm intervals but at an unspecified depth. Thermocouples were simply inserted into the streambed of two gravel streams. The temperature gradient in bedrock material was found by removing boulders similar to the streambed, fitting them with thermocouples, and then placing them in water baths which simulate stream temperatures. Although the bedrock measurements were not in situ, Brown concluded that up to 25 percent of the energy absorbed by a bedrock bottom stream may be transferred to the bed. No consideration was given to the fate of this thermal energy. Brown (1969, p. 74) concluded that:

Consideration of this energy budget component was essential for accurate temperature prediction. The rock acted as an energy sink during midday hours and as an energy source later in the day. In contrast, gravel bottoms seem to be insignificant energy sinks. Although temperature gradients were measured in the gravel-bottomed stream, thermal conductivities of the water-gravel mixture, approximately 0.05 Btu/ft²-inch-min °F, were too low to provide any heat exchange that noticeably affected the predictions.

In later work, Brown (1970) simplified the temperature change equation by reducing the energy budget ϕ_T to net radiation, ϕ_{NR} . Rationale for this simplification was the observation that, for the stream studied, 95 percent of the heat input during the midday period of midsummer was accounted for by solar radiation. Streambed conduction was not included in this less sophisticated model.

The simplified model was the forerunner to an improved temperature prediction model for small streams (Brown, 1972). This study included further observations of streambed conduction. Thermocouples were placed at 1 cm vertical intervals and at an unspecified depth in gravel bottomed streams and in a bedrock boulder, but on this occasion the boulder was returned to the stream.

Results of this study showed gravel-bottomed streams to be effectively isothermal in the upper 20 cm layer. Gradients of $0.05^{\circ}\text{C}/\text{cm}$ or less were observed between the 5 cm layer and the surface. A maximum gradient of 1.1°C was observed between the 20 cm layer and the surface. Midday temperature gradients of $0.45^{\circ}\text{C}/\text{cm}$ were observed in the upper layers of the bedrock. This was about 18 percent of the incoming heat load. Preliminary results from a probe in the gravel bed of Spawn Creek also show isothermal conditions in the upper zone. However, below this zone a significant temperature gradient was observed.

Brown (1972) considered that the isothermal conditions in the top 20 cm of the gravel streambed was due to the free circulation of surface water within this layer because of its open porous nature. He concluded that conductive heat transfer is restricted by point-to-point contact between gravel particles together with the efficient heat transfer between particles and the circulating intergravel water.

Brown (1972) concluded that in bedrock bottom streams, 15 to 20 percent of the net all-wave radiation absorbed by the stream may be lost to the bed. On this basis the magnitude of predicted temperature was reduced by 15 to 20 percent.

Meteorologic considerations

Past models of stream temperature have considered solar radiation to be the major component of the energy budget. In addition, it is often assumed that radiation is completely absorbed at the air-water interface (Edinger et al., 1968; Edinger and Geyer, 1965; Parker and Krenkel, 1969). This may be valid for deep, turbid rivers, but this assumption is false for clear, shallow streams (Pivovarov, 1973; Viskanta and Toor, 1972). Some investigators recognized transmission of solar energy through water, but considered its effect equilibrated over depth by turbulence (Novotny and Krenkel, 1973).

The streambed is considered to be a diffuse reflector of radiation. Reflectance of the bottom material is assumed to be gray (independent of wavelength) and equal to $0 < \rho < 1$ where $\rho = 1$ is a perfectly reflecting bottom and $\rho = 0$ is a perfectly absorbing bottom.

In the case of a perfectly reflecting bottom ($\rho = 1$), the rate of internal absorption of water is increased, but in cases when $\rho < 1$, which is most often the case in natural waters, the portion which is absorbed by the bed (not reflected) is neglected in this model. However, through interpretation of their graphic results, nearly 50 percent of the total flux incident on the water surface is absorbed by the bottom when $\rho = 0$ and depth is 1 meter, and 25 percent of the total flux is absorbed by the bottom when $\rho = 0.5$.

CHAPTER 3
DYNAMIC STREAM TEMPERATURE
MODEL DESCRIPTION

Introduction

The Dynamic Stream Temperature Model (DSTEMP) described in this chapter is designed to be used in conjunction with a flood routing technique (DNRT) developed by the Hydrologic Research Laboratory of the National Weather Service, National Oceanic and Atmospheric Administration. Stream geometry and streamflow data generated by the Implicit Dynamic Routing Program (DNRT) (Fread, 1973; Fread, 1974) are used in the temperature model, DSTEMP. Alternatively, these stream geometry and streamflow data may be input directly to DSTEMP without using DNRT. Program capabilities, model formulation, and numerical solution are described below. The various heat exchange processes acting over the air-water and soil-water interfaces are represented by mathematical submodels described in this chapter. A flowchart, input data and decision parameters description, program listing, and two examples of input and output are contained in the DSTEMP Users Manual (Appendix A).

Program Capabilities

DSTEMP can be applied to the prediction of mean daily stream temperatures or to the prediction of the diurnal variation of stream temperatures. Time and space steps in DNRT and DSTEMP are specified by the user. Successive time steps need not be of equal length. Also subreaches of different lengths can be specified. The program is structured in a flexible manner so that individual components of heat transfer across the stream boundaries can be omitted through user options. Lack of data may necessitate the use of this option for streambed conduction, for example. A choice between three alternative techniques of calculating incident and solar radiation flux at the stream surface is provided. These techniques range from the direct use of observed data, to the calculation of solar radiation flux from meteorologic and astronomical data. The calculation approach requires some coefficient estimation before it can be applied but in return it takes account of local factors affecting solar radiation. A separate subroutine is used to calculate each component of net heat transfer at the stream surface and streambed. Therefore, a technique currently used to estimate one of the heat transfer components may be readily replaced by another technique without changing the main program unless new data requirements are introduced.

Two important features of the meteorologic data requirements are the use of meteorologic data sets and meteorologic time intervals that differ from the computational time intervals. A meteorologic data set comprises a complete set of data for all the meteorologic variables required in DSTEMP. Several meteorologic data sets may be used for modeling a stream system. Each data set is applied to a different group of subreaches for which the observed meteorologic data in the data set are considered representative. Meteorologic data are often available on a daily basis whereas the computational time interval for a diurnal study may be 3 hours, for example. By specifying the ratio of the meteorologic time increment to the computational time increment (IMDT), the user may opt to reuse meteorologic data for several computational time intervals contained within the meteorologic time interval. Figure 3.1 illustrates this feature. In addition, several options to reduce the data preparation requirements were included in the input procedure.

Meteorologic data are assumed to be constant over each computational time interval in which they are used. Thus meteorologic data are treated as cumulated or averaged values over the computational time interval. Examples include dry-bulb temperature which is assumed to be averaged over the computational time interval, and observed solar radiation which is assumed to be the cumulated value in the same interval. In contrast, hydraulic and stream

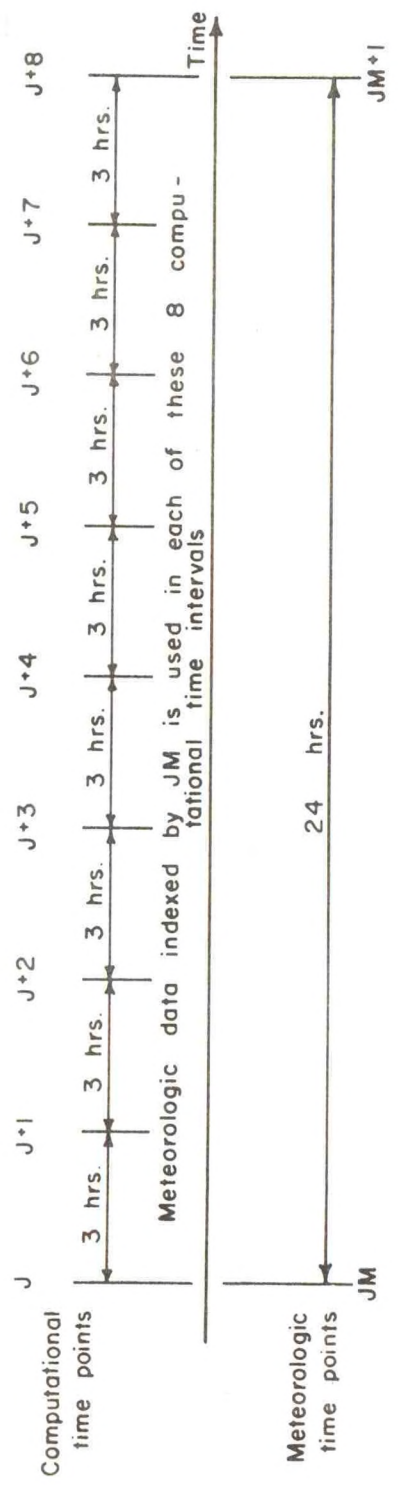


Figure 3.1. Relationship between computational time intervals and meteorologic time intervals for the case where $IMDT = 8$ and $DT(JJ) = 3, JJ = J, (J + 8)$.

temperature data are treated as instantaneous values at each time point. These distinctions are made in the input description contained in the Users Manual (Appendix A), and in the development of the numerical solution in this chapter.

Units used in DNRT and DSTEMP are those used by the National Weather Service and United States Geological Survey in published data which are likely to be used in applications of the models. When programming DSTEMP, an attempt was made to facilitate a future program option in which S.I. or British units could be used. The S.I. option is not available in the current version of DSTEMP.

Provision has been made to treat surface and subsurface lateral inflows separately. A different temperature may be specified for each. In this way unmodeled tributaries, overland flow, interflow, return flows, etc., can be separated from baseflow originating in the groundwater body. Both surface and subsurface lateral inflows can be negative in which case they are outflows from the river and the temperature associated with them is the stream temperature.

Any number of first order tributaries to the main stream can be handled by DNRT and DSTEMP providing dimension statements are adjusted to the appropriate size. Following the technique used in DNRT, tributary flows are input to the main stream as surface lateral inflow uniformly distributed over a specified subreach. Therefore, stream temperatures for a time point are predicted along all the tributaries before

predictions commence on the main stream (see flowchart in Appendix A). In this way the surface lateral inflow temperatures of tributary inflows are available when they are required for temperature predictions on the main stream.

Thermal loads located as point sources are handled by a simple heat balance procedure. Stream temperatures immediately upstream and downstream of the location at which the point load enters the stream are calculated and output.

All data input are printed at the beginning of the program output. Two types of output tables are used: a table of stream temperatures, advective heat sources, and hydraulic data for each computational point at each time point; and a table of components of heat exchange at stream surface and bed for each subreach at each time interval.

Implicit Dynamic Routing Program (DNRT)

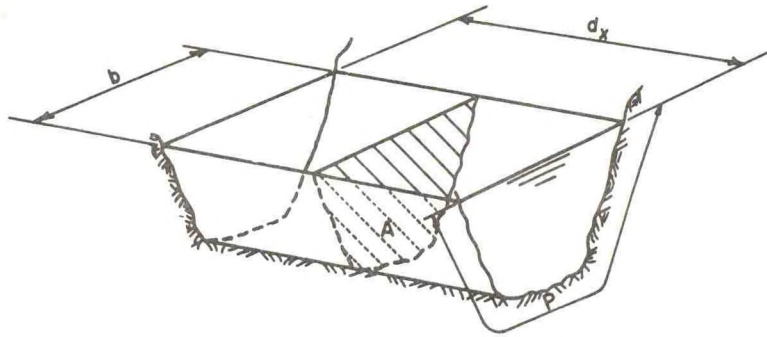
DNRT is a technique for streamflow forecasting in which transient stages and discharges are computed for various forecast points along a river from a given stage or discharge hydrograph at the upstream boundary of a river reach in which a flood wave is propagating (Fread, 1974). The interaction of storage and dynamic effects between a river and its tributaries may be efficiently simulated using DNRT (Fread, 1973). Stages and discharges are computed by an implicit dynamic routing technique in which the complete one

dimensional differential equations of unsteady flow are solved by an implicit four-point finite difference method which necessitates the solution of successive systems of nonlinear equations. A very efficient solution for the nonlinear systems is provided by the Newton-Raphson iterative method used in conjunction with an extrapolation technique and a special quad-diagonal Gaussian elimination procedure. DNRT has been verified on several floods and hurricane surges in the Lower Mississippi River.

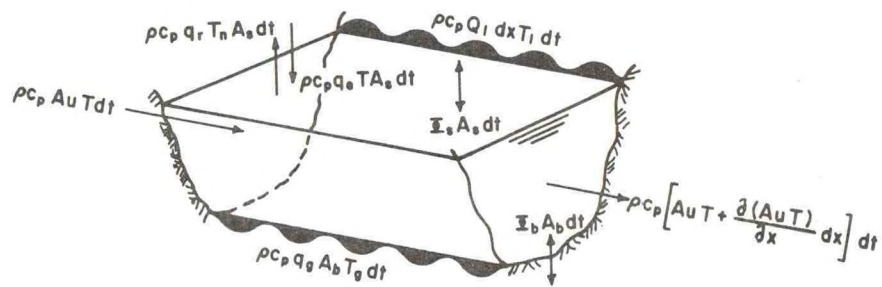
Hydraulic and stream geometry data transferred to DSTEMP from DNRT are described in detail by read statements 2 through 13 in the DSTEMP input description contained in Appendix A. These data include: computational time intervals, subreach lengths, cross-sectional areas, top widths of flow, wetted perimeters, streamflow rates, stream stages, and surface lateral inflow rates.

Model Formulation

The model for prediction of average and diurnal stream temperatures was formulated by performing a heat balance on a control volume in the stream (Figure 3.2). Two important assumptions were made: complete and instantaneous mixing over each stream cross-section; and negligible longitudinal diffusion. In addition, heat resulting from biological and chemical processes and from fluid friction was disregarded. Also no attempt was made to represent the situation in



(i) Stream geometry



(ii) Heat fluxes

Figure 3.2. Sub-reach control volume.

which ice formation occurs.

The assumption of complete and instantaneous mixing implies that transverse temperature gradients over a stream cross-section can be neglected. Usually only one stream temperature measurement is available at each water quality station and therefore transverse temperature gradients would be impossible to define except in a few well instrumented streams. The assumption permitted the use of a one-dimensional analysis instead of the more complex two- and three-dimensional approaches (Jobson and Yotsukura, 1973). Thus stream temperatures represented by the model were assumed to be average temperatures across the stream cross-section. It should be noted that the cross-section averaged predicted stream temperatures were compared with stream temperatures observed at a single location in the stream cross-section.

Fischer (1973) has stated that longitudinal diffusion, either molecular or turbulent, is relatively unimportant compared to the effect of velocity upon the longitudinal temperature distribution and is, therefore, usually ignored. By neglecting diffusion a first-order rather than a second-order analysis was required. This simplification permitted the use of the implicit four-point finite difference technique which is applicable only to first-order equations. By using the same numerical scheme in both the hydraulic and stream temperature models it is intended that space and time steps will be compatible

in both models. The implicit four-point finite difference scheme allows for variable size space and time steps.

Although frictional heat added to the stream due to boundary roughness was neglected in the current version of DSTEMP, Vugts (1974) indicated that it may not be unimportant. According to Pluhowski (1970) friction heat flux, ϕ_f , can be calculated as follows:

$$\phi_f = \frac{Q \rho s dx}{J} \quad \dots \dots \dots (3.1)$$

in which

- Q streamflow rate (cfs)
- ρ density of water (62.32 lbs. ft⁻³)
- s slope of subreach (ft. ft⁻¹)
- dx computational space interval on length of subreach (ft)
- J a constant (778 ft.lbs. BTU⁻¹)

Four types of heat flux were considered in the heat balance on the control volume (Figure 3.2):

1. Nonadvective heat exchange across the stream surface.
2. Nonadvective heat exchange across the streambed.
3. Advection of heat associated with stream velocity.
4. Other advective heat fluxes by lateral inflow, tributary inflow, groundwater infiltration and seepage, rainfall and snowfall, and evaporation.

For the purpose of developing the heat balance only the net quantities of nonadvective heat exchange across the stream surface and streambed are considered; these quantities are represented by Φ_s and Φ_b , respectively. Each of the components comprising these net terms are described in a later section.

A heat balance over the time interval dt for the subreach control volume shown in Figure 3.2 was obtained by equating the sum of the four types of heat flux to the net change in total heat contained in the control volume. The sign convention adopted was positive for heat fluxes associated with advection of mass into the stream. Heat exchange, such as radiation, which is not associated with mass transfer was treated as positive when the transfer of heat was into the stream.

1. surface heat exchange

$$\Phi_s A_s dt$$

2. streambed heat exchange

$$+ \Phi_b A_b dt$$

3. stream velocity heat flux

$$+ \rho c_p A u dt - \rho c_p \left[AuT + \frac{\partial}{\partial x} (AuT) dx \right] dt$$

4. other advective heat fluxes

$$+ \rho c_p Q_\ell dx T_\ell dt + \rho c_p q_g A_b T_g dt + \rho c_p q_r A_s T_r dt - \rho c_p q_e A_s T_s dt$$

change in total heat in control volume

$$= \rho c_p d(AT)dx \quad . \quad . \quad . \quad . \quad . \quad . \quad (3.2)$$

in which

- c_p specific heat of water at constant pressure
(0.9988 BTU lbs⁻¹ deg. F⁻¹)
- A cross-sectional area of stream (ft²)
- u stream velocity (ft. s⁻¹)
- dt computational time interval (s)
- dx computational space interval or subreach length (ft)
- T stream temperature (deg. F)
- Φ_s net nonadvective heat exchange across water surface
(BTU ft⁻² s⁻¹)
- A_s stream surface area (ft²)
- Φ_b net nonadvective heat exchange across streambed
(BTU ft⁻² s⁻¹)
- A_b streambed area (ft²)
- Q_l rate of surface lateral inflow (overland flow plus interflow)
per unit length of subreach (cfs ft⁻¹)
- T_l temperature of surface lateral inflow (deg. F)

respectively. When Q_ℓ and q_g are negative (Q_ℓ^- , q_g^-) then T is used instead of T_ℓ and T_g .

Net surface and streambed exchange, Φ_s and Φ_b , are each calculated from the summation of a number of component heat transfers which are described in a later section. Some of these components are nonlinear in T and to simplify the numerical solution procedures most stream temperature models employ a linearized approximation for Φ_s and Φ_b . Two notable exceptions to this are the parabolic approximations used by Wunderlich (1968) and Morse (1970, 1972a, 1972b). Wunderlich proposed that, depending on the required accuracy and the temperature range of interest, Φ_s may be determined from either

$$\Phi_s = C'' + B'' T + A'' T^2 \quad (3.6)$$

or

$$\Phi_s = C' + B' T \quad (3.7)$$

in which C'' , B'' , A'' , C' and B' are determined by least square regression of Φ_s against T . Values of Φ_s were calculated for a range of values of T and using monthly averages of daily meteorologic data. Morse refined Wunderlich's work to 3 hour time intervals and used least squares to estimate a set of values of C'' , B'' , A'' , C' , and B' for each of the eight 3 hour time intervals in a day. Meteorologic

data for calculating Φ_s was obtained for each of the eight 3 hour time intervals in a day by averaging over the same 3 hour periods in several successive days. Morse (1970) reported that the parabolic relationship provided a statistically better fit than the linear relationship when applied to calculated surface heat exchange for the Columbia River over a 10 day period in July, 1966. By averaging meteorologic data over a period of several days, it is assumed that these data are essentially constant over the averaging period. A cooling trend during one study period led Morse (1972a) to the observation that more representative results can be obtained from shorter averaging periods. However, as fewer days are used to estimate the least square coefficients statistical confidence in the estimated values decreases.

The approach of Wunderlich and Morse to developing a parabolic approximation for the net surface exchange by least squares can be applied to development of the linear relationship in Equation 3.7. Other linearization procedures include the concept of an equilibrium temperature, the use of a truncated Taylor series expansion of the nonlinear terms in Φ_s and Φ_b , and the use of empirical linear approximations to the nonlinear terms in Φ_s and Φ_b .

Equilibrium temperature, T_E , is the stream temperature at which Φ_s is zero. Edinger and Geyer (1965) first proposed the use

of equilibrium temperature for linearizing the net surface exchange as follows:

$$\Phi_s = -K(T - T_E) \quad \cdot \quad \cdot \quad \cdot \quad \cdot \quad \cdot \quad \cdot \quad \cdot \quad \cdot \quad \cdot \quad \cdot \quad (3.8)$$

in which K is the surface heat transfer coefficient ($\text{BTU ft}^{-2} \text{s}^{-1} \text{ deg. F}^{-1}$). T_E must be obtained by a cumbersome trial and error procedure and its value can vary by up to 90 deg. F on a diurnal basis (Edinger et al., 1968). Therefore in their discussion of linearization techniques for Φ_s Jobson and Yotsukura (1973) describe the equilibrium temperature concept as "inadequate for predicting diurnal fluctuations in water temperature." They concluded that "the introduction of the equilibrium temperature concept has been both unnecessary and inconvenient."

Another approach to linearizing nonlinear terms in Φ_s is by using the first two terms in the Taylor series expansion about an arbitrary reference temperature, T_R . By careful selection of T_R linearization errors may be minimized (Jobson and Yotsukura, 1973).

In DSTEMP empirical linear approximations, piecewise-linear approximations, and least squares linear approximations to nonlinear components of Φ_s and Φ_b are employed. Thus Φ_s and Φ_b are expressed in the linear forms:

$$\Phi_s = C_1 + C_2 T = \sum_{i=1}^n (c_1^i + c_2^i T) \cdot \cdot \cdot \quad (3.9)$$

$$\Phi_b = C_3 + C_4 T = \sum_{i=1}^m (c_3^i + c_4^i T) \cdot \cdot \cdot \quad (3.10)$$

in which each of the n components of Φ_s are expressed in the linear form $c_1^i + c_2^i T$ and each of the m components of Φ_b are expressed in the linear form $c_3^i + c_4^i T$. Calculation of c_1^i , c_2^i , c_3^i , and c_4^i is discussed in a later section in which estimation of the surface and streambed heat exchange components are described. Coefficients C_1 , C_2 , C_3 , and C_4 were obtained as follows:

$$C_1 = \sum_{i=1}^n c_1^i \cdot \cdot \cdot \quad (3.11)$$

$$C_2 = \sum_{i=1}^n c_2^i \cdot \cdot \cdot \quad (3.12)$$

$$C_3 = \sum_{i=1}^m c_3^i \cdot \cdot \cdot \quad (3.13)$$

$$C_4 = \sum_{i=1}^m c_4^i \cdot \cdot \cdot \quad (3.14)$$

The rearranged form of Equation 3.2, including the substitution of Equations 3.3, 3.4, 3.5, 3.9, and 3.10, and the addition of the extra terms associated with negative surface and groundwater lateral inflows is as follows:

$$\frac{\partial(AT)}{\partial t} + \frac{\partial(QT)}{\partial x} - \left[\frac{bC_1 + PC_3}{\rho c_p} + Q_l^+ T_l + q_g^+ PT_g + q_r bT_r \right] - \left[\frac{bC_2 + PC_4}{\rho c_p} + Q_l^- + q_g^- P - q_e b \right] T = 0 \quad . \quad . \quad (3.15)$$

Numerical Solution

Implicit four-point finite difference scheme

Explicit finite difference techniques applied to the solution of the unsteady flow equations are restricted by numerical stability considerations to very small computational time steps of the order of minutes or seconds. Therefore, the explicit method is very inefficient for stream simulations lasting several days or weeks. In contrast implicit finite difference techniques have no restrictions on the size of the specified time interval due to computational stability; however, accuracy constraints may limit its size.

The generalized implicit four-point finite difference scheme utilized by Fread in DNRT allows for variable size space intervals Δx and time intervals Δt . Figure 3.3 contains a four-point grid identified by the intersections of the vertical lines x_i and x_{i+1} with the horizontal lines t^j and t^{j+1} . Finite differencing is carried out for a point M within the four-point grid. At the point M the

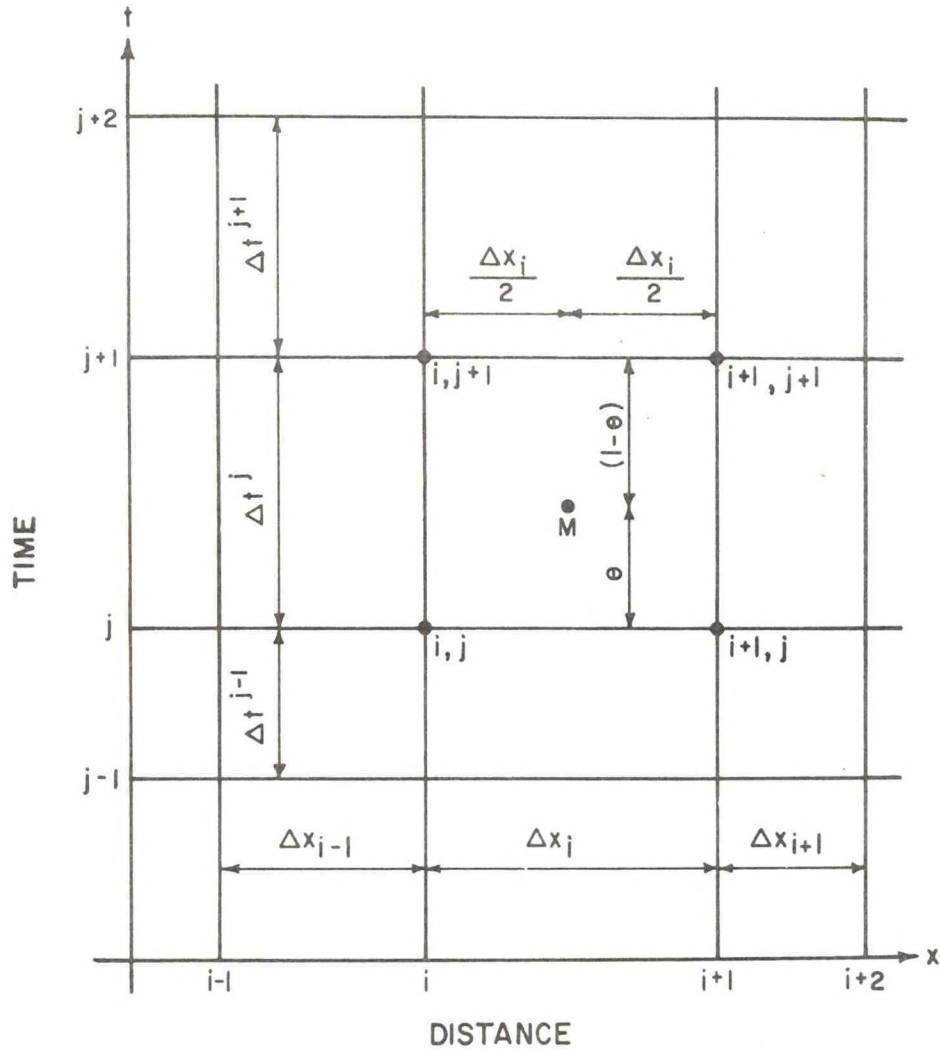


Figure 3.3 Network of points on (x, t) plane for the generalized implicit four-point finite difference method (adapted from Amein and Fang, 1970).

value of a function $K(M)$ is represented by:

$$K(M) \approx \theta \left(\frac{K_i^{j+1} + K_{i+1}^{j+1}}{2} \right) + (1 - \theta) \left(\frac{K_i^j + K_{i+1}^j}{2} \right) \quad (3.16)$$

in which θ is a weighting factor determining the location of M between the two adjacent time lines t^j and t^{j+1} . Space and time partial derivatives of $K(M)$ are approximated by:

$$\frac{\partial K(M)}{\partial x} \approx \theta \left(\frac{K_{i+1}^{j+1} - K_i^{j+1}}{\Delta x_i} \right) + (1 - \theta) \left(\frac{K_{i+1}^j - K_i^j}{\Delta x_i} \right) \quad (3.17)$$

$$\frac{\partial K(M)}{\partial t} \approx \frac{K_i^{j+1} + K_{i+1}^{j+1} - K_i^j - K_{i+1}^j}{2 \Delta t^j} \quad \dots \quad (3.18)$$

Fread (1974) found that for slowly varying transients in large rivers $\theta = 0.55$ minimizes the loss of accuracy associated with greater values while avoiding the possibility of a weak or pseudo-instability.

Numerical solution of advection equations

The generalized implicit four-point finite difference scheme used in the routing model DNRT (Fread, 1973; Fread, 1974) was also applied in DSTEMP. Substituting Equations 3.16, 3.17, and 3.18 into the advection equation (Equation 3.15) yields the following:

$$\begin{aligned}
& \frac{1}{2\Delta t^j} \left[(AT)_i^{j+1} + (AT)_{i+1}^{j+1} - (AT)_i^j - (AT)_{i+1}^j \right] \\
& + \frac{\theta}{\Delta x_i} \left[(QT)_{i+1}^{j+1} - (QT)_i^{j+1} \right] + \frac{(1-\theta)}{\Delta x_i} \left[(QT)_{i+1}^j - (QT)_i^j \right] \\
& - \frac{\theta}{2} \left\{ \frac{C_1}{\rho c_p} \left[b_i^{j+1} + b_{i+1}^{j+1} \right] + \frac{C_3}{\rho c_p} \left[P_i^{j+1} + P_{i+1}^{j+1} \right] \right. \\
& + \left[(Q_\ell^+ T_\ell)_i^{j+1} + (Q_\ell^+ T_\ell)_{i+1}^{j+1} \right] + \left[(q_g^+ PT_g)_i^{j+1} + (q_g^+ PT_g)_{i+1}^{j+1} \right] \\
& \left. + \left[(q_r b T_r)_i^{j+1} + (q_r b T_r)_{i+1}^{j+1} \right] \right\} \\
& - \frac{(1-\theta)}{2} \left\{ \frac{C_1}{\rho c_p} \left[b_i^j + b_{i+1}^j \right] + \frac{C_3}{\rho c_p} \left[P_i^j + P_{i+1}^j \right] \right. \\
& + \left[(Q_\ell^+ T_\ell)_i^j + (Q_\ell^+ T_\ell)_{i+1}^j \right] + \left[(q_g^+ PT_g)_i^j + (q_g^+ PT_g)_{i+1}^j \right] \\
& \left. + \left[(q_r b T_r)_i^j + (q_r b T_r)_{i+1}^j \right] \right\} \\
& - \frac{\theta}{2} \left\{ \frac{C_2}{\rho c_p} \left[(b T)_i^{j+1} + (b T)_{i+1}^{j+1} \right] + \frac{C_4}{\rho c_p} \left[(P T)_i^{j+1} + (P T)_{i+1}^{j+1} \right] \right. \\
& + \left[(Q_\ell^- T)_i^{j+1} + (Q_\ell^- T)_{i+1}^{j+1} \right] + \left[(q_g^- PT)_i^{j+1} + (q_g^- PT)_{i+1}^{j+1} \right] \\
& \left. - \left[(q_e b T)_i^{j+1} + (q_e b T)_{i+1}^{j+1} \right] \right\}
\end{aligned}$$

$$\begin{aligned}
& - \frac{(1-\theta)}{2} \left\{ \frac{C_2}{\rho c_p} \left[(b T)_i^j + (b T)_{i+1}^j \right] + \frac{C_4}{\rho c_p} \left[(P T)_i^j + (P T)_{i+1}^j \right] \right. \\
& + \left[(Q_\ell^- T)_i^j + (Q_\ell^- T)_{i+1}^j \right] + \left[(q_g^- P T)_i^j + (q_g^- P T)_{i+1}^j \right] \\
& \left. - \left[(q_e b T)_i^j + (q_e b T)_{i+1}^j \right] \right\} = 0 \quad (3.19)
\end{aligned}$$

In DSTEMP Q_ℓ^+ , Q_ℓ^- , and T_ℓ were assumed invariant over a subreach Δx_i . In the general nomenclature of Equations 3.16, 3.17, and 3.18 this invariance can be expressed as:

$$K_i^j = K_{i+1}^j \quad (3.20)$$

and

$$K_i^{j+1} = K_{i+1}^{j+1} \quad (3.21)$$

Also q_g^+ , q_g^- , T_g , q_r , T_r , and q_e were assumed invariant over a subreach Δx_i and a time interval Δt^j . In the case of invariance of T_r over Δt^j , for example, it was assumed that the value of wet-bulb temperature was the average value over the time interval Δt^j . Invariance of q_r over Δt^j implies that q_r is the depth of precipitation cumulated over the time interval Δt^j . In the general nomenclature of Equations 3.16, 3.17, and 3.18 the invariance over Δx_i and Δt^j can be expressed as:

$$K_i^j = K_{i+1}^j = K_i^{j+1} = K_{i+1}^{j+1} \quad (3.22)$$

Equation 3.19 was rearranged into the following general form after substitution of Equations 3.20, 3.21, and 3.22 applied to the appropriate variables:

$$A_i T_i^{j+1} + B_i T_{i+1}^{j+1} = C_i T_i^j + D_i T_{i+1}^j + E_i \quad (3.23)$$

in which A_i , B_i , C_i , D_i , and E_i are coefficients that are independent of T . Equation 3.23 was then solved for T_{i+1}^{j+1} :

$$T_{i+1}^{j+1} = \frac{C_i T_i^j + D_i T_{i+1}^j + E_i - A_i T_i^{j+1}}{B_i} \quad (3.24)$$

To improve the program efficiency "array look-ups" and repeated identical calculations were minimized by the introduction of dummy variables defined in Table 3.1. In terms of these dummy variables, the coefficients in Equations 3.23 and 3.24 are defined as follows:

$$A_i = D5 * D27 - D6 * (Q)_i^{j+1} - D2 * (D14 * D17 + D13 * D21 + D15) \quad (3.25)$$

$$B_i = D5 * D28 - D6 * D25 - D2 * (D14 * D18 + D13 * D22 + D15) \quad (3.26)$$

$$C_i = D5 * D29 + D7 * (Q)_i^j + D3 * (D14 * D19 + D13 * D23 + D16) \quad (3.27)$$

$$D_i = D5 * D30 - D7 * (Q)_{i+1}^j + D3 * (D14 * D20 + D13 * D24 + D16) \quad (3.28)$$

Table 3.1 Definition of dummy variables used in DSTEMP and in Equations 3.25 through 3.29.

Dummy variable	Equation form	Program form
D1	$(1 - \theta)$	1 - THETA
D2	$\theta/2$	THETA/2
D3	$(1 - \theta)/2$	D1/2
D4	$1/\rho c_p$	1/(RHO*CP)
D5	$1/2\Delta t^j$	1/(2*DT(J))
D5A	$1/\Delta t^j$	2*D5
D6	$\theta/\Delta x_i$	THETA/DX
D7	$(1 - \theta)/\Delta x_i$	D1/DX
D8	$C_1/\rho c_p$	D4*C1
D9	$C_2/\rho c_p$	D4*C2
D10	$C_3/\rho c_p$	D4*C3
D11	$C_4/\rho c_p$	D4*C4
D12	$\frac{C_3}{c_p} + (q_g^+ T_g)_i$	D10+QGP*D31
D13	$\frac{C_4}{c_p} + (q_g^-)_i$	D11+QGM
D14	$\frac{C_2}{c_p} - (q_e)_i^j$	D9-QEE
D15	$(Q_l^-)_{i}^{j+1}$	QLM(2)
D16	$(Q_l^-)_i^j$	QLM(1)

Table 3.1 Continued.

Dummy variable	Equation form	Program form
D17	$(b)_i^{j+1}$	BD(I, J1, K)
D18	$(b)_{i+1}^{j+1}$	BD(I1, J1, K)
D19	$(b)_i^j$	BD(I, J, K)
D20	$(b)_{i+1}^j$	BD(I1, J, K)
D21	$(P)_i^{j+1}$	PM(I, J1, K)
D22	$(P)_{i+1}^{j+1}$	PM(I1, J1, K)
D23	$(P)_i^j$	PM(I, J, K)
D24	$(P)_{i+1}^j$	PM(I1, J, K)
D25	$(Q)_{i+1}^{j+1}$	QS(I1, J1, K)
D26	$\frac{C_1}{c_p} + (q_r T_r)_i^j$	D8+QRR*TRR
D27	$(A)_i^{j+1}$	CSA(I, J1, K)
D28	$(A)_{i+1}^{j+1}$	CSA(I1, J1, K)
D29	$(A)_i^j$	CSA(I, J, K)
D30	$(A)_{i+1}^j$	CSA(I1, J, K)
D31	$(T_g)_i$	TG(I, K)

$$\begin{aligned}
E_i = & D2*[D26*(D17+D18) + D12*(D21 + D22) + 2*(Q_\ell^+ T_\ell)_i^{j+1}] \\
& + D3*[D26*(D19+D20) + D12*(D23 + D24) + 2*(Q_\ell^+ T_\ell)_i^j] \\
& \dots \dots \dots (3.29)
\end{aligned}$$

Point loads

Thermal loads associated with a point inflow to the stream can also be handled by DSTEMP. Point sources must be located in-between subreaches at computational points. Therefore, it follows from the assumption of instantaneous and complete mixing, that point loads do not enter into the heat balance on the subreach control volume. If point loads are modeled when DSTEMP is used in conjunction with DNRT some care must be exercised. This is because the current version of DNRT does not allow for point loads to be input at a single point. Instead they are represented as lateral inflow over a short subreach. This may not be a realistic means of representing return flows from a cooling process for example, that are small in quantity in comparison to the streamflow rate but significant in their impact on stream temperature. Such a point load could probably be neglected in DNRT, but should be included in DSTEMP when seeking to provide a good representation of the stream temperature regime. If a point load is handled as a lateral inflow in DNRT it must be handled in the same manner in DSTEMP and thus its temperature

must be specified as a surface lateral inflow temperature. If a point load is neglected in DNRT because it is small in flowrate but it is thermally significant, then it should be treated as a point load in DSTEMP.

Continuing the assumption of complete and instantaneous mixing point loads are handled by a simple heat balance at the point of entry to the stream:

$$(T')_{i+1}^{j+1} = \frac{(QT)_{i+1}^{j+1} + Q_p T_p}{(Q)_{i+1}^{j+1} + Q_p} \quad \dots \quad (3.30)$$

in which

$(T')_{i+1}^{j+1}$ stream temperature immediately downstream of point load (indexed by $L=1$ in program) (deg. F)

Q_p flowrate of point load (cfs)

T_p temperature of point load (deg. F)

Both the values of stream temperature immediately upstream and immediately downstream of the point load are stored in the computer program and printed in the DSTEMP output.

Heat Exchange Components

General

The general linear forms of heat exchange components of net nonadvective heat exchange across the surface and streambed are:

$$\phi_{\text{ith surface component}} = c_1^i + c_2^i T \quad . \quad . \quad . \quad . \quad . \quad . \quad (3.31)$$

$$\phi_{\text{ith bed component}} = c_3^i + c_4^i T \quad . \quad . \quad . \quad . \quad . \quad . \quad (3.32)$$

In this section the physical constants, empirical coefficients, and meteorologic, astronomical, and other data required to estimate each component of nonadvective heat exchange as a function of stream temperature are described.

Components of net nonadvective heat exchange across the stream surface are:

$$\Phi_s = (\phi_s - \phi_{sr}) + (\phi_v - \phi_{vr}) + (\phi_a - \phi_{ar}) - \phi_b - \phi_e + \phi_c - \phi_{sn} - \phi_w \quad . \quad . \quad . \quad . \quad . \quad . \quad (3.33)$$

in which

- ϕ_s solar radiation flux incident at stream surface
- ϕ_{sr} solar radiation flux reflected from stream surface
- ϕ_v vegetative radiation flux incident at stream surface
- ϕ_{vr} vegetative radiation flux reflected from stream surface
- ϕ_a atmospheric radiation flux incident at stream surface
- ϕ_{ar} atmospheric radiation flux reflected from stream surface
- ϕ_b back radiation flux emitted by stream surface
- ϕ_e heat flux due to latent heat of vaporization associated with evaporation from stream
- ϕ_c conductive flux across stream surface

ϕ_{sn} heat flux due to latent heat of fusion associated with melting of snow falling into the stream

ϕ_w heat flux by surface layer renewal

Components of net nonadvective heat exchange across the streambed are:

$$\Phi_b = \phi_{bs} + \phi_{bb} + \phi_{bc} \quad . \quad . \quad . \quad . \quad . \quad . \quad . \quad . \quad . \quad (3.34)$$

in which

ϕ_{bs} solar radiation flux absorbed by streambed

ϕ_{bb} back radiation flux emitted by streambed

ϕ_{bc} conductive flux across streambed

The units of each component are $\text{BTU ft}^{-2} \text{hr}^{-1}$. User options have been included in DSTEMP to permit inclusion or exclusion of individual components. In this way studies of the sensitivity of stream temperatures to individual components are facilitated. Also components for which adequate data is unavailable can be omitted. However, care must be exercised when excluding components from predictive runs; for example, it is difficult to conceive of a situation in which solar radiation could justifiably be omitted.

Several components are not modeled in the current version of DSTEMP. For these components methods of estimation are proposed in this section. Users could readily introduce these methods into the

empty subroutine shells of the present program if desired.

Equation 3.2 in the model formulation section shows that Φ_s and Φ_b were considered to act over the areas A_s and A_b , respectively. ϕ_{bs} was considered to act on an area equal to A_s projected onto the streambed. Therefore, the ϕ_{bs} component was included in Φ_s instead of Φ_b in the program form of the numerical solution but appears as a component of Φ_b in all output tables.

Solar radiation

Three techniques for estimating incident and reflected solar radiation flux are included in the current version of DSTEMP:

1. Solar radiation flux calculated.
2. Total daily observed solar radiation flux distributed in parabolic manner between sunrise and sunset.
3. Observed solar radiation flux in computational time interval used directly.

Results from these techniques will be compared and factors to be considered when selecting one of the techniques will be discussed. Firstly, each of the techniques will be described.

Technique 1 - calculated solar radiation. A method of calculating solar radiation flux described in detail by Wunderlich (1972) was adapted to DSTEMP. The method is divided into three steps:

1. Solar radiation flux received at the top of the atmosphere.

2. Solar radiation flux received at the ground under a clear sky.
3. Solar radiation flux received at the ground under a cloudy sky.

The computation of solar radiation flux received at the top of the earth's atmosphere, the extraterrestrial solar radiation flux, is based on measured values of radiation emitted by the sun and the trigonometric relationship to express the direct solar beam intensity on a horizontal (tangential) plane (List, 1963). With extraterrestrial radiation flux known, the clear sky solar radiation flux received at the ground is principally a function of atmospheric transmittance. The method used for computation was selected by Wunderlich (1972) as the method that accounts for the maximum effect of local factors (Bolsenga, 1964). Attenuation of solar radiation by clouds is difficult to predict because of the great variety of types, distributions, and albedos of clouds, and the lack of analytical parameters to satisfactorily express this combined effect on solar radiation (Wunderlich, 1972).

Only a summary of the computational technique is presented below. For further details the reader is referred to Wunderlich (1972).

Declination of sun

$$\begin{aligned} \sin \delta = & \sin \left(\frac{23.445 \pi}{180} \right) \sin \left[\frac{2 \pi}{360} \left(279.9348 + \frac{360}{2 \pi} d \right. \right. \\ & + 1.914827 \sin d - 0.079525 \cos d \\ & \left. \left. + 0.019938 \sin 2d - 0.001620 \cos 2d \right) \right] \dots \dots \dots (3.35) \end{aligned}$$

in which

δ declination of sun (radians)

$$d = \frac{2 \pi}{365.242} (D-1) \quad (\text{radians}) \quad \dots \dots \dots (3.36)$$

D day number in the year

Relative distance of earth-sun

$$r = 1 + 0.017 \cos \left[\frac{2 \pi}{365} (186-D) \right] \dots \dots \dots (3.37)$$

in which

r relative distance of earth-sun (dimensionless)

Hour angle of sunrise

$$\cos h_{sr} = \frac{\sin \alpha_{sr} - \sin \phi \sin \delta}{\cos \phi \cos \delta} \dots \dots \dots (3.38)$$

in which

h_{sr} hour angle of sunrise (radians)

α_{sr} solar altitude at sunrise (radians)

ϕ latitude of the location (radians)

Hour angle of sunset

$$\cos h_{ss} = \frac{\sin \alpha_{ss} - \sin \phi \sin \delta}{\cos \phi \cos \delta} \quad . \quad . \quad . \quad . \quad . \quad (3.39)$$

in which

h_{ss} hour angle of sunset (radians)

α_{ss} solar altitude at sunset (radians)

Standard time of sunrise and sunset

$$STR = \frac{12}{\pi} h_{sr} - 12 + DTSL - ET \quad . \quad . \quad . \quad . \quad . \quad (3.40)$$

$$STS = \frac{12}{\pi} h_{ss} + 12 + DTSL - ET \quad . \quad . \quad . \quad . \quad . \quad (3.41)$$

in which

STR standard time of sunrise (hours)

STS standard time of sunset (hours)

DTSL time difference between local and standard meridian

(hours). DTSL is a constant for the location and is

computed by:

$$DTSL = \frac{e}{15} (LSM - LLM) \quad . \quad . \quad . \quad (3.42)$$

LSM longitude of standard meridian (degrees from Greenwich)

LLM longitude of local meridian (degrees from Greenwich)

$e = -1$ for west longitude

$e = +1$ for east longitude

ET equation of time (hours) given by:

$$\begin{aligned} ET = & -60 (0.123570 \sin d \\ & - 0.004289 \cos d + 0.153809 \sin 2d \\ & + 0.060783 \cos 2d) \quad . \quad . \quad . \quad . \quad . \quad (3.43) \end{aligned}$$

Hour angle-time relationships

$$h_B = \frac{\pi}{12} (ST_B - DTSL + ET + \epsilon) \quad . \quad . \quad . \quad . \quad . \quad (3.44)$$

$$h_E = \frac{\pi}{12} (ST_E - DTSL + ET + \epsilon) \quad . \quad . \quad . \quad . \quad . \quad (3.45)$$

in which

h_B hour angle of the beginning of computational time interval
(radians)

h_E hour angle of the end of computational time interval
(radians)

ST_B standard time of the beginning of computational time
interval (hours)

ST_E standard time of the end of computational time interval
(hours)

$\epsilon = +12$ for standard time before noon

$\epsilon = -12$ for standard time after noon

Solar altitude

$$\sin \alpha = \sin \phi \sin \delta + \cos \phi \cos \delta \cos h \quad . \quad . \quad . \quad . \quad . \quad (3.46)$$

in which

$$\alpha \quad \text{solar altitude, } \phi \leq \alpha \leq \frac{\pi}{2} \quad (\text{radians})$$

Extraterrestrial solar radiation integrated over computational time interval

$$q_o = \frac{12}{\pi} \frac{I_o}{r} [\sin \phi \sin \delta (h_E - h_B) + \cos \phi \cos \delta (\sin h_E - \sin h_B)] \quad . \quad . \quad . \quad . \quad . \quad (3.47)$$

in which

$$q_o \quad \text{extraterrestrial solar radiation flux for period } (h_E - h_B) \\ (\text{BTU ft}^{-2} \text{ hr}^{-1})$$

$$I_o \quad \text{solar constant } (429 \text{ BTU ft}^{-2} \text{ hrs}^{-1})$$

Precipitable water content of the atmosphere

$$w = \exp(0.0341 T_d - 2.0762) \quad . \quad . \quad . \quad . \quad . \quad (3.48)$$

in which

$$w \quad \text{precipitable water content of the atmosphere (ins.)}$$

$$T_d \quad \text{dew point temperature (deg. F)}$$

Optical air mass

$$m_p = \frac{(1 - 0.000006879Z)^{5.256}}{\sin \alpha + 0.15 \left(\frac{180}{\pi} \alpha + 3.885 \right)^{-1.253}} \quad . \quad . \quad . \quad . \quad . \quad (3.49)$$

in which

- m_p optical air mass adjusted to local altitude (dimensionless)
 Z elevation of subreach above mean sea level (ft)

Mean atmospheric transmission coefficients

$$a' = \exp \left\{ - (0.465 + 0.134 w) [0.129 + 0.171 \exp(-0.880 m_p)] m_p \right\} \quad \dots \dots \dots (3.50)$$

$$a'' = \exp \left\{ - (0.465 + 0.134 w) [0.179 + 0.421 \exp(-0.721 m_p)] m_p \right\} \quad \dots \dots \dots (3.51)$$

in which

- a' mean atmospheric transmission coefficients after scattering (cm)
 a'' mean atmospheric transmission coefficient after scattering and absorption (cm)

Solar short wave radiation flux incident at stream surface

$$q_i = q_o \frac{[a'' + 0.5 (1 - a' - d_p)]}{[1 - 0.5 R_g (1 - a' - d_p)]} (1 - 0.0065 C^2) (1 - S) \quad (3.52)$$

in which

- q_i incident solar radiation flux at stream surface
 (BTU ft⁻² hr⁻¹)
 R_g albedo of ground adjacent to stream (Table 3.2)
 (dimensionless)

Table 3.2. Total dust depletion coefficient, d_p . (Summarized by Bolsenga (1964) based on data by Kimball (1927, 1928, 1930).)

Season	Washington, D.C.		Madison, Wisc.		Lincoln, Nebr.	
	$m^a = 1$	$m = 2$	$m = 1$	$m = 2$	$m = 1$	$m = 2$
Winter	-	0.13	-	0.08	-	0.06
Spring	0.09	0.13	0.06	0.10	0.05	0.08
Summer	0.08	0.10	0.05	0.07	0.03	0.04
Fall	0.06	0.11	0.07	0.08	0.04	0.06

^aOptical air mass $m = 1 / [\sin \alpha + 0.15 (\alpha + 3.885)^{-1.253}]$.

- d_p total dust depletion coefficient of the atmosphere (Table 3.3) (dimensionless)
- C cloud cover in an integer number of tenths of cover
- S fraction of sky shaded from the stream surface by vegetation or other obstructions excluding cloud cover (dimensionless)

Solar short wave radiation flux reflected at stream surface

$$q_r = q_i R_t \dots \dots \dots (3.53)$$

in which

q_i reflected solar radiation flux at stream surface
(BTU ft⁻² hr⁻¹)

R_t reflectivity of water surface given by:

$$R_t = 1.18 \left(\frac{180}{\pi} \alpha \right)^{-0.77} \dots \dots \dots (3.54)$$

Technique 2 - distributed observed solar radiation. A method of distributing solar radiation flux in a parabolic manner between sunrise and sunset was adapted from Albertson et al. (1974). The choice of a parabolic distribution was made on the basis of radiation data collected by Raphael (1962). Solar radiation flux incident at the stream surface during the time period ($h_E - h_B$) was computed as follows (Figure 3.4):

$$q_i = \frac{12 I_{obs}}{L^3} \left[\frac{L}{4} (X_2^2 - X_1^2) - \frac{1}{6} (X_2^3 - X_1^3) (1 - S) \right] \dots \dots (3.55)$$

Table 3.3. Albedo of ground surface, R_g . (After Buttner (1953) and Sutton (1953).)

Ground Condition	R_g
Meadows and Fields	0.14 ^a
Leave and Needle Forest	0.07 - 0.09 ^a
Dark, Extended Mixed Forest	0.045 ^a
Heath	0.10 ^a
Flat Ground, Grass Covered	0.25 - 0.33
Flat Ground, Rock	0.12 - 0.15
Sand	0.18
Vegetation Early Summer, Leaves with High Water Content	0.19
Vegetation Late Summer, Leaves with Low Water Content	0.29
Fresh Snow	0.83
Old Snow	0.42 - 0.70

^aMay be too low.

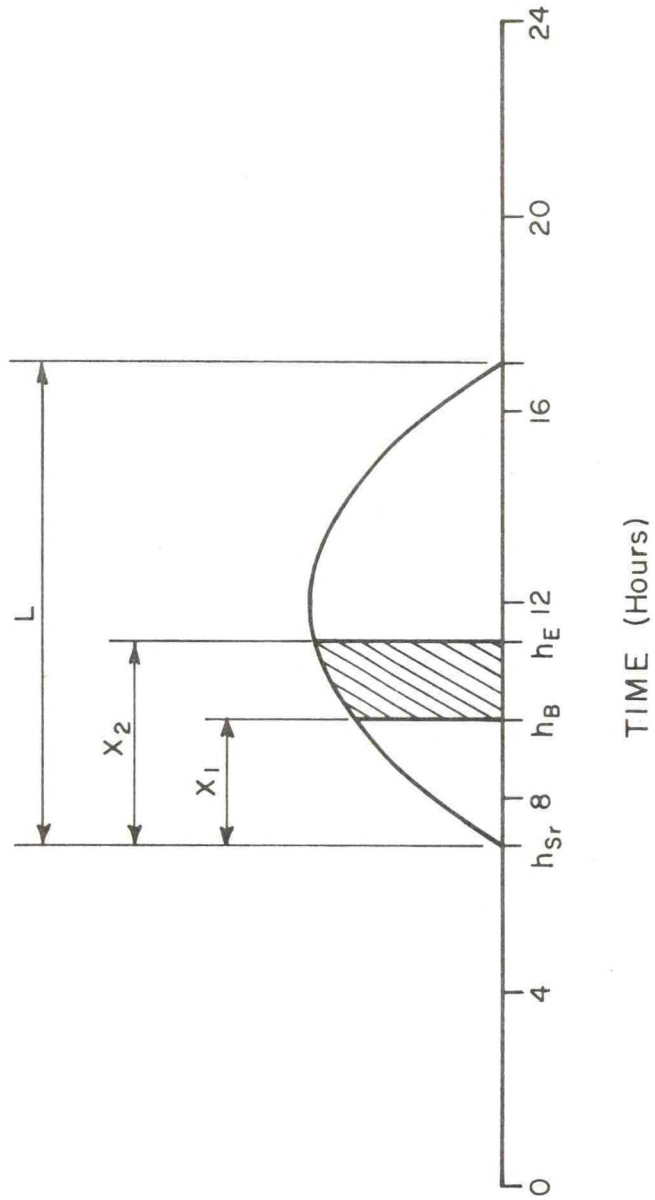


Figure 3.4. Parabolic distribution of daily solar radiation flux by technique 2 (adapted from Albertson et al., 1974).

in which

q_i	solar radiation flux incident at the stream surface during the time period ($h_E - h_B$) ($\text{BTU ft}^{-2} \text{hr}^{-1}$)
I_{obs}	observed total daily solar radiation flux ($\text{BTU ft}^{-2} \text{hr}^{-1}$)
$L = h_{\text{ss}} - h_{\text{sr}}$	sunrise - sunset period (hours)
$X_1 = h_B - h_{\text{sr}}$	time from sunrise to beginning of computational time interval, h_B (hours)
$X_2 = h_E - h_{\text{sr}}$	time from sunrise to end of computational time interval, h_E (hours)
S	fraction of sky shaded from the stream surface by vegetation or other obstructions excluding cloud cover (dimensionless)

Solar radiation flux reflected at the stream surface during the time period ($h_E - h_B$) was computed in the following way:

$$q_r = q_i R_t \quad \cdot \cdot \cdot \cdot \cdot \cdot \cdot \cdot \cdot \cdot \cdot \cdot \quad (3.56)$$

in which

R_t reflectivity of water surface as input by the user (dimensionless)

Technique 3 - observed solar radiation. In this approach solar radiation flux incident at the stream surface was equated to the observed solar radiation in each computational time interval modified

only by a shading factor:

$$q_i = I_{obs} (1 - S) \quad (3.57)$$

and reflected solar radiation at stream surface was estimated by:

$$q_r = q_i R_t \quad (3.58)$$

In the general form of Equation 3.31 incident and reflected solar radiation flux at the stream surface are given by:

$$\phi_s = q_i \quad (3.59)$$

$$\phi_{sr} = q_r \quad (3.60)$$

Techniques compared. The principal source of error in predicting incident solar radiation lies in handling the effects of cloud cover (Wunderlich, 1972). When observed solar radiation data at one location are used for stream temperature predictions at another location the differences in cloud cover at the two locations can introduce considerable error to surface heat exchange calculations. Times of sunrise and sunset vary for different subreaches in a stream because of the effects of channel orientation and topographic features above which the sun must rise before the solar beam is incident on the water surface. Other factors influencing the amount of solar radiation flux incident on the stream surface include the albedo of the ground

surface adjacent to the stream, R_g , and the atmospheric transmittance depending in part on the dust depletion coefficient d_p .

Technique 1 has the advantages of accounting for the variation in local factors such as orientation and topographic effects (described by α_{sr} and α_{ss}) and the ground surface albedo, R_g . It has the disadvantage of depending heavily on good cloud cover data. However, unless observed solar radiation data are available close to the study subreaches techniques 2 and 3 also may provide unrealistic estimates of incident and reflected solar radiation. When diurnal predictions are made using daily data technique 2 gives the solar radiation data a distribution which approximates the distribution expected under constant cloud cover conditions. If observed solar radiation data are available at less than a daily frequency then technique 3 should be used if it is considered that these observed data provide a more realistic distribution of solar radiation throughout the day than the parabolic approximation in technique 2. Another approach is to calibrate technique 1 to the site at which solar radiation data were observed. Calibration is achieved by estimating α_{sr} , α_{ss} , R_g , and d_p for the site and then adjusting these coefficients within a reasonable range of values until the observed solar radiation is closely matched. Both the times of sunset and sunrise and also the total amount of observed daily solar radiation should be closely matched. Technique 1

could then be used on each subreach by giving α_{sr} , α_{ss} , and R_g values appropriate to each subreach. The calculation approach requires some coefficient estimation before it can be applied but in return it takes account of local factors affecting solar radiation.

Figures 3.5 and 3.6 contain the results of sensitivity studies on two coefficients (R_g and d_p) in the computational method of estimating incident and reflected solar radiation flux at the stream surface (technique 1). By raising R_g from its lower limit for without-snow conditions (0.05 from Table 3.3) to its upper limit for without-snow conditions (0.45) the cumulative incident solar radiation in a 24 hour period was increased by 27 percent. When R_g was further increased to the upper limit for fresh snow conditions (0.85) the increase in cumulative incident solar radiation over the case where $R_g = 0.05$ was 72 percent.

Albedo of snow decreases with age over the range 0.85 to 0.4. Because of the importance of R_g in determining the incident solar radiation flux it appears that a snowpack simulation to determine the presence of snow and the albedo of the snow surface should be developed. The relative importance of solar radiation to the total heat budget in times of snow should be evaluated before proceeding with the snowpack simulation. A snowpack routine applied by Bowles et al. (1975) in a watershed simulation model could be adapted for this purpose.

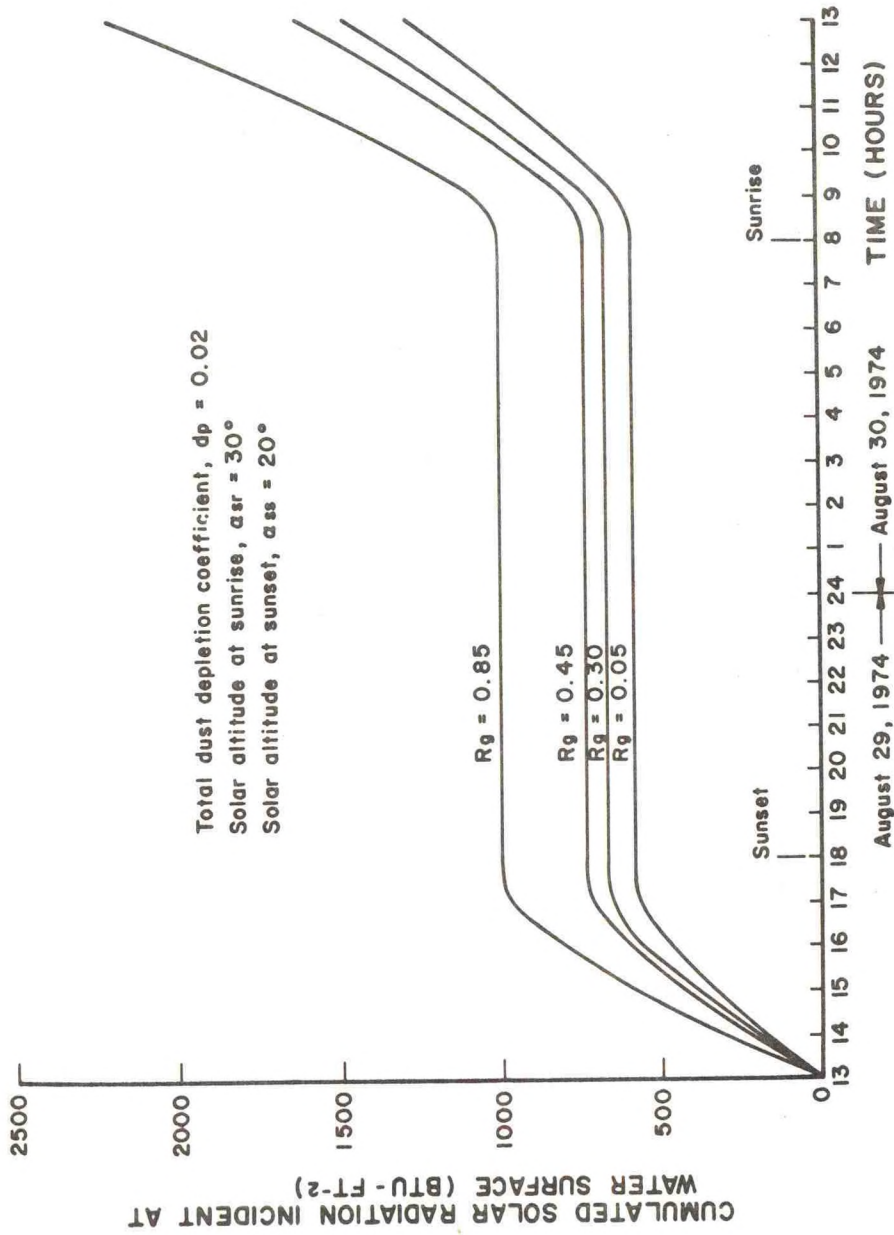


Figure 3.5. Sensitivity of incident solar radiation to reflectivity of ground adjacent to stream (R_g).

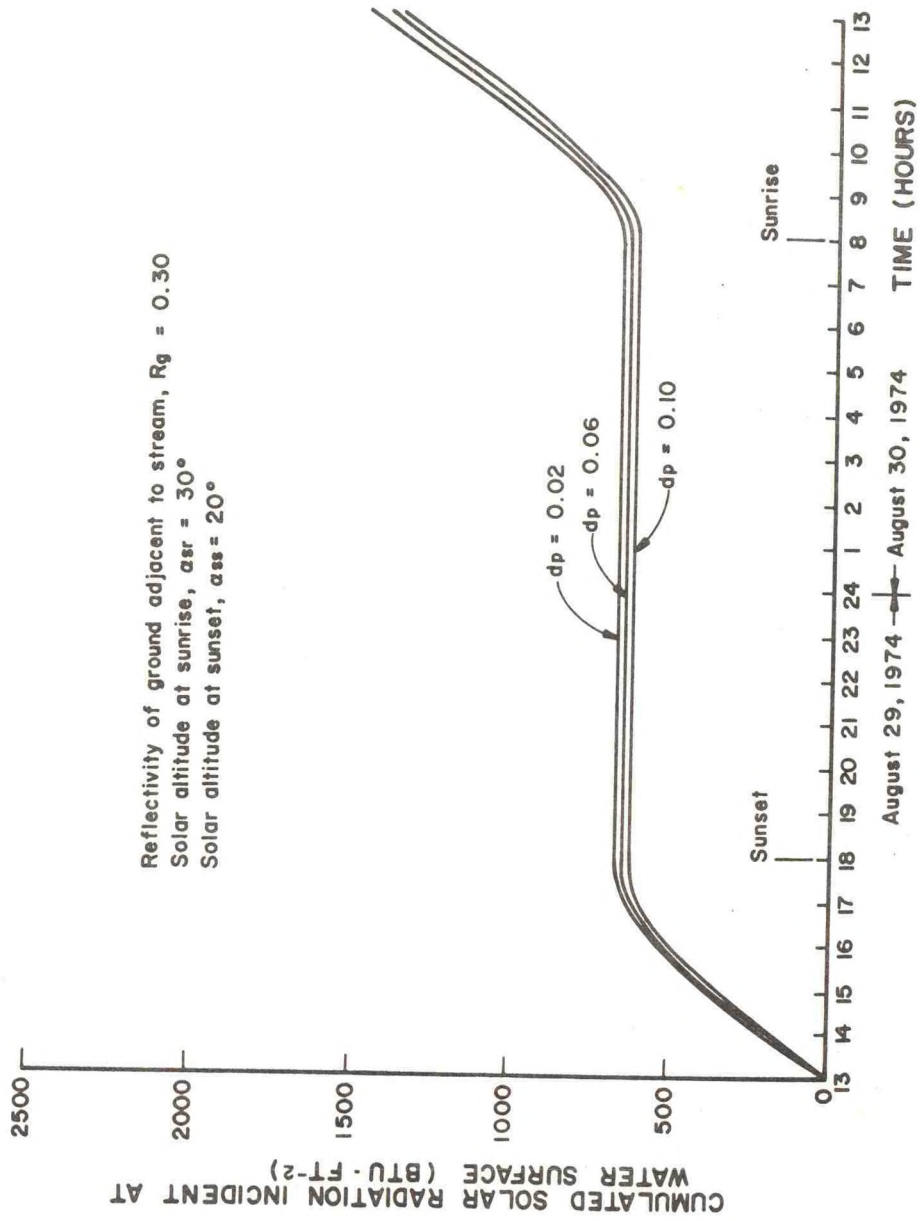


Figure 3.6. Sensitivity of incident solar radiation to total dust depletion coefficient (d_p).

Incident solar radiation flux was shown to be fairly insensitive to the dust depletion coefficient, d_p (Figure 3.6). By varying d_p over its range for the summer season, 0.02 to 0.10 (Table 3.2) cumulative incident solar radiation decreased by less than 4 percent.

Figure 3.7 is a comparison of cumulated incident solar radiation calculated by the three techniques available in DSTEMP. Observed data were recorded at Utah State University (USU) which is located 15 miles (24 km) southwest of the study stream, Spawn Creek. The discrepancy between the calculated (ITECH = 1) and observed (ITECH = 3) lines can be attributed to several factors: topographic differences between the measurement site and study stream (different α_{sr} and α_{ss}); different albedos of adjacent ground (R_g) at measurement site and study area; and cloud cover (C) differences between the valley location of the measurement site and the mountain location of the study stream. If the observed data were adjusted for topographic, and ground albedo differences, it is believed that the value of R_g could be reduced to a more realistic value for Spawn Creek and that the results from techniques 1 and 3 would be closer over the entire 24 hour period.

Technique 2 represents a different distribution of the same total amount of radiation that is predicted in technique 3. An important factor determining the different distributions is that sunrise and sunset times used in technique 2 were estimated for Spawn Creek and not

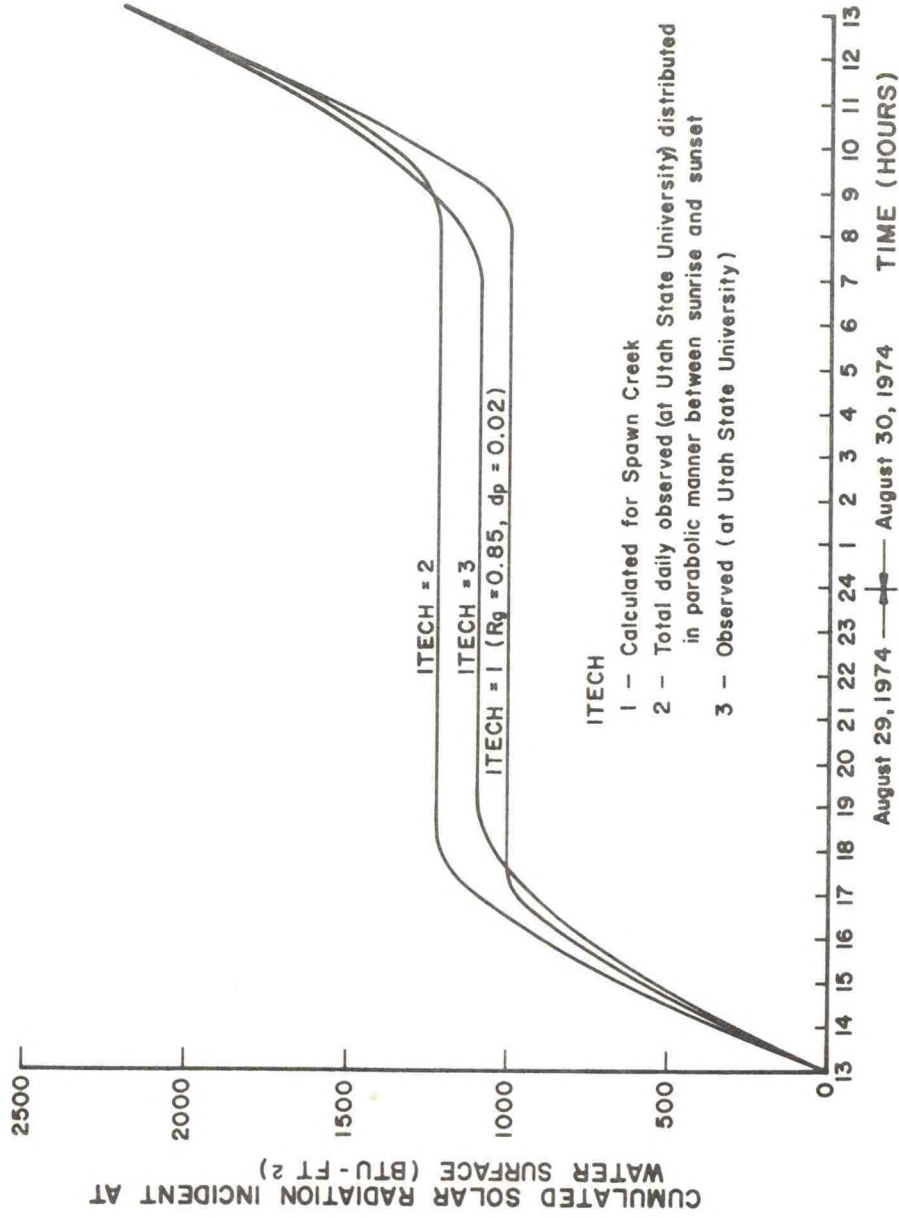


Figure 3.7. Comparison of solar radiation calculated by the three techniques.

the USU measurement site. The earlier sunset and later sunrise used in technique 2, compared with those observed in technique 3, reflects the greater degree of topographic obstruction at Spawn Creek. If sunset and sunrise times in technique 2 were set equal to those observed in technique 3 a better correspondence would be expected between these two approaches.

Vegetative radiation

Long-wave radiation emitted by the forest canopy was not accounted for in the current version of DSTEMP. Pluhowski (1970) proposed applying Stefan-Boltzmann's law to the problem of estimating incident and reflected vegetative radiation at the stream surface. Written directly in the form of Equation 3.31, Pluhowski's approach was:

$$\phi_v = \epsilon \sigma (T_a + 459.67)^4 \quad . \quad . \quad . \quad . \quad . \quad . \quad (3.61)$$

$$\phi_{vr} = R_l \phi_v \quad . \quad . \quad . \quad . \quad . \quad . \quad (3.62)$$

in which

ϵ emissivity factor for forest canopy ($\epsilon = 1.0$ for solid canopy)

σ Stefan-Boltzmann constant (1.74×10^{-9} BTU hrs⁻¹ ft⁻² deg. R⁴)

- T_a absolute temperature of the air above the ground as an approximation to the effective leaf temperature (deg. R)
- R_ℓ reflectivity of water surface to long-wave radiation
($R_\ell = 0.03$ according to Harbeck, 1958)

This component would probably be important in subreaches flowing through densely forested areas.

Atmospheric radiation

Anderson (1954) proposed the following empirical relationship for incident long-wave atmospheric radiation flux:

$$\phi_a = \beta \epsilon \sigma (T_a + 459.67)^4 \quad \dots \dots \dots (3.63)$$

in which

- β atmospheric radiation factor (dimensionless)
- ϵ emissivity of the atmosphere ($\epsilon = 1.0$)

Based on a statistical analysis of Anderson's results and on later work by Burt (1958), Raphael (1962) developed Figure 3.8 in which β was represented as a function of vapor pressure and cloud cover:

$$\beta = AA(C) + BB(C) e_a \quad \dots \dots \dots (3.64)$$

in which

- C cloud cover in an integer number of tenths of cover
- AA(C), BB(C) empirical coefficients in Equation 3.64 with different values for $C = 0, 10$. The values used in

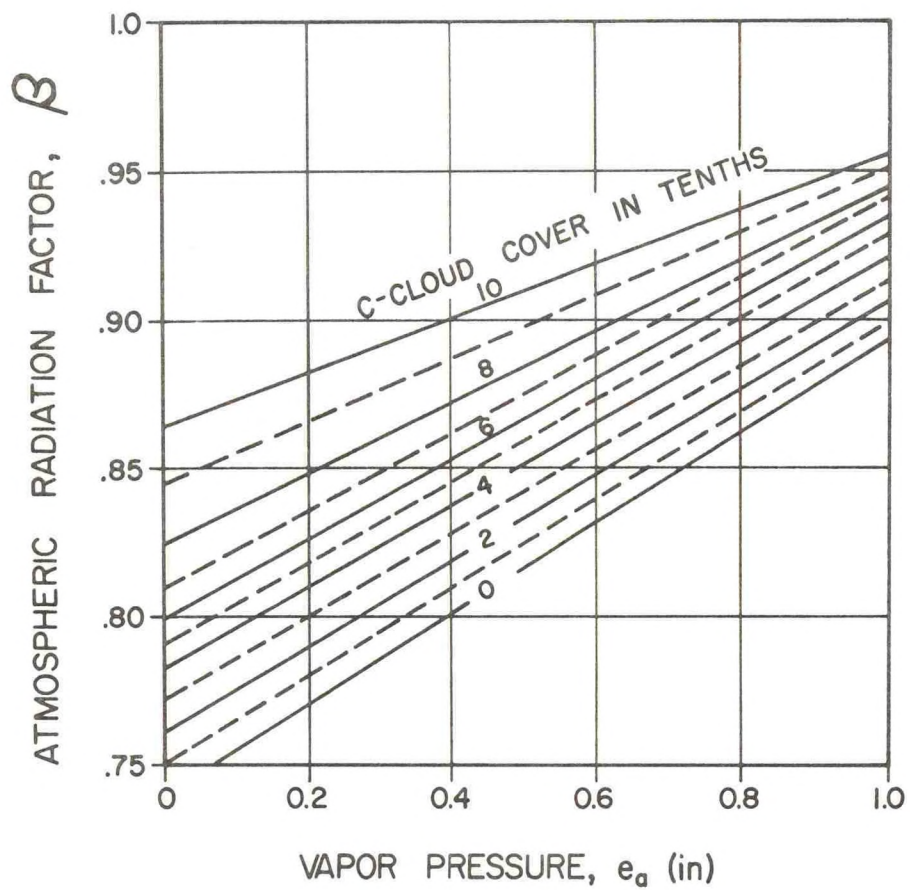


Figure 3.8. Atmospheric radiation factor, β (after Raphael, 1962).

AA(C) and BB(C) were taken from Novotny and Krenkel (1971) and are contained in the input description for read statements 32 and 33 in the DSTEMP input description (Appendix A)

e_a vapor pressure of air (ins. Hg)

Vapor pressure of air was calculated using a modified version of the Magnus-Tetens formula (Kleinschmidt, 1935):

$$e_a = \exp \left[\frac{8.642 T_d - 683.0}{0.5556 T_d + 219.5} \right] \cdot \cdot \cdot \quad (3.65)$$

in which

T_d dew point temperature (deg. F)

Long-wave atmospheric radiation flux reflected at the stream surface was estimated by:

$$\phi_{ar} = R_l \phi_a \cdot \cdot \cdot \cdot \cdot \cdot \cdot \cdot \cdot \cdot \quad (3.66)$$

Back radiation

Countering the incoming fluxes of heat from the sun, atmosphere, and forest is the long-wave radiation emitted by the stream itself.

Long-wave back radiation from the stream was computed by a piecewise-linear approximation to Stefan-Boltzmann's law with an emissivity factor for water of $\epsilon = 0.97$ (Anderson, 1954):

$$\phi_b = B1(T) + B2(T)T \quad . \quad . \quad . \quad . \quad . \quad . \quad . \quad . \quad (3.67)$$

in which

T stream temperature (deg. F)

B1(T), B2(T) coefficients in the piecewise-linear approximation
to Stefan-Boltzmann's law depending on stream
temperature range:

T	B1	B2
32 - 68	68.27	0.8815
68 - 104	54.25	1.084

Latent heat of vaporization associated
with evaporation

Many empirical formulas are available for estimating evaporation from water bodies (Wunderlich, 1972). Each of these formulas involves coefficients that should be estimated from field experiments. A generalized version of the empirical evaporation equation was adapted for use in DSTEMP. Latent heat of vaporization removed from the stream by the evaporating water mass was estimated by:

$$\phi_e = \rho L_v Nu (e_s - e_a) \quad . \quad . \quad . \quad . \quad . \quad . \quad . \quad . \quad (3.68)$$

in which

ρ density of water (62.3 lbs. ft⁻³)

L_v latent heat of vaporization of water (1053 BTU lbs⁻¹)

N mass transfer coefficient (evaluated by field experiment)

- or during model calibration procedure) (ins. Hg⁻¹)
- u wind speed (mph)
- e_s saturation vapor pressure of air (ins. Hg)
- e_a vapor pressure of air (ins. Hg)

Saturation vapor pressure of air was calculated by a piecewise-linear approximation (Wunderlich, 1972) to the Magnus-Tetens formula (Equation 3.65) in which T was substituted for T_d:

$$e_s = ES1(T) + ES2(T)T \quad . \quad . \quad . \quad . \quad . \quad . \quad (3.69)$$

in which

ES1(T), ES2(T) coefficients in the piecewise-linear approximation to Magnus-Tetens formula depending on stream temperature range. Values used for ES1(T) and ES2(T) are listed in the input description for read statements 35 and 36 in the DSTEMP input description (Appendix A).

Conduction

Bowen (1926) related heat losses to the air by conduction across a water surface, to latent heat of vaporization associated with evaporation from the water surface:

$$R = \frac{\phi_c}{\phi_e} = 6.49 \left[\frac{T - T_a}{e_s - e_a} \right] \frac{P}{P_o} \quad . \quad . \quad . \quad . \quad (3.70)$$

in which

R Bowen's ratio (a dimensionless constant, see Bowen, 1926)

P atmospheric pressure at study area (ins. Hg)

P_o atmospheric pressure at sea level

Heat losses by conduction were estimated by substituting Equation 3.68 and P_o = 29.92 ins. Hg into Equation 3.70 and then solving for ϕ_c :

$$\phi_c = 0.217 (T - T_a) P \rho L_v Nu \quad . \quad . \quad . \quad . \quad . \quad (3.71)$$

Latent heat of fusion associated with snowfall

The current version of DSTEMP does not include an estimation of the latent heat of fusion and other heat required to convert snow falling into the stream to water. Adapting an approach used by Jeppson (1975) the heat lost by the stream in melting snow is given by:

$$\phi_{sn} = q_{sn} \rho [L_f + C_{sn} (T - T_r)] \quad . \quad . \quad . \quad . \quad . \quad (3.72)$$

in which

q_{sn} snow (ft. s⁻¹)

L_f latent heat of fusion (143.5 BTU lbs⁻¹)

C_{sn} specific heat of ice (0.50 BTU lbs⁻¹ deg. F⁻¹)

Surface layer renewal

Heat supply or removal by surface renewal was also omitted from the current version of DSTEMP. It could be represented using an approach proposed by Novotny and Krenkel (1971):

$$\phi_w = k_w (T_s - T) \quad \dots \dots \dots \quad (3.73)$$

$$k_w \approx 3.96 \times 10^4 k \left(\frac{U}{H}\right)^{0.33} \quad \dots \dots \dots \quad (3.74)$$

in which

- T_s surface water temperature (deg. F)
- k coefficient of thermal conductivity (BTU ft⁻¹ s⁻¹ deg. F⁻¹)
- U velocity of stream (ft. s⁻¹)
- H depth of flow (ft.)

To calculate ϕ_w an estimate of T_s is required. Novotny and Krenkel (1971) proposed a technique for calculating T_s from T , the bulk water temperature, by applying a heat balance at the air-water interface. If T_s is estimated it should also be used in place of T in the estimation of ϕ_b (Equation 3.67), ϕ_e (Equation 3.68), and ϕ_c (Equation 3.70).

Solar radiation absorbed
by streambed

After reflection at the stream surface the remainder of the incident solar radiation flux enters the stream. Approximately 60

percent of the solar radiation (Novotny and Krenkel, 1971) entering the stream is immediately absorbed in the water surface (Figure 3.9). Within the stream solar radiation is absorbed in an exponential manner which can be described fairly well by Beer's law. Thus the solar radiation flux absorbed by the streambed was estimated by:

$$\phi_{bs} = (1 - R_b)(1 - s)(\phi_s - \phi_{sr}) \exp(-\eta H) \quad . \quad . \quad . \quad (3.75)$$

in which

R_b reflectivity of streambed (found experimentally or in calibration procedure) (dimensionless)

s proportion of solar radiation entering stream that is absorbed in the water surface (usually 0.6)

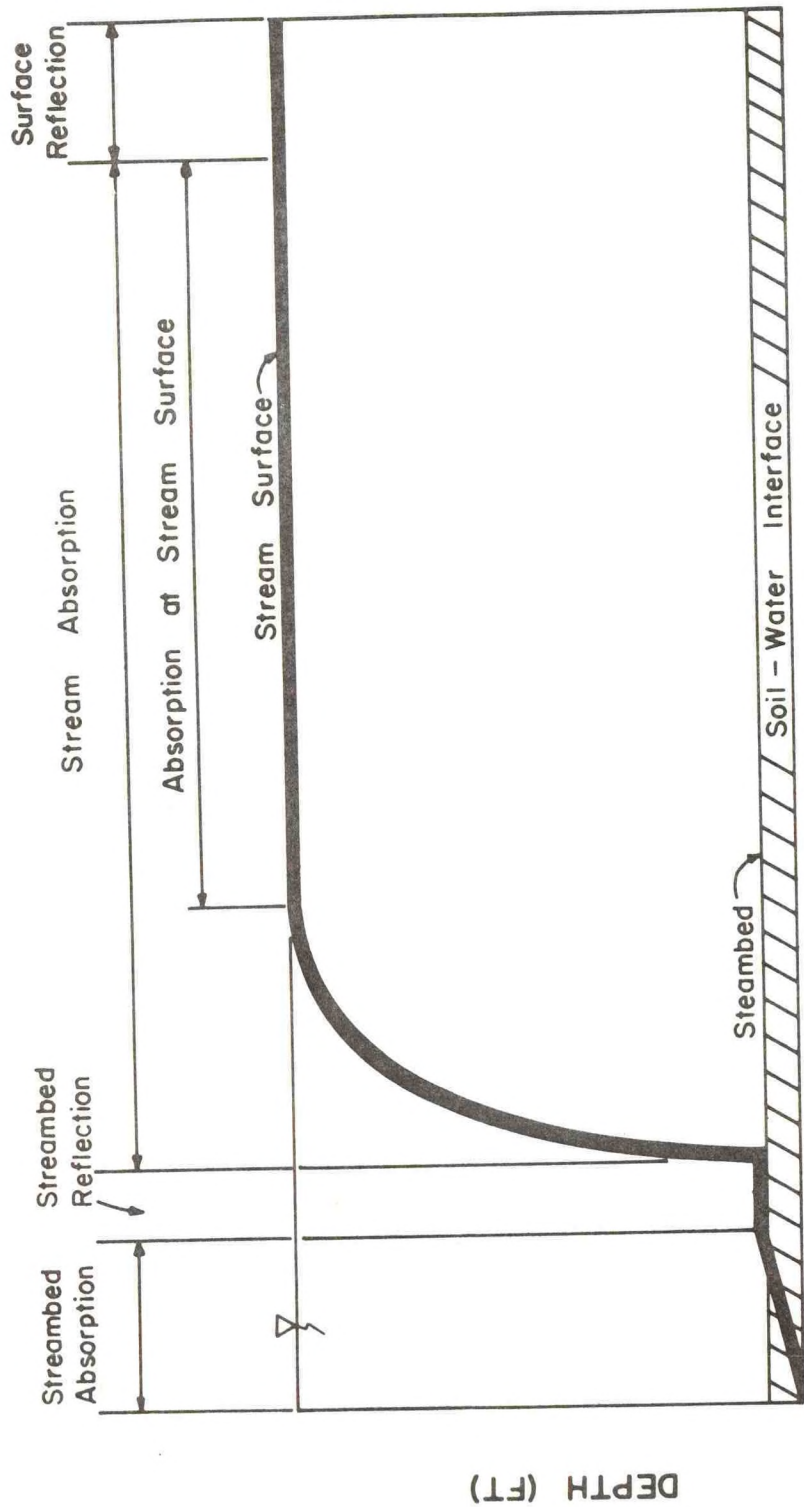
η bulk extinction coefficient (mean value for solar radiation 0.008 ft^{-1} , Roesner, 1969) (ft^{-1})

Back radiation from streambed

This component was not modeled in the current version of DSTEMP. If an emissivity of the streambed could be established then it is proposed that the Stefan-Boltzmann's law could be applied based on the temperature of the streambed-stream interface.

Conductive flux across streambed

In Comer et al. (1975) a regression relationship was developed to predict conductive flux across the streambed of Spawn Creek based on



SOLAR RADIATION FLUX (BTU-FT⁻²)

Figure 3.9. Dissipation of incident solar radiation flux.

experimental data:

$$\phi_{bc} = \alpha_1 + \alpha_2 \phi_{bs} + \alpha_3 T_g + \alpha_4 T \quad . \quad . \quad . \quad (3.76)$$

in which

$\alpha_1, \alpha_2, \alpha_3, \alpha_4$ regression coefficients

T_g groundwater temperature (deg. F)

CHAPTER 4
APPLICATION OF DSTEMP TO
BRAZOS-LITTLE RIVERS, TEXAS

Introduction

A search was made for a river system on which to demonstrate the Dynamic Stream Temperature Model (DSTEMP) and its linkage to the Implicit Dynamic Routing Program (DNRT). The following criteria were selected for the river system:

- 1) A river-tributary system is preferred to a single river
- 2) Streamflow and stream temperature data should be available at the upstream boundaries of the main river and tributary and at the downstream boundary of the main river
- 3) Streamflow at the upstream boundaries of the river system should contribute the major portion of the streamflow at the downstream boundary and therefore lateral inflow is small
- 4) No reservoirs between upstream and downstream boundaries
- 5) No major sources of thermal pollution or streamflow for which records do not exist

The third criterion was established because streamflow-stream temperature modeling in a river system with large lateral inflow becomes mainly a problem of estimating lateral inflow rates and lateral inflow temperatures. In the absence of these lateral inflow data they should be estimated using a two-dimensional hydrology-water temperature model applied to the catchment areas of the river system. At present, such a

model does not exist for water temperature. In order that the predictions from DSTEMP should not be dominated by lateral inflow temperature estimates a river system with small lateral inflow was sought such that hydrograph-thermograph routing and meteorologic considerations were the most important aspects of the stream temperature simulation.

After an extensive search with the assistance of the Chief, Branch of Quality of Water, USGS, and several USGS District Chiefs, the Brazos-Little Rivers in Texas were found to closely satisfy the criteria listed above. In the remainder of this chapter the data collection, streamflow modeling, DSTEMP problem set-up, and results of the Brazos-Little application are described.

Brazos-Little River System

The section of the Brazos-Little River System modeled in this study was bounded by USGS streamflow gages at Highbank, Cameron, and College Station (Figure 4.1). Stream temperature records were available at the Highbank and Cameron gages but not at College Station. Therefore, stream temperature records from the Bryan gage, 9 miles downstream, were used for comparison with stream temperatures predicted by the DSTEMP model at college stations. On the basis of channel characteristics the 65.5 mile section of the Brazos River was divided into 13 subreaches, and the 33.6 mile section of the Little River was divided into 8 subreaches. At the confluence of the rivers an arbitrarily small subreach was

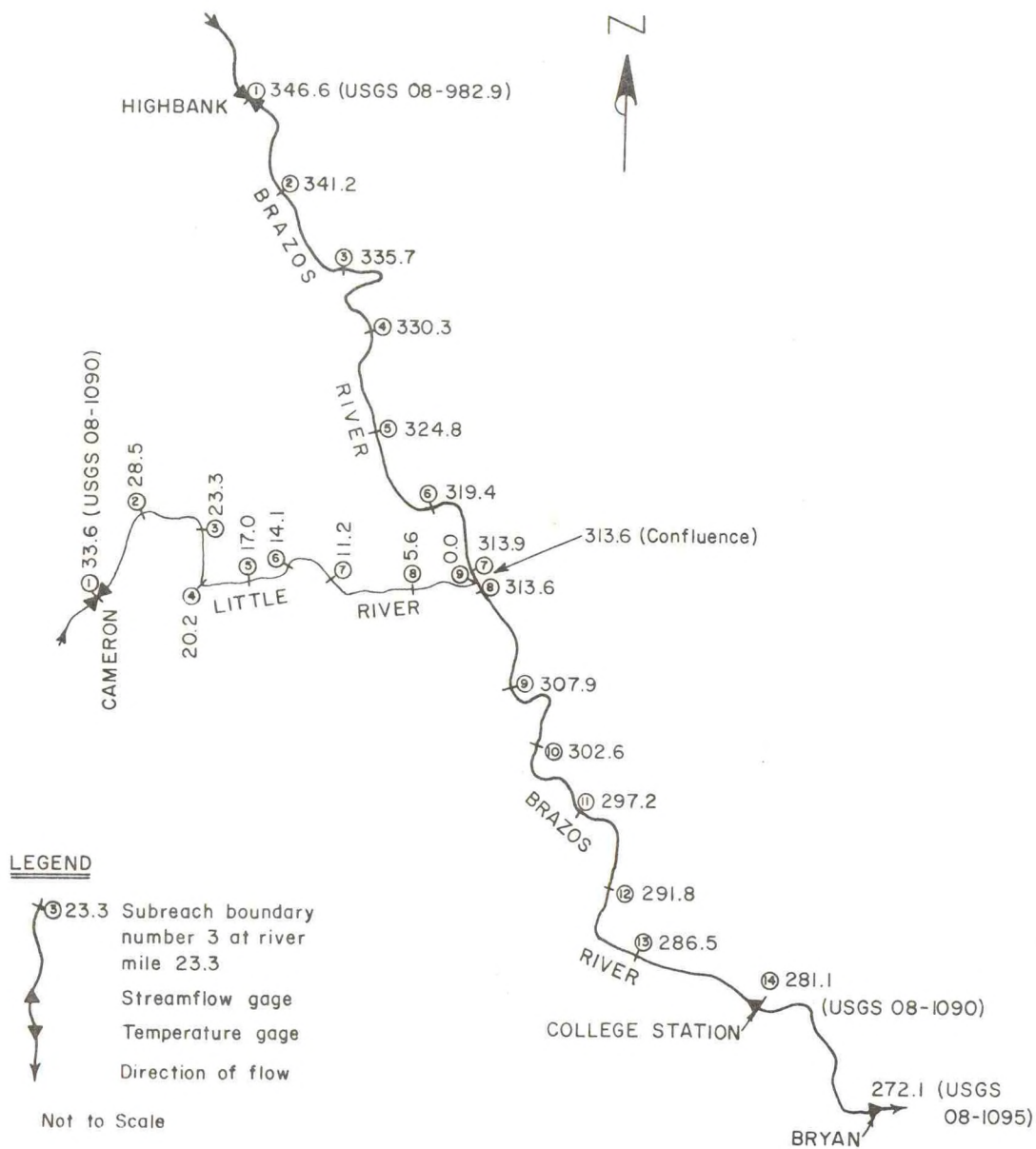


Figure 4.1. Schematic of Brazos-Little River System.

defined on the Brazos River for addition of the Little River treated as lateral inflow over the small subreach.

Data Sources

Several storms during the 1973 water year were selected for possible simulation. Streamflow and stream temperature data were obtained from the USGS Surface Water Records and Water Quality Records. Topographic quadrangle maps, and rating curves and cross-sections for the gaging stations were furnished by the USGS, Austin, Texas.

Meteorologic data were taken from Local Climatic Data published by NOAA. Additional unpublished meteorologic data for College Station were supplied on microfilm from the National Climatic Center, Asheville, North Carolina. Solar radiation data observed at College Station were made available by the Texas State Climatologist.

Streamflow Modeling

Data preparation for application of DNRT to the Brazos-Little Rivers was undertaken jointly by the contractors (Utah Water Research Laboratory) and the client (Hydrologic Research Laboratory, National Weather Service, NOAA). Final calibration of DNRT for unsteady flow conditions was accomplished by D. L. Fread of NOAA. Output from the calibrated DNRT model was written onto computer disc storage files at Utah State University, and then read as input by the DSTEMP model.

DSTEMP Problem Set-Up

A partial listing of DSTEMP model input is contained in Figure 4.2. The listing was obtained using the print option, IPRT = 1, which excludes hydraulic and stream geometry data generated by DNR T. All components of surface heat transfer available in the current version of DSTEMP were used, but streambed heat transfer components were considered negligible. Solar radiation was calculated using the third technique (ITECH = 3). A 12 hour computational time increment was used.

Surface and subsurface components of lateral inflow were lumped together and no point sources of thermal effluents were represented. Initial temperatures along the river system were estimated by linear interpolation between the upstream and downstream boundaries while maintaining a heat balance at the confluence of the two rivers. Comparison of observed and predicted stream temperatures was possible at only one location, the downstream boundary.

Standard values of the various meteorologic coefficients listed in Appendix A were used in this application. Three meteorologic data groups were defined:

- 1) Brazos River, subreaches 1-7: using precipitation and dry bulb air temperatures observed at Highbank and other meteorologic data from Waco.
- 2) Little River, subreaches 1-8: using precipitation and dry bulb air temperatures observed at Cameron and other meteorologic data from Waco.

3) Brazos River, subreaches 9-13: using meteorologic data observed at College Station

Observed solar radiation data at College Station were used in all the meteorologic data groups. These data were adjusted for an instrument bias by adding 20% to the reported value. All meteorologic data were input for a meteorologic time interval of 24 hours except solar radiation data which were input for the 12 hour computational time intervals.

Results

Figures 4.3a and c show the upstream streamflow boundary conditions for the dynamic routing model, DNRT, for the period of December 5-28, 1972. A comparison of the observed and predicted hydrographs at the downstream boundary is represented by Figure 4.3e. This figure indicates that very good agreement was achieved between model responses and observed flows.

The strategy for calibration of DSTEMP was as follows:

- 1) Adjust coefficients affecting surface heat transfer components
- 2) Adjust estimate of lateral inflow thermograph

During the early stage of model calibration the first technique (ITECH=1) for calculating solar radiation was used. However, a comparison of solar radiation predicted by this technique with values observed at College Station indicated that low values were generally over-estimated and that high values were generally under-estimated. It was not feasible to draw any conclusions about the technique for estimating solar radiation.

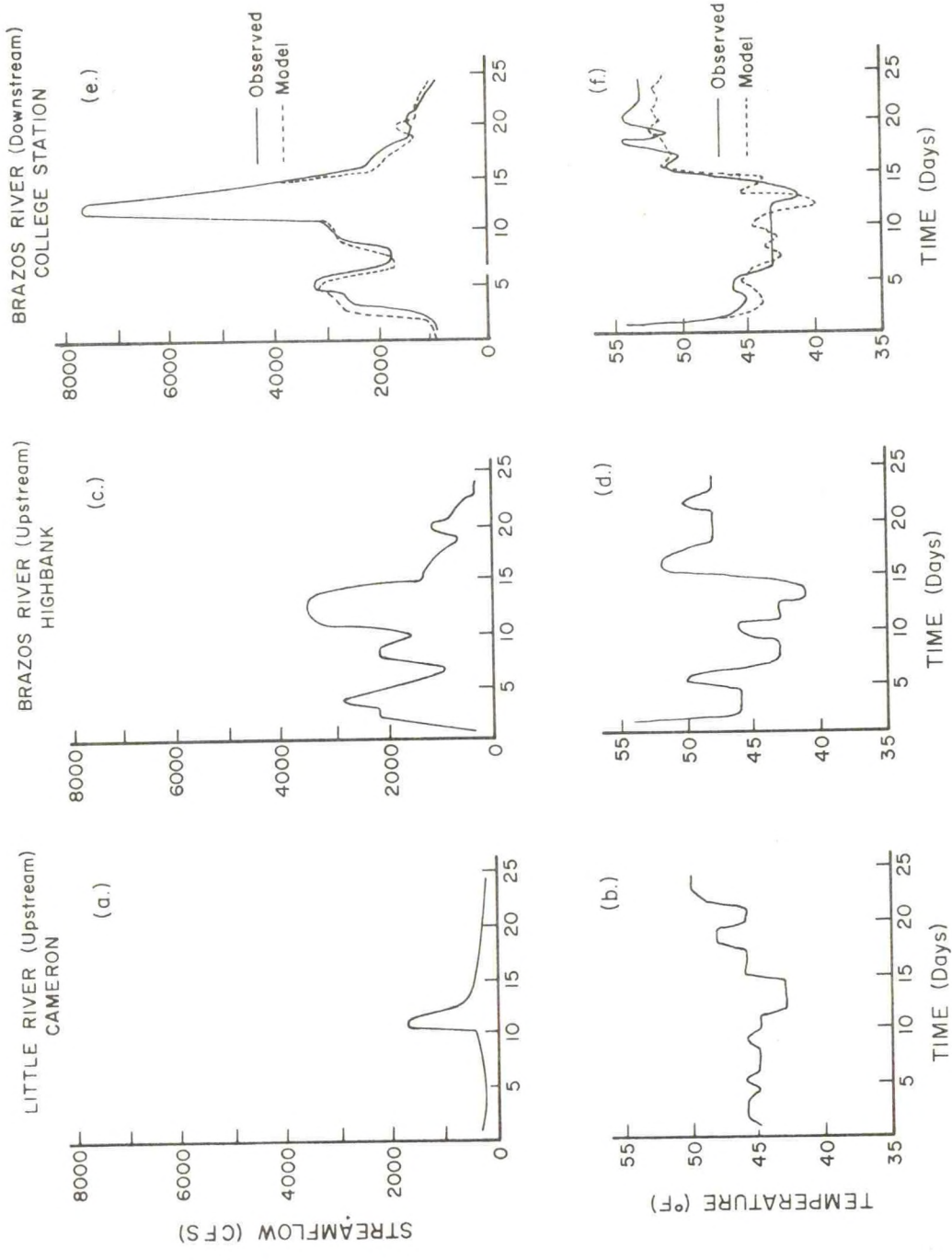


Figure 4.3. Hydrographs and thermographs at upstream and downstream boundaries of Brazos-Little River System including model predictions (December 5-28, 1972).

based on these results since the instrument with which solar radiation⁹⁷ data were observed was known to be out of adjustment (Griffiths, 1975, personal communication). However, because the predicted stream temperature reflected the apparent discrepancies in the solar radiation predictions it was decided to use the observed solar radiation data adjusted for instrument bias (i. e. ITECH=3).

The USGS at Austin, Texas, estimated shading on the Brazos River to be 5% and on the Little River to be 25%. These values were reduced to 0% and 15% respectively for winter conditions.

Heat transfer by evaporation and conduction across the stream surface are directly proportional to the mass transfer coefficient, N (see Equations 3.68 and 3.71). A value of $N = 0.00005 \text{ ins. Hg}^{-1}$ was found to yield reasonable values of evaporation and conduction.

During the storm period the lateral inflow thermograph was considered to be highly dependent on air temperature. Therefore a lateral inflow thermograph (Figure 4.4) was assumed based on the variation in air temperature.

The following factors should be considered when evaluating the adequacy of the simulation results:

- 1) Thermographs used by the USGS are rated by the manufacturer as accurate to within 2°F (Rawson, 1970)
- 2) Observed stream temperatures used in this study were based on instantaneous values selected randomly within 24 hour intervals on the continuous thermograph trace. In contrast, model predictions were for time points spaced twelve hours apart. Therefore, a comparison between a predicted and an observed mean temperature may be a comparison between temperatures with up to 24 hours difference in occurrence.

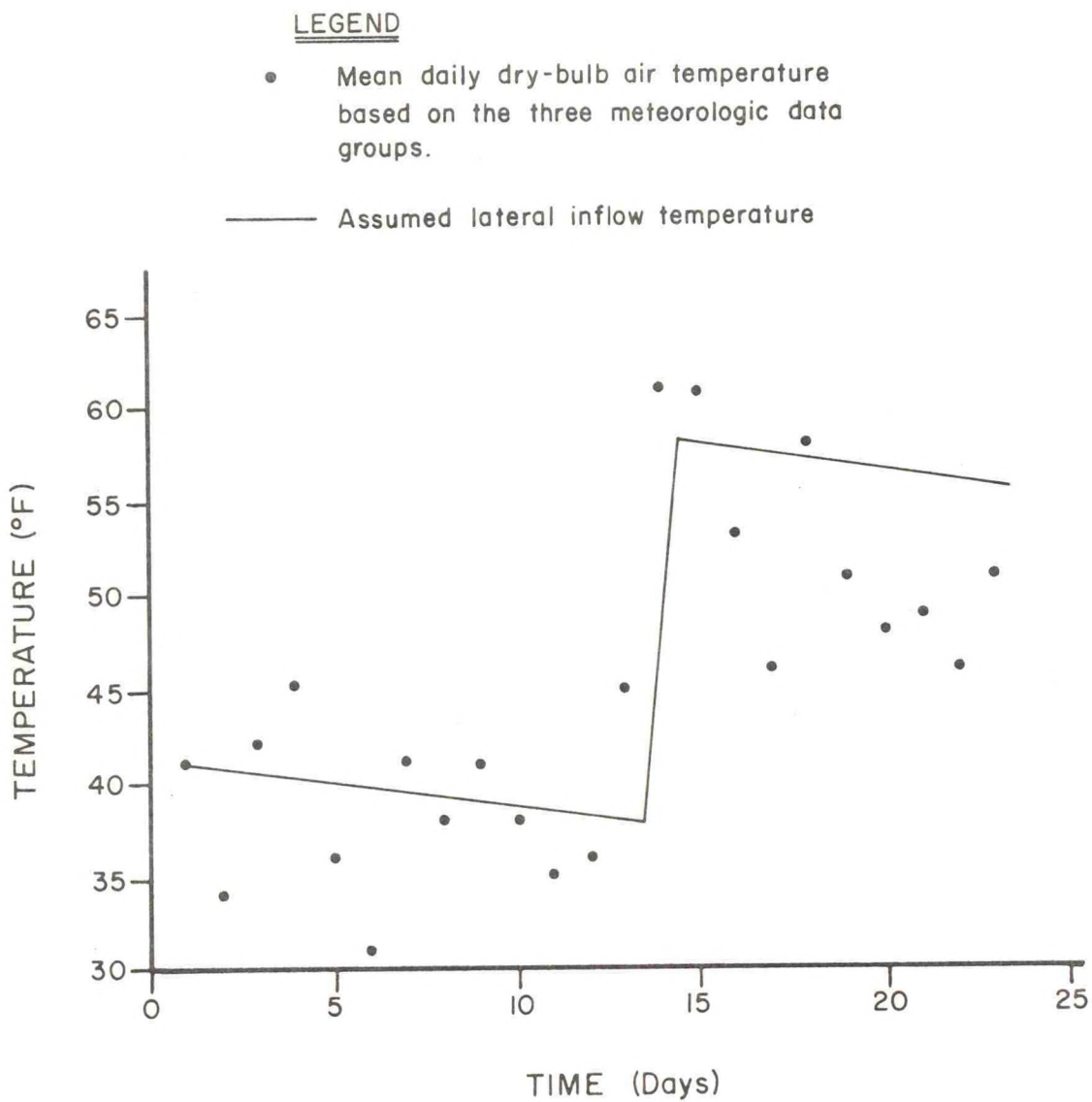


Figure 4.4. Assumed lateral inflow thermograph.

3) DSTEMP predicts stream temperatures that are average for the stream cross-section, whereas observed stream temperatures are measured at single locations in the cross-section.

4) The observed thermograph in this study was located 9 miles downstream of the point at which stream temperatures were predicted.

Upstream boundary conditions for stream temperature are shown in Figures 4.3b and d. Observed and predicted thermographs at the downstream boundary are represented by Figure 4.3f. A trough in the predicted thermograph coincides with the peak of the hydrograph (Figure 4.3e) at day 12 but misses the trough in the observed thermograph by one day. Predicted temperatures after day 16 are generally low compared with observed temperatures. Overall agreement is quite good with a correlation coefficient, R^2 , equal to 84%.

CHAPTER 5

CONCLUSIONS AND FURTHER WORK

A Dynamic Stream Temperature Model (DSTEMP) has been developed and tested. The current version of DSTEMP is suitable for application in temperature simulations on small streams or large river systems. This versatility is enhanced by the capability of substituting different methods of calculating heat transfer components, or suppressing components that are unimportant on certain streams. Thus process studies such as those performed on Spawn Creek (Comer, et al., 1975) can be handled by DSTEMP. Also, the simulation of stream temperature regimes in large river systems is facilitated by the meteorologic data group concept described in Chapter 3 and Appendix A. Dynamic aspects of the flow and temperature representation by DNR T-DSTEMP are essential to obtain predictions of critical, but transient, stream temperature conditions that may endanger aquatic environment.

Although the current versions of DNR T-DSTEMP offer a very flexible tool for dynamic simulation of streamflow - stream temperature there remain some areas of further work. Suggestions for further work on DNR T and DSTEMP are listed below:

DNRT

- 1) Distinguish between surface and subsurface lateral inflow contributions. Could be achieved through linkage to a two-dimensional hydrology model.
- 2) Add capability for handling point loads.

DSTEMP

- 1) Generate thermographs for lateral inflows by linkage with a two-dimensional hydrology -- water temperature model. At present the estimation of these thermographs is mainly the result of intuitive guesses and trial-and-error matching of observed and predicted thermographs after the nonadvective heat transfer processes are calibrated.
- 2) Add frictional heat flux and those components of heat exchange omitted from the current version.
- 3) Add to the solar radiation subroutine, for ITECH = 1, an algorithm for calculating the variation of snow albedo with the age of snowpack adjacent to the stream.
- 4) Input cloud type and vary coefficients in Equation 3.54 as described by Anderson (1954).
- 5) Allow for computational time intervals different to the data time interval by interpolating between input data (does not apply to meteorologic data).
- 6) Calculate statistics to summarize model performances based on observed stream temperatures.
- 7) Plot predicted and observed stream temperatures to assist in model calibration or evaluation of model predictions.
- 8) Include an ice formation and melt algorithm to extend the temperature range over which the model is applicable.
- 9) Add a reservoir algorithm.
- 10) Complete the option to use S. I. units.

11) Apply estimation theory to the real time stream temperature forecasting problem. This will facilitate "updating" as data become available. It could also be used to provide "best" estimates of lateral inflow temperatures.

It is considered that the addition of the above features to the DNR T-DSTEMP models will further enhance their practical value to river forecasters.

REFERENCES

- Albertson, O. L., B. A. Tichenor, J. Seaders, and F. J. Burgess. 1974. Stream temperature prediction by digital computer techniques. Department of Civil Engineering, Oregon State University, Corvallis, Oregon. 27 p.
- Amein, M., and C. S. Fang. 1970. Implicit flood routing in natural channels. *Journal of the Hydraulics Division, ASCE*, 96(HY 12): 2481-2500. December.
- Anderson, E. R. 1954. Energy-budget studies, water loss investigations: Lake Hefner studies. SCS Professional Paper 269.
- Bolsenga, S. T. 1964. Daily suns of global radiation for cloudless skies. Technical Report No. 160. U.S. Army Material Command, Cold Regions Research and Engineering Laboratory, Hanover, New Hampshire. November.
- Bowen, I. S. 1926. The ratio of heat losses by conduction and by evaporation from any water surface. *Physical Review*, 27:779-787. July.
- Bowles, D. S., J. P. Riley, and G. B. Shih. 1975. An application of the Utah State University Watershed Simulation Model to the Entiat Experimental Watershed, Washington State. Final report to Pacific Northwest Forest and Range Experiment Station, United States Forest Service.
- Brown, G. W. 1969. Predicting temperature in small streams. *Water Resources Research* 5:68-75.
- Brown, G. W. 1970. Predicting the effect of clearcutting on stream temperature. *J. Soil and Water Conserv.* 25:11-13.
- Brown, G. W. 1972. An improved temperature prediction model for small streams. Oregon State University, Water Resources Research Institute, WRRI-16.
- Burt, W. V. 1958. Heat budget terms for Middle Snake River Reservoirs. Technical Report No. 6, Reference 58-7. School of Science, Oregon State College, Corvallis, Oregon. December.

- Buttner. 1953. Linke's Meteorologisches Taschenbuch, Volume 2. Geest and Portig K. G., Leipzig.
- Comer, L. E., D. S. Bowles, and W. J. Grenney. 1975. Field investigations and mathematical model for heat transfer processes in the bed of a small stream. Utah Water Research Laboratory, College of Engineering, Utah State University, Logan, Utah 84322. 103 p.
- Dailey, J. E., and D. R. F. Harleman. 1972. Numerical model for the prediction of transient water quality in estuary networks. Ralph M. Parsons Laboratory for Water Resources and Hydrodynamics, Report No. 158, Department of Civil Engineering, M.I.T. October.
- Dake, J. M. K., and D. R. F. Harleman. 1969. Thermal stratification in lakes: analytical and laboratory studies. Water Resources Research 5(2):484-495. April.
- Dingman, S. L., and A. Assur. 1967. The effect of thermal pollution on river--ice conditions--Part 1. United States Army Cold Regions Research and Engineering Laboratory, Hanover, N.H. December.
- Edinger, J. E., D. W. Duttweiler, and J. C. Geyer. 1968. The response of water temperatures to meteorological conditions. Water Resources Research, 4(5):1137-1143. October.
- Edinger, J. E., and J. C. Geyer. 1965. Heat exchange in the environment. EEI Publication No. 65-902, Edison Electric Institute, New York, New York. 259 p.
- Fischer, H. B. 1973. Longitudinal dispersion and turbulent mixing in open-channel flow. In: Annual review of fluid mechanics. Annual Reviews Inc., Palo Alto, California. p. 59-78.
- Fread, D. L. 1973. Technique for implicit dynamic routing in rivers with tributaries. Water Resources Research 9(4):918-926. August.
- Fread, D. L. 1974. Implicit dynamic routing of floods and surges in the Lower Mississippi. Presented at the American Geophysical Union Spring National Meeting in Washington, D.C. April 8-12. p. 26.

- Harbeck, G. E. 1958. Water loss investigations: Lake Mead Studies. USGS Professional Paper 298.
- Harleman, D. R. F., D. N. Borcard, and T. O. Majarian. 1973. A predictive model for transient temperature distributions in unsteady flows. Ralph M. Parsons Laboratory for Water Resources and Hydrodynamics, Report No. 175, Department of Civil Engineering, M.I.T. November.
- Harper, Martin E. 1972. Development and application of a multi-parametric mathematical model of water quality. Doctor of Philosophy Dissertation, University of Washington.
- Jeppson, R. W. 1975. Prediction of stream temperature and rate of ice formation. Unpublished manuscript.
- Jobson, H. E., and N. Yotsukura. 1973. Mechanics of heat transfer in nonstratified open-channel flows. Chapter 8 in Environmental impact on rivers (River Mechanics Vol. III). Edited by H. W. Shen. Water Resource Publications, Fort Collins, Colorado. 680 p.
- Kimball, H. H. 1927, 1928, 1930. Measurements of solar radiation intensity and determination of its depletion by the atmosphere. Monthly Weather Review, Volumes 55, 56, and 58.
- Kleinschmidt, E. 1935. Handbuch der Meteorologischen Instrumente. Springer, Berlin. p. 201.
- List, R. T. 1963. Smithsonian Meteorologic Tables (6th Edition) Smithsonian Institution, Washington, D.C.
- McKee, J. E., and H. W. Wolf. 1963. Water quality criteria. Second Edition, Sacramento, Calif. 548 p.
- Morse, W. L. 1970. Stream temperature prediction model. Water Resources Research, 6(1):290-302. February.
- Morse, W. L. 1972a. Stream temperature prediction under reduced flow. Proc. ASCE, Journal of Hydraulics Division, 98 (HY6): 1031-1047. June.
- Morse, W. L. 1972b. Stochastic stream temperature model. In Proc. International Symposium on Uncertainties in Hydrologic and Water Resource Systems, Tucson, Arizona. pp. 324-339. Dec. 11-14.

- Novotny, V., and P. A. Krenkel. 1971. Heat transfer in flowing streams. Report No. 7, Department of Environmental and Water Resources Engineering, Vanderbilt University School of Engineering, Nashville, Tennessee. September.
- Pailey, P. P., E. O. Macagno, and J. F. Kennedy. 1974. Winter-regime thermal response of heated streams. *Journal of the Hydraulics Division, Proc. ASCE* 100(HY4):531-550. April.
- Parker, F. L., and P. A. Krenkel. 1969. Engineering aspects of thermal pollution. Vanderbilt University Press. 340 p.
- Pivovarov, A. A. 1973. Thermal conditions in freezing lakes and rivers. The Israeli Program for Scientific Translation. Jerusalem. (Russian edition, 1972). 136 p.
- Pluhowski, E. J. 1970. Urbanization and its effect on the temperature of the streams on Long Island, New York. USGS Professional Paper 627-D. 110 p.
- Raphael, J. M. 1962. Prediction of temperature in rivers and reservoirs. *Journal of the Power Division, ASCE*, 88(PO2):157-181. July.
- Rawson, J. 1970. Reconnaissance of water temperature of selected streams in southeastern Texas. Report 105, Texas Water Development Board. p. 2.
- Roesner, L. A. 1969. Mathematical models for the net heat rate of heat transfer through the air-water interface of a flowing stream. Ph.D. dissertation, University of Washington.
- Texas Water Development Board. 1971. Simulation of water quality in streams and canals. Texas Water Development Board, report 128.
- Timofeyev, M. P., and S. P. Malevskiy-Malevich. 1967. Patterns of thermal regime of the surface layer of water. In *Soviet Hydrology: Selected Papers 1967*. No. 1, 102.
- Sutton, G. O. 1953. *Micrometeorology*. McGraw Hill, New York, New York. 333 p.
- Viskanta, R., and J. S. Toor. 1972. Radiant energy transfer in waters. *Water Resources Research* 8(3):595-608. June.

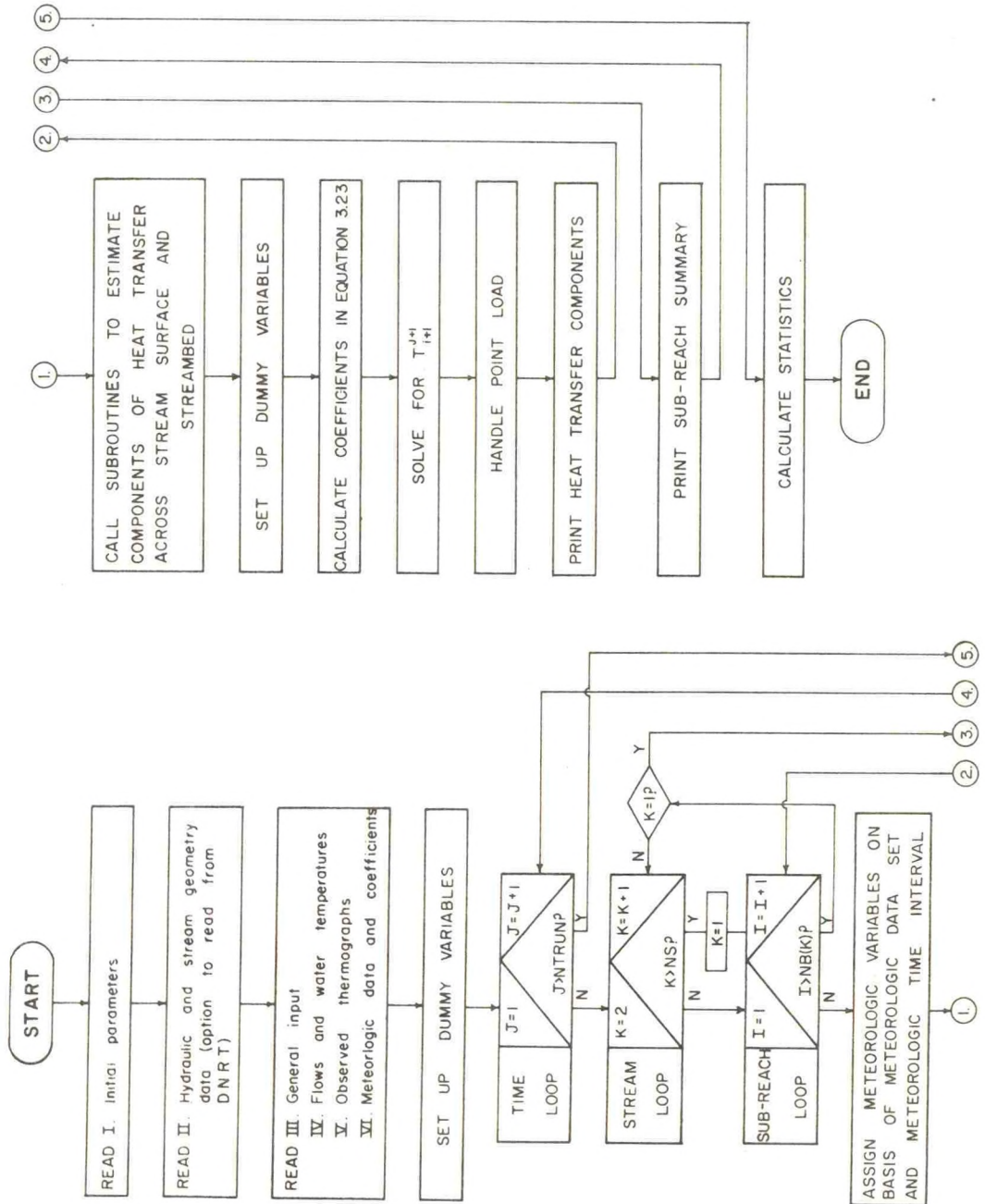
- Vugts, H. F. 1974. Calculation of temperature variations of small mountain streams. *Journal of Hydrology*, 23:267-278.
- Wunderlich, W. O. 1968. The water temperature regime of fully-mixed streams. Report No. 15 (preliminary), Tennessee Valley Authority, Water Resources Research Laboratory, Norris, Tennessee. 64 p.
- Wunderlich, W. O. 1972. Heat and mass transfer between a water surface and the atmosphere. Report No. 14, Tennessee Valley Authority, Water Resources Research Laboratory, Norris, Tennessee. 173 p. April.

APPENDIX A

Users Manual for Dynamic Stream Temperature
Model (DSTEMP)

	Page
1. Overall flow chart	109
2. Input data and decision parameter description	110
3. Program listing	133
4. Examples of input and output	
a. Main stream only	143
b. Main stream and one tributary	146

1. Overall Flowchart of Dynamic Stream Temperature Model(DSTEMP).



2. Input Data and Decision Parameters for Dynamic
Stream Temperature Model (DSTEMP)

110

Notes

1. Input data and decision parameters for DSTEMP are divided into six groups:
 - I Initial parameter
 - II Hydraulic and stream geometry data
 - III General input
 - IV Flows and water temperatures
 - V Observed thermographs
 - VI Meteorologic data and coefficients
2. Computer mnemonics are defined at their first appearance in a read statement. Three important subscripts used are:
 - I Computational point or sub-reach index
 - J Time point or time interval index
 - K Stream index
3. Each 80 column input record contains a 10 character card identification followed by seven 10 character data fields. Each read statement described below commences with a four character code defining the card type. Columns 5 to 10 may be used for identifiers such as the indices I, J, and K, and card sequence numbers.
4. The beginning and end of DO-loops are indicated by notes in parenthesis immediately before and after the first and last read statements respectively, in DO-loops.
5. Units for the variables to be read are included in the following descriptions of input data. The units are those used by the National Weather Service and United States Geological Survey in published data which are likely to be used in applications of DSTEMP. In an attempt to allow for a future option in which S. I. units will be used, coefficients, physical constants and headings in which units are printed are all read as input. When the S. I. option is introduced S. I. equivalents will be substituted for the British units used at present.
6. When all seven data fields are used on the last card read in a read statement, a blank card must be placed after that card. This measure is necessary because of a limitation in the structure of the FORTRAN read formats.
7. "b" indicates a blank column in the card identification field.

I. Initial Parameters

1. "KRRb", "KRR, ITECH, NTRUN, IOSS, IDTCST, IPRT - Format (A10, 6I10)

"KRRb" Card type identification

KRR Number of computer input unit from which output from Dynamic Routing Program (DNRT) is read. Transfer of hydraulic and stream geometry data may be accomplished via disc, magnetic tape, punched cards, etc. Alternatively these data may be directly input to DSTEMP.

ITECH

Technique option for calculating solar radiation.

ITECH = 1 Solar radiation calculated

ITECH = 2 Total daily observed solar radiation distributed between sunrise and sunset in parabolic manner.

ITECH = 3 Solar radiation observed in each time interval DT(J) used directly.

NTRUN

Number of time intervals to be run. $NTRUN \leq NT$ (Use during calibration to execute only first NTRUN time intervals - hence reduce computer time during initial stages of calibration). If $NTRUN = 0$, then NTRUN will be set equal to NT by the program.

IOSS

Input option for reading steady state hydraulic and stream geometry data (Applies to read statements 8 to 13)

IOSS = 0 Unsteady flows

IOSS = 1 Steady state flows (Useful if steady state hydraulic and stream geometry data are input directly to DSTEMP without the use of DNRT)

IDTCST Input option for constant time step (Applies to read statement 3 - if transferring data from DNRT then set IDTCST = 0)
 IDTCST = 0 time step varies - read a value for each time interval DT(J)
 IDTCST = 1 constant time step - read only the constant value of the time step

IPRT Print option for selective output of input data and decision parameters
 IPRT = 0 All input data and decision parameters are printed (Use to provide complete record at first calibration run)
 IPRT = 1 All input data and decision parameters except hydraulic and stream geometry data (read statements 3-13) are printed (Use when removing errors from punched card input)
 IPRT = 2 Only coefficients, parameters, and data that are varied during calibration are printed (Use during calibration)

II. Hydraulic and stream geometry data (transferred from DNRT or directly input to DSTEMP)

2. "NTNS," NT, NS - Format (A10, 2I10)

"NTNS" Card type identification

NT Number of time points (equals number of time intervals plus one)

NS Number of streams

 NS = 1 Main stream only

 NS = 2 Main stream and 1 tributary, etc.

3. "DTbb", (DT(J), J = 1, NTI) - Format (A10, 7 F10.0/(10X, 7 F10.0))

"DTbb" Card type identification

J Time point or time interval index

DT(J) Length of Jth time interval in hours (DT(J) ≤ 24 hours)

NTI Number of time intervals to be read

NTI = NT - 1 if IDTCST = 0

NTI = 1 if IDTCST = 1

4. "NBbb", (NB(K), K = 1, NS) - Format (A10, 7 I10/(10X, 7 I10))

"NBbb" Card type identification

K Stream index

K = 1 main stream

K = 2, NS tributaries

NB(K) Number of computational points on nodes in Kth stream
(NB(K) ≥ 2)

(Omit read statement 5 if NS = 1)

5. "NJUN", (NJUN(K), K = 2, NS) - Format (A10, 7 I10/(10X, 7 I 10))

"NJUN" Card type identification

NJUN(K) Number of main stream reach over which Kth tributary
enters main stream

(Read statements 6 to 12 are read for one stream (K subscript) at a time)

6. "Xbbb", (X(I,K), I = 1, NX) - Format (A10, 7F10.0/(10X, 7F10.0))

"Xbbb" Card type identification

I Computational point or sub-reach index

X(I,K) River distance in miles at the Ith computational point

NX NB(K)

7. "DDXb", (DDX(I,K), I = 1, NX1) - Format (A10, 7F10.0/(10X, 7F10.0))

"DDXb" Card type identification

DDX(I,K) Length in feet of Ith sub-reach between Ith and (I+1)th computational points

NX1 Number of sub-reaches = NB(K) - 1

(Read statements 8 to 12 are read for one time point (J subscript) at a time. A total of NTI time points are read: NTI = NT if IOSS = 0, NTI = 1 if IOSS = 1)

8. "CSAb", (CSA(I,J,K), I = 1, NX) - Format (A10, 7F10.0/(10X, 7F10.0))

"CSAb" Card type identification

CSA(I,J,K) Cross-sectional area of flow in feet² at Ith computational point.

9. "BDbb", (BD(I,J,K), I = 1, NX) - Format (A10, 7F10.0/(10X, 7F10.0))

"BDbb" Card type identification

BD(I,J,K) Top width of flow in feet at Ith computational point

10. "PMbb", (PM(I,J,K), I = 1, NX) - Format (A10, 7F10.0/(10X, 7F10.0))

"PMbb" Card type identification

PM(I,J,K) Wetted perimeter in feet at Ith computational point

11. "QSbb", (QS(I,J,K), I = 1, NX) - Format (A10, 7F10.0/(10X, 7F10.0))

"QSbb" Card type identification

QS(I,J,K) Streamflow rate in cfs at Ith computational point

12. "ELVT", (ELVTN(I,J,K), I = 1, NX) - Format (A10, 7F10.0/(10X, 7F10.0))

"ELVT" Card type identification

ELVTN(I,J,K) Elevation of water surface at Ith computational point in feet above mean sea level.

13. "QLbb", (QL(I,J,K), I = 1, NX1) - Format (A10, 7F10.0/(10X, 7F10.0))

"QLbb" Card type identification

QL(I,J,K) Surface lateral inflow in cfs . ft.⁻¹ over Ith sub-reach
(Include tributary inflow to main stream)

(End of J- and K- loops)

III. General input

14. (TITLE(L), L = 1, 30) - Format (20A4/10A4)

TITLE(L) Title for DSTEMP output tables. Should describe stream location, period of data, and purpose of model run.

15. (UNIT(L), L = 1, 30) - Format (20A4/10A4)

UNIT(L) Part of the heading in an output table. UNIT contains the units of the following variables:

	<u>Columns</u>	<u>British Units</u>	<u>SI Units</u>
X(I, K)	5 to 12	"MILES"	"KM"
CSA(I, J, K)	13 to 21	"FT2"	"M2"
BD(I, J, K)	22 to 28	"FT"	"M"
PM(I, J, K)	29 to 35	"FT"	"M"
DDX(I, J, K)	36 to 44	"FT"	"M"
QL(I, J, K)	48 to 52	"FT2S-1"	"M2S-1"
QG(I, J, K)	53 to 59	"FTS-1"	"MS-1"
QP(I, J, K)	60 to 66	"CFS"	"M3S-1"
QS(I, J, K)	67 to 75	"CFS"	"M3S-1"
TL(I, J, K)	76 to 84	"DF"	"DC"
TG(I, J, K)	85 to 90	"DF"	"DC"
TP(I, J, K)	91 to 96	"DF"	"DC"
Heat Exchange	97 to 102	"BTU"	"KJ"
Stream Temperature	103 to 108	"DF"	"DC"
	109 to 114	"DF"	"DC"
	115 to 120	"DF"	"DC"

16. "IOHT", (IOHTC(IC), IC = 1, 11) - Format (A10, 7I10/(10X, 4I10))

"IOHT"	Card type identification
IC	Component of heat transfer index
IOHTC(IC)	Option to include or exclude different components of heat transfer across the air-water and water-streambed interfaces.

- IC Component
1. Incident and reflected solar radiation at stream surface
 2. Incident and reflected long wave radiation from adjacent vegetation at stream surface¹
 3. Incident and reflected atmospheric radiation at stream surface
 4. Back radiation from stream
 5. Latent heat of vaporization associated with evaporation from stream surface
 6. Conduction across stream surface
 7. Latent heat of fusion associated with snow falling on stream¹
 8. Surface renewal losses¹
 9. Absorption of solar radiation by streambed and streambed conduction
 10. Back radiation from streambed¹

IOHTC(IC) = 0 Exclude ICth component
 IOHTC(IC) = 1 Include ICth component

¹This component is not modeled in the current version of DSTEMP - set IOHTC(IC) = 0

17. "PROP", RHO, CP, FLHV, FLHF, ATREF, ATEN, SURABS, SOLREF - Format (A10, 7F10.0/(10X, F10.0))

"PROP" Card type identification (Properties of water)
 RHO Density of water (62.317 lbs. ft.⁻³)

CP Specific heat of water at constant pressure ($0.9988 \frac{\text{Btu. lbs.}^{-1} \text{ deg. F}^{-1}}$)

FLHV Latent heat of vaporization of water ($1053 \frac{\text{Btu. lbs.}^{-1}}$)

FLHF Latent heat of fusion of water ($143.5 \frac{\text{Btu. lbs.}^{-1}}$)

ATREF Proportion of incident atmospheric radiation reflected at water surface (usually 0.03)

ATEN Bulk extinction coefficient (Equation 3.75) for attenuation of solar radiation transmitted through stream depth (usually $0.015 \frac{\text{ft.}^{-1}}$)

SURABS Proportion of solar radiation entering water surface that is immediately absorbed (usually 0.6)

SOLREF Proportion of incident solar radiation reflected at water surface (can leave blank if ITECH = 1)

18. "TIME", IDAY2, FHR2, FLAT, DTSL, FHSS - Format (A10, I10, 5F10.0)

"TIME" Card type identification

IDAY2 Day number counting from January 1st of DT(1), the first time point

FHR2 Time in hours measured from midnight of DT(1), the first time point. Daylight saving time should be corrected to standard time if ITECH = 1

FLAT Latitude in degrees of streams to be modeled (can leave blank if ITECH \neq 1)

DTSL Time difference between local and standard meridian in hours (can leave blank if ITECH \neq 1) Computed by:

$$DTSL = \frac{e}{15} (\text{LSM} - \text{LLM})$$

in which

LSM longitude of standard meridian in degrees from Greenwich
(75°W for Eastern Standard Time)

LLM longitude of local meridian in degrees from Greenwich

e = - 1 for west longitude

e = + 1 for east longitude

- FHSR Standard time of sunrise in hours measured from midnight (can leave blank if ITECH \neq 2)
- FHSS Standard time of sunset in hours measured from midnight (can leave blank if ITECH \neq 2)
19. "COF1", THETA, SOLCST, DSTDEP, FMTC, SIGMA, BOTREF - Format (A10, 3F10.0, 2E10.5, F10.0)
- "COF1" Card type identification
- THETA Weighting factor for implicit four-point finite difference technique (THETA = 0.55 minimizes the loss of accuracy associated with greater values while avoiding the possibility of a weak or pseudo-instability in many cases of slowly varying transients in large rivers (Fread, 1974); can range 0.5-1.0)
- SOLCST Solar constant (429 Btu. ft. ⁻² hrs. ⁻¹)
- DSTDEP Total dust depletion coefficient of the direct solar beam by scattering and absorption (See Table 3.2)
- FMTC Mass transfer coefficient in ins. Hg. ⁻¹
- SIGMA Stefan - Boltzmann constant (1.74 E-9 Btu. hrs. ⁻¹ ft. ⁻² °R⁴)
- BOTREF Reflectivity of streambed
20. "COF2", (COEF(L), L = 1,4) - Format (A10, 4F10.0)
- "COF2" Card type identification
- COEF(L) Regression coefficients for predicting streambed conduction (Equation 3.76) (leave blank if IOHTC(9) = 0)

IV. Flows and water temperatures

21. "IOQT", IOQGTG, IOTL, NTL, NP - Format (A10, 4F10.0)

"IOQT" Card type identification

IOQGTG Input option for reading QG (I, K) and TG (I, K)
(Applies to read statements 22 and 23)

IOQGTG = 0 do not read QG(I, K) and TG(I, K)
IOQGTG = 1 read QG(I, K) (in cfs. ft.₋₁) and TG(I, K)
IOQGTG = 2 read QG(I, K) (in cfs. ft.₋₁) and TG(I, K)

IOTL Input option for reading TL (I, J, K) (Applies to read statement 24)

IOTL = 0 do not read TL (I, J, K)
IOTL = 1 read TL (I, J, K) and set (TL(I, J, K), I = 2, NX1) =
TL(1, J, K) i.e., the same TL vs. time data ("background
thermograph") is to be used for each sub-reach of the Kth
stream

NTL Number of sub-reaches in which "background thermograph" read in read statement 24 is to be overwritten. This option might be used in sub-reaches where un-modeled tributaries enter and therefore the lateral inflow thermograph would be different to the "background thermograph" read in read statement 24. (Applies to read statement 25)

NP Number of point loads to be read in.

(Read statements 22 and 23 are read if IOQGTG = 1 and are read for one stream (K subscript) at a time)

22. "QGbbs", (QG(I, K), I = 1, NX1) - Format (A10, 7F10.0/(10X, 7F10.0))

"QGbbs" Card type identification

QG(I, K) Steady state value of groundwater exchange between Ith reach and groundwater body. Infiltration to the groundwater body must be given a negative sign and seepage from the groundwater body must be given a positive sign. If units of QG(I, K) are cfs. ft. $\frac{-2}{-1}$ then set IOQGTG = 1 and if cfs. ft. $\frac{-1}{-1}$ then set IOQGTG = 2. (in read statement 21).

23. "TGbb", (TG(I,K), I = 1 NX1) - Format (A10, 7F10.0/(10X, 7F10.0))

"TGbb" Card type identification

TG(I, K) Steady state temperature in deg. F of groundwater below Ith sub-reach and at a depth such that the variation in temperature is negligible over the period for which the model is run. Seeping groundwater is assumed to leave the stream at the temperature of the stream.

(End of K-loop)

(Read statement 24 is read if IOTL = 1 and is read for one stream (K subscript) at a time)

24. "TLBG", (TL(1, J, K), J = 1, NT) - Format (A10, 7F10.0/(10X, 7F10.0))

"TLBG" Card type identification

TL(1, J, K) "Background thermograph" in deg. F for Kth stream. Thermograph is read into first sub-reach position (I=1) in TL array and then the remaining sub-reaches (I=2, NX1) are assigned the same thermograph values.

(End of K-loop)

(Read statement 25 is read NTL times and is omitted if $NTL = 0$)

25. "TLKI", K, I, (TL(I, J, K), J = 1, NT) - Format (A4, 2I2, 2X, 7F10.0/(10X, 7F10.0))

"TLKI" Card type identification

TL(I, J, K) Thermograph in deg. F for Ith sub-reach on the Kth stream. This thermograph replaces the "background thermograph" in the Ith sub-reach on the Kth stream. These thermographs may, for example, be developed from temperatures of unmodeled tributary streams entering the main stream. For sub-reaches in which modeled tributaries enter the main stream, the computed tributary temperatures at the point of confluence will be assigned to TL(I, J, K) by the program. Therefore there is no need to input a thermograph for sub-reaches in which tributaries enter the main stream.

(Read statement 26 is read for one stream (K subscript) at a time)

26. "TSIC", (TS(I, 1, K, L), I = 1, NX) - Format (A10, 7F10.0/(10X, 7F10.0))

"TSIC" Card type identification

TS(I, 1, K, L) Initial condition ($J = 1$) of stream temperature in deg. F for Ith computational point. If $NP \geq 0$ then TS(I, 1, K, L) is read consecutively for $L = 1$ and $L = 2$. The purpose of the subscript L in the TS array is to store two values of stream temperature at computational points where point loads enter the stream. Because of the assumption of instantaneous and complete mixing at each stream section predicted values of stream temperature will jump at the location of a point load. $L = 1$ indexes stream temperature immediately downstream (after point load) of the computational point and $L = 2$ indexes the stream temperature immediately upstream (before point load) of the computational point. At computational points where point loads do not enter the stream, the stream temperatures indexed under $L = 1$ and $L = 2$ are identical. If $NP = 0$ then only $L = 1$ values are read.

(End of K-loop)

(Read statement 27 is read for one stream (K subscript) at a time)

27. "TSUS", (TS(1,J,K,1), J = 1, NT) - Format (A10, 7F10.0/(10X, 7F10.0))

"TSUS" Card type identification

TS(1,J,K,1) Upstream (I = 1) boundary condition for stream temperature in deg.F

(End of K-loop)

(Read statements 28 and 29 are read NP times and are omitted if NP = 0)

28. "QPbb", K,I, (QP(I,J,K), J = 1, NT) - Format (A4, 2I2, 2X, 7F10.0/(10X, 7F10.0))

"QPbb" Card type identification

QP(I,J,K) Flowrate in cfs of point load entering stream at Ith computational point on Kth stream. At present point loads are not accounted for in the Dynamic Routing Program (DNRT). Therefore to maintain a mass balance, point loads in DSTEMP should have a flowrate that is not significant when compared with the streamflow rate. Point loads that are significant thermally and in terms of flow should be treated as lateral inflow over a short sub-reach and input through DNRT.

29. "TPbb", K,I, (TP(I,J,K), J = 1, NT) - Format (A4, 2I2, 2X, 7F10.0/(10X, 7F10.0))

"TPbb" Card type identification

TP(I,J,K) Thermograph in deg.F for point load entering stream at Ith computational point on Kth stream

V. Observed thermographs

30. "NOTb", NOT - Format (A10, I10)

"NOTb" Card type identification

NOT Number of computational points for which observed thermographs are to be input

(Read statement 31 is read NOT times and is omitted if NOT = 0)

31. "TSOb", K,I, (TSO(INOT,J), J = 1,NT) - Format (A4, 2I2, 2X, 7F10.0/(10X, 7F10.0))

"TSOb" Card type identification

INOT Index for observed thermographs (INOT = 1, NOT). The index INOT is stored in array INOTN(I,K).

TSO(INOT, J) INOTth observed thermograph in deg.F

VI. Meteorologic data and coefficients

32. "AAbb", (AA (IC), IC = 1, 11) - Format (A10, 7F10.0/(10X, 4F10.0))

"AAbb" Card type identification

AA(IC) Coefficients in the empirical expression (Equation 3.64) for the atmospheric radiation factor β . Standard values are:
(0.740, 0.750, 0.760, 0.771, 0.783, 0.793, 0.800, 0.810, 0.825, 0.845, 0.866)

33. "BBbb", (BB(IC), IC = 1, 11) - Format (A10, 7F10.0/(10X, 4F10.0))

"BBbb" Card type identification

BB(IC) Coefficients in the empirical expression (Equation 3.64) for the atmospheric radiation factor β . Standard values are:
(0.150, 0.150, 0.150, 0.143, 0.138, 0.137, 0.135, 0.130, 0.120, 0.105, 0.090)

34. "TEbb", (TE(IE), IE = 1, 3) - Format (A10, 3F10.0)
- "TEbb" Card type identification
- TE(IE) Temperatures in deg.F that divides the linear approximations to the empirical expression (Equation 3.69) for saturation vapor pressure. Standard values: (50, 68, 86)
35. "ES1b", (ES1(IE), IE = 1, 4) - Format (A10, 4F10.0)
- "ES1b" Card type identification
- ES1(IE) Coefficients in the empirical expression (Equation 3.69) for saturation vapor pressure. Standard values: (-0.138, -0.548, -1.440, -3.133) in.Hg.
36. "ES2b", (ES2(IE), IE = 1, 4) - Format (A10, 4F10.0)
- "ES2b" Card type identification
- ES2(IE) Coefficients in the empirical expression (Equation 3.69) for saturation vapor pressure. Standard values: (0.0098, 0.0180, 0.0312, 0.0509) (in.Hg.) (deg.F)
- (Read statements 37 to 40 are read for one stream (K subscript) at a time)
(Omit read statements 37 to 39 if ITECH \neq 1)
37. "ALSR", (ALSR (I, K), I = 1, NX1) - Format (A10, 7F10.0/(10X, 7F10.0))
- "ALSR" Card type identification
- ALSR(I, K) Solar altitude in degrees for Ith sub-reach at sunrise. For flat, unobstructed horizon ALSR(I, K) = 0 deg.

38. "ALSS", (ALSS(I, K), I = 1, NX1) - Format (A10, 7F10.0/(10X, 7F10.0))

"ALSS" Card type identification

ALSS(I, K) Solar altitude in degrees for Ith sub-reach at sunset. For flat, unobstructed horizon $ALSS(I, K) = 0$ deg.

39. "GRDR", (GRDRF(I, K), I = 1, NX1) - Format (A10, 7F10.0/(10X, 7F10.0))

"GRDR" Card type identification

GRDRF(I, K) Albedo of ground surface adjacent to stream (see Table 3.3)

40. "SHAD", (SHADE(I, K), I = 1, NX1) - Format (A10, 7F10.0/(10X, 7F10.0))

"SHAD" Card type identification

SHADE(I, K) Fraction of sky shaded from the stream surface by vegetation or other obstructions excluding cloud cover in Ith sub-reach. Shading is expressed as a decimal fraction; for example, 25% shading should be input as 0.25. Figure A1 may be useful when estimating the amount of shading.

(End of K-loop)

41. "NGbb", NG, IMDT - Format (A10, 2I10)

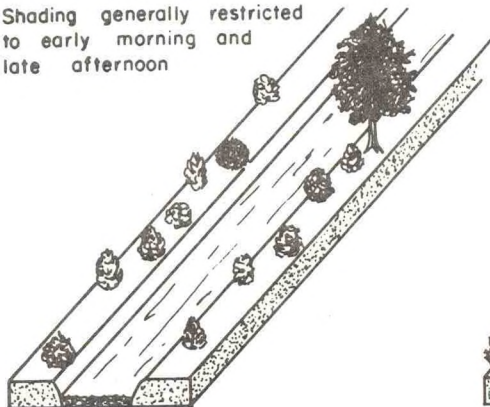
"NGbb" Card type identification

NG

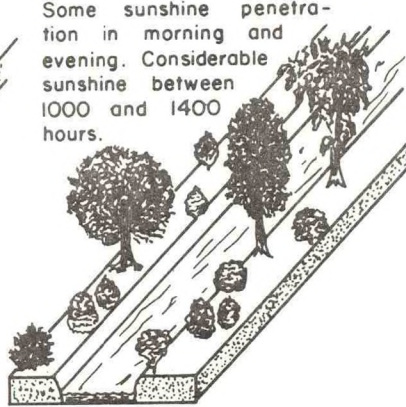
Number of sets of observed meteorologic data to be read. A meteorologic data set is a complete set of data for all the meteorologic variables required in DSTEMP. Several meteorologic groups may be used for modeling a stream system. Each set of meteorologic data is applied to a different group of sub-reaches for which the observed data is considered representative. Several types of data are required for each meteorologic data set. For applications in which National Weather Service meteorologic data are used some data types, such as air temperature, are available at many more locations than other variables. In these

SHADE FACTOR 0-0.25

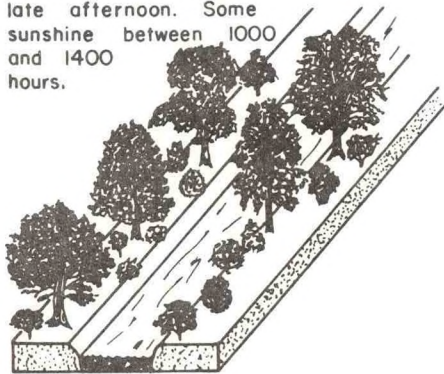
Shading generally restricted to early morning and late afternoon

**SHADE FACTOR 0.25-0.50**

Some sunshine penetration in morning and evening. Considerable sunshine between 1000 and 1400 hours.

**SHADE FACTOR 0.50-0.75**

Very little sunshine penetration in morning or late afternoon. Some sunshine between 1000 and 1400 hours.

**SHADE FACTOR 0.75-1.0**

Very little sunshine penetration even at midday.



Figure A.1. Aid to estimating shade factor (after Pluhowski, 1970).

cases the same values of the less available variables, such as wind velocity and atmospheric pressure, may be reused in several meteorologic data sets in which air temperature is the only variable that changes from data set to data set. The decision on the number of meteorologic data sets to be used will depend on the relative location of meteorologic stations and the study reaches, and also on meteorologic variability.

IMDT Ratio of number of computational time intervals (NT-1) to the number of meteorologic time intervals. For example: if the computational time interval is 3 hours and meteorologic data is available at daily intervals then $IMDT = 24/3 = 8$ (See Figure 3.1). In this example meteorologic data for the first meteorologic time interval will be reused for each of the first 8 computational time intervals. Meteorologic data from the second meteorologic time interval will be reused for each of the computational time intervals 9 to 16 and so on. IMDT should be set to 1 the computational time interval is variable. (Applies to read statements 44 to 53).

42. "IObb" IOQE, IOQR, IOTR, IORH, IOATPR, IOICL - Format (A10, 6I10)
- "IObb" Card type identification
- IOQE Input option for reading QE(IG, JM). (Applies to read statement 44)
- IOQE = 0 do not read QE(IG, JM)
- IOQE = 1 read QE(IG, JM)
- IOQR Input option for reading QR(IG, JM). (Applies to read statement 45)
- IOQR = 0 do not read QR(IG, JM)
- IOQR = 1 read QR(IG, JM)
- IOTR Input option for reading TR(IG, JM). (Applies to read statement 46)
- IOTR = 0 do not read TR(IG, JM). In this case TR(IG, JM) is set equal to TA(IG, JM) by the program

IOIR = 1 read TR(IG, JM)

IOIRH Input option for reading TD(IG, JM). (Applies to read statement 48)

IOIRH = 0 Dew point temperatures read into TD(IG, JM)

IOIRH = 1 Relative humidities read into TD(IG, JM) and
converted to dew point temperatures by the program.

IOATPR Input option for reading ATPR(IG, JM). (Applies to read statement 49)

IOATPR = 0 do not read ATPR(IG, JM). In this case ATPR(IG, JM)
is estimated on the basis of elevation above mean sea level.

IOATPR = 1 read ATPR(IG, JM)

IOICL Input option for reading ICL(IG, JM). (Applies to read statement 52)

IOICL = 0 do not read ICL(IG, JM). In this case ICL(IG, JM) is set
equal to ICS(IG, JM) by the program

IOICL = 1 read ICL(IG, JM)

(Read statement 43 is read for one stream (K subscript) at a time)

43. "NRGb", (NRG(I, K), I = 1, NX1) - Format (A10, 7I10/(10X, 7I10))

"NRGb" Card type identification

NRG(I, K) Number of the meteorologic data set to be used in the Ith sub-reach.
The selection of the data set for the Ith reach should be based on the
representativeness of the selected data set to the meteorologic conditions
in the Ith sub-reach

(End K-loop)

(Read statements 44 to 53 and read for one meteorologic data set (IG subscript) at a time - total of NG sets)

(Omit read statement 44 if IOQE = 0)

44. "QEbb", (QE(IG, JM), JM = 1, NTM) - Format (A10, 7F10.0/(10X, 7F10.0))

"QEbb" Card type identification

IG Meteorologic data set index

JM Meteorologic time intervals index

NTM Number of time intervals for which meteorologic data is to be read, where

$$NTM = (NT-1)/IMDT$$

QE(IG, JM) Evaporation in inches per computational time interval for the IGth meteorologic data set.

(Omit read statement 45 if IOQR = 0)

45. "QRbb", (QR(IG, JM), JM = 1, NTM) - Format (A10, 7F10.0/(10X, 7F10.0))

"QRbb" Card type identification

QR(IG, JM) Precipitation in inches per computational time interval for the IGth meteorologic data set

(Omit read statement 46 if IOTR = 0)

46. "TRbb", (TR(IG, JM), JM = 1, NTM) - Format (A10, 7F10.0/(10X, 7F10.0))

"TRbb" Card type identification

TR(IG, JM) Wet - bulb temperature (used as rainfall temperature) in deg. F averaged over the computational time interval for the IGth meteorologic data set.

47. "TAbb", (TA(IG, JM), JM = 1, NTM) - Format (A10, 7F10.0/(10X, 7F10.0))
- "TAbb" Card type identification
- TA(IG, JM) Dry - bulb temperature in deg. F averaged over the computational time interval for the IGth meteorologic data set.
48. "TDRH", (TD(IG, JM), JM = 1, NTM) - Format (A10, 7F10.0/(10X, 7F10.0))
- "TDRH" Card type identification
- TD(IG, JM) If IORH = 0 then TD(IG, JM) is dew point temperature in deg. F averaged over the computational time interval for the IGth meteorologic data set.
- If IORH = 1 then TD(IG, JM) is relative humidity as a percentage averaged over the computational time interval for the IGth meteorologic data set.
- (Omit read statement 49 if IOATPR = 0)
49. "ATPR", (ATPR(IG, JM), JM = 1, NTM) - Format (A10, 7F10.0/(10X, 7F10.0))
- "ATPR" Card type identification
- ATPR(IG, JM) Atmospheric pressure in inches Hg. averaged over the computational time interval for the IGth meteorologic data set.
50. "WDVE", (WDVEL(IG, JM), JM = 1, NTM) - Format (A10, 7F10.0/(10X, 7F10.0))
- "WDVE" Card type identification
- WDVEL(IG, JM) Wind speed in miles per hour averaged over the computational time interval for the IGth meteorologic data set.

51. "ICSb", (ICS(IG, JM), JM = 1, NTM) - Format (A10, 7I10/(10X, 7I10))

"ICSb" Card type identification

ICS(IG, JM) Cloud cover in an integer number of tenths of cover averaged over the computational time interval for the IGth meteorologic data set. If the meteorologic time interval is 24 hours then ICS(IG, JM) is the average cloud cover between sunrise and sunset.

(Omit read statement 52 if IOICL = 0)

52. "ICLb", (ICL(IG, JM), JM = 1, NTM) - Format (A10, 7I10/(10X, 7I10))

"ICLb" Card type identification

ICL(IG, JM) Cloud cover in an integer number of tenths of cover averaged over the computational time interval for the IGth meteorologic data set. If the meteorologic time interval is 24 hours then ICL(IG, JM) is the average cloud cover over the 24 hour period.

(Omit read statement 53 if ITECH = 1)

53. "DYSL", (DYSL(IG, JM), JM = 1, NTM) - Format (A10, 7F10.0/(10X, 7F10.0))

"DYSL" Card type identification

DYSL(IG, JM) If ITECH = 2 then DYSL(IG, JM) is total incident solar radiation observed between sunset and sunrise in Btu. ft.⁻² day⁻¹. If the meteorologic time interval is not equal to 24 hours then repeat the value of total incident solar radiation for all meteorologic time intervals contained in the 24 hour period.

If ITECH = 3 then DYSL(IG, JM) is total incident solar radiation observed over the computational time interval in Btu. ft.⁻²DT(J)⁻¹.

(End of IG-loop)

3. Program listing.

```

FILE 5-IINPUT
FILE 6-OUTPUT
FILE 8-KIND=PACK, TITLE='NOAOUT', MAXRECSIZE=80, BLOCKSIZE=720,
-UNITS=CHARACTERS, AREASIZE=20, AREAS=1000, SAVEFACTOR=999)
C *****
C ***** DYNAMIC STREAM TEMPERATURE MODEL (DSTEMP) *****
C *****
C DAVID S BOWLES, UTAH WATER RESEARCH LABORATORY, LOGAN, UTAH 84322
DOUBLE PRECISION ACOD
COMMON/GEOM/MB(2), NJUN(2), DD(14,2), CSA(14, 300,2),
  BOK(14, 300,2), PK(14, 300,2), FLAT, ELVTNC(14, 300,2), ELV,
  ALSR(14,2), ALSS(14,2), ALSRR, ALSRS, GRDRF(14,2),
  SHADE(14, 2), DPAV
COMMON/TIME/DYTC(300), TIME(300), IDAY(300), DYSL, DTHR, FHR1, FHR2,
  IDAY1, IDAY2, FHSR, FHSS
COMMON/FLOW/BS(14, 300,2), QL(14, 300,2), BGR(14,2), OP(14, 300,2),
  OR(3, 300), PCE(3, 300), BRR, OEE, OLP(2), QLM(2), GGP, GGM,
  GEL(14,2)
COMMON/MET/PCSS(14, 300), CCS(2), CC(4,2), HWVEL(3, 300),
  RW, FLAV, PMT, SORCS, OS, TRP(3, 300), ATREF, SIGM,
  DVS(13, 300), DAYSQL, ATEM, ROTREF, SUBRS, S, DLREF,
  AK(11), RB(11), TFC(1), ES(4), CTD(14, 300,2)
COMMON/TEMP/TSL(14, 300,2), TSM(2, 300), IJNDN(14,2), IJG(11,4,2),
  TIL(14, 300,2), TGL(14,2), TRC(3, 300), TRR, TPC(14, 300,2),
  TAC(3, 300), TDC(3, 300), T SAV, TOD, TAA
COMMON/STAT/
COMMON/GENL/JUNIT(30), Jp, K, IG, PI, PI2, DTOR, KM,
  ET, IOHTCC(10), ITECH, COEF(6), D31
500 FORMAT(10,7F10,2)/(10X,7F10,0)
501 FORMAT(20, A10,7F10,2)/(10X,7F10,4)
502 FORMAT(40,7I10P(10,7I10))
503 FORMAT(10, A10,7I10/(10, 10X,7I10))
504 FORMAT(A6,2I2,2X,7F10,0)/(10X,7F10,0)
505 FORMAT(A6,4I4,2I2,2X,7F10,0)/(10X,7F10,0)
506 FORMAT(A16,1I6,6F10,0)/(10X,7F10,0)
507 FORMAT(10, A10,1I6,6F10,0)/(10X,7F10,0)
508 FORMAT(A16,3F10,0,2E10,5,2F10,0)
509 FORMAT(10, A10,3F10,3,2E10,5,2F10,0)
510 FORMAT(10, A10,3F10,3,2E10,5,2F10,0)
511 FORMAT(20, A10,4)
512 FORMAT(10, A10,4)
513 FORMAT(10, A10,4)
514 FORMAT(10, A10,4)
515 FORMAT(10, A10,4)
516 FORMAT(10, A10,4)
517 FORMAT(10, A10,4)
518 FORMAT(10, A10,4)
519 FORMAT(10, A10,4)
520 FORMAT(10, A10,4)
521 FORMAT(10, A10,4)
522 FORMAT(10, A10,4)
523 FORMAT(10, A10,4)
524 FORMAT(10, A10,4)
525 FORMAT(10, A10,4)
526 FORMAT(10, A10,4)
527 FORMAT(10, A10,4)
528 FORMAT(10, A10,4)
529 FORMAT(10, A10,4)
530 FORMAT(10, A10,4)
531 FORMAT(10, A10,4)
532 FORMAT(10, A10,4)
C *** INITIALISE
K=5
K=6
PI=3.141592654
PI2=2*PI
DTOR=57.29577951
WRITE(K,512)
READ(K,502)ACOD,KRR,ITECH,MTROM,IOSS,IOICST,IPRT
WRITE(K,503)ACOD,KRR,ITECH,MTROM,IOSS,IOICST,IPRT
C *****
C *** READ OUTPUT FROM NOAA FLOOD ROUTING PROGRAM *****
C READ(KRR,502)ACOD,MT,NS
WRITE(K,503)ACOD,MT,NS
MTI=MT-1
IF(MTRUN)MTI2,10,5
IF(MTRUN)5,10
5 NTRUN=MT
10 IF(DTCST)23,23,15
15 READ(KRR,500)ACOD,DTCL
IF(IPRT,1,0)WRITE(K,501)ACOD,DTCL(1)
DO 20 J=2,MT1
  DT(J)=DT(1)
20 CONTINUE
GOTO 23
23 IF(IPRT,0,503)ACOD,DT(J),J=1,MT1
IF(IPRT,0,0)WRITE(K,501)ACOD,DT(J),J=1,MT1
25 READ(KRR,502)ACOD,4*MB(K),K=1,NS)
IF(IPRT,0,0)WRITE(K,503)ACOD,4*MB(K),K=1,NS)
IF(MS-1)28,28,26
26 READ(KRR,502)ACOD,(NJUN(K),K=2,NS)
IF(IPRT,0,0)WRITE(K,503)ACOD,(NJUN(K),K=2,NS)
C READ STREAM-BY-STREAM
DC,NO,X=L,NS
NXX=NR(K)
WRITE(K,500)ACOD,(X,L),J=1,NXX)
IF(IPRT,1,0)WRITE(K,501)ACOD,(X,L),J=1,NXX)

```

3. Program listing (continued).

```

29 READ(KR+500)ACD*(DXX(I,K),I=1,NX1)
   IF(IPRT-EO,0)WRITE(KM+501)ACD*(DXX(I,K),I=1,NX1)
   NII=NT
   IF(I0SS)30,30,29
30 NII=1
   DO 35 J=1,NTI
   READ(KR+500)ACD*(CSA(I,J,K),I=1,NX1)
   IF(IPRT-EO,0)WRITE(KM+501)ACD*(CSA(I,J,K),I=1,NX1)
   READ(KR+500)ACD*(BDC(I,J,K),I=1,NX1)
   IF(IPRT-EO,0)WRITE(KM+501)ACD*(BDC(I,J,K),I=1,NX1)
   READ(KR+500)ACD*(PM(I,J,K),I=1,NX1)
   IF(IPRT-EO,0)WRITE(KM+501)ACD*(PM(I,J,K),I=1,NX1)
   READ(KR+500)ACD*(PH(I,J,K),I=1,NX1)
   IF(IPRT-EO,0)WRITE(KM+501)ACD*(PH(I,J,K),I=1,NX1)
   READ(KR+500)ACD*(QSC(I,J,K),I=1,NX1)
   IF(IPRT-EO,0)WRITE(KM+501)ACD*(QSC(I,J,K),I=1,NX1)
   READ(KR+500)ACD*(CELVN(I,J,K),I=1,NX1)
   IF(IPRT-EO,0)WRITE(KM+501)ACD*(CELVN(I,J,K),I=1,NX1)
   READ(KR+500)ACD*(COL(I,J,K),I=1,NX1)
   IF(IPRT-EO,0)WRITE(KM+501)ACD*(COL(I,J,K),I=1,NX1)
   CONTINUE
35 IF(I0SS)40,40,36
36 DO 38 J=2,NT
   DO 37 I=1,NX
   CSA(I,J,K)=CSA(I-1,K)
   BDC(I,J,K)=BDC(I-1,K)
   PM(I,J,K)=PM(I-1,K)
   PH(I,J,K)=PH(I-1,K)
   QSC(I,J,K)=QSC(I-1,K)
   CELVN(I,J,K)=CELVN(I-1,K)
   COL(I,J,K)=COL(I-1,K)
   CONTINUE
37 CONTINUE
38 CONTINUE
40 CONTINUE
C *****
C ON MAIN STREAM - REMOVE WHEN CORRECT QL READ FROM DNRT
DO 42 K=2,MS
  I=NJUN(K)
  I1=I-1
  NX=NB(K)
  DO 41 J=1,NT
    QL(I,J,1)=QL(I1,J,1)+65(NX-J,K)/DXX(I,1)
  CONTINUE
41 CONTINUE
42 CONTINUE
C *****
C READ INPUT DATA TO DYNAMIC STREAM TEMPERATURE MODEL (DSTEMP) *****
C *****
C #1 GENERAL
C # HEADINGS
  READ(KR+515)(TITLE(L),L=1,30)
  WRITE(KM+532)(TITLE(L),L=1,30)
  READ(KR+515)(UNIT(L),L=1,30)
  IF(IPRT-LI,2)WRITE(KM+532)(UNIT(L),L=1,30)
C # HEAT TRANSFER COMPONENT CALCULATION OPTIONS
  READ(KR+502)ACD*(ICHTC(IC),IC=1,10)
  IF(IPRT-LI,2)WRITE(KM+503)ACD*(ICHTC(IC),IC=1,10)
C # PROPERTIES OF WATER
  READ(KR+500)ACD*(RHO,CP,FLHW,FLHF,ATREF,ATEN,SURABS,SOLREF)
  IF(IPRT-LI,2)WRITE(KM+501)ACD*(RHO,CP,FLHW,FLHF,ATREF,ATEN,SURABS,SOLREF)
C # TIME FACTORS
  READ(KR+506)ACD*(IDAY2,FHR2,FLAT,DTSL,FMSR,FHSS)
  IF(IPRT-LI,2)WRITE(KM+507)ACD*(IDAY2,FHR2,FLAT,DTSL,FMSR,FHSS)
  FLAT=FLAT/DTOR
C # WEIGHTING FACTOR FOR IMPLICIT FOUR-POINT FINITE DIFFERENCE METHOD

```


3. Program listing (continued).

```

87 DO 90 IP=1,NP
  READKR=500)ACD0,K,I,(QPI,J,K),J=1,NT)
  IF(IPRT-LT-2)WRITE(KM=500)ACD0,K,I,(QPI,J,K),J=1,NT)
  READKR=500)ACD0,K,I,(PPI,J,K),J=1,NT)
  IF(IPRT-LT-2)WRITE(KM=500)ACD0,K,I,(PPI,J,K),J=1,NT)
  CONTINUE
C *3 OBSERVE THERMOGRAPHS
  READKR=500)ACD0,MOT
  IF(IPRT-LT-2)WRITE(KM=500)ACD0,MOT
  IF(MOT)I02=I02-92
  DO 100 I02=1,N02
  READKR=500)ACD0,K,I,(TSO(I02),J),J=1,NT)
  IF(IPRT-LT-2)WRITE(KM=500)ACD0,K,I,(TSO(I02),J),J=1,NT)
  IMOT(K)=IMOT
CONTINUE
C *4 METEOROLOGIC
C * MET COEFFICIENTS
  READKR=500)ACD0,(CAKIC),IC=1,11)
  READKR=500)ACD0,(CBKIC),IC=1,11)
  IF(IPRT-LT-2)WRITE(KM=500)ACD0,(CAKIC),IC=1,11)
  IF(IPRT-LT-2)WRITE(KM=500)ACD0,(CBKIC),IC=1,11)
  READKR=500)ACD0,(CEKIE),IE=1,3)
  IF(IPRT-LT-2)WRITE(KM=500)ACD0,(CEKIE),IE=1,3)
  READKR=500)ACD0,(CESIE),IE=1,4)
  IF(IPRT-LT-2)WRITE(KM=500)ACD0,(CESIE),IE=1,4)
  READKR=500)ACD0,(CESIE),IE=1,4)
  IF(IPRT-LT-2)WRITE(KM=500)ACD0,(CESIE),IE=1,4)
  READ STREAM=BY-STREAM
  DO 110 K=1,NS
  NX=M8(K)
  NXI=NX-1
  IF(ITECH=2)I04=I04+108,108
  READKR=500)ACD0,(ALSIR,I,K),I=1,NXI)
  IF(IPRT-LT-2)WRITE(KM=500)ACD0,(ALSIR,I,K),I=1,NXI)
  READKR=500)ACD0,(ALSIC,I,K),I=1,NXI)
  IF(IPRT-LT-2)WRITE(KM=500)ACD0,(ALSIC,I,K),I=1,NXI)
  DO 105 I=1,NX
  ALSR(I,K)=ALSR(I,K)/DTR
  ALSX(I,K)=ALSX(I,K)/BTOR
CONTINUE
105 READKR=500)ACD0,(GRBRF,I,K),I=1,NXI)
  IF(IPRT-LT-2)WRITE(KM=500)ACD0,(GRBRF,I,K),I=1,NXI)
  READKR=500)ACD0,(SHADE,I,K),I=1,NXI)
  IF(IPRT-LT-2)WRITE(KM=500)ACD0,(SHADE,I,K),I=1,NXI)
CONTINUE
C * READ MET GROUP ASSIGNMENTS FOR SUB-REACHES AND MET INPUT OPTIONS
  READKR=502)ACD0,NG,IMDT
  IF(IPRT-LT-2)WRITE(KM=502)ACD0,NG,IMDT
  READKR=502)ACD0,I08,I08B,I08R,I08M,I08P,I08T
  IF(IPRT-LT-2)WRITE(KM=502)ACD0,I08,I08B,I08R,I08M,I08P,I08T
  IF(I08=1)I117=I117-112
  DO 115 K=1,NS
  NXI=M8(K)-1
  READKR=502)ACD0,(NRG(I,K),I=1,NXI)
  IF(IPRT-LT-2)WRITE(KM=502)ACD0,(NRG(I,K),I=1,NXI)
CONTINUE
115 GOTO 120
117 NXI=M8(K)-1
  DO 119 K=1,NS
  MRG(I,K)=1
  DO 118 I=1,NXI
  MRG(I,K)=1
CONTINUE
118 CONTINUE
119 CONTINUE
C READ MET DATA GROUP=BY-GROUP
120 MTM=NTI/IMDT
  DO 140 IG=1,NG
  IF(I08E=1)I23=I23+122
  READKR=500)ACD0,(QEGIG,JM),JM=1,NTM)
  IF(IPRT-LT-2)WRITE(KM=500)ACD0,(QEGIG,JM),JM=1,NTM)
  IF(I08R=1)I30=I30+130+126
  READKR=500)ACD0,(CORIG,JM),JM=1,NTM)
  IF(IPRT-LT-2)WRITE(KM=500)ACD0,(CORIG,JM),JM=1,NTM)
  IF(I08S=1)I36=I36+132+131
  READKR=500)ACD0,(FRIIG,JM),JM=1,NTM)
  IF(IPRT-LT-2)WRITE(KM=500)ACD0,(FRIIG,JM),JM=1,NTM)
  READKR=500)ACD0,(FACIG,JM),JM=1,NTM)
  IF(IPRT-LT-2)WRITE(KM=500)ACD0,(FACIG,JM),JM=1,NTM)
  READKR=500)ACD0,(TACIG,JM),JM=1,NTM)
  IF(IPRT-LT-2)WRITE(KM=500)ACD0,(TACIG,JM),JM=1,NTM)
  IF(IPRT-LT-2)WRITE(KM=500)ACD0,(TDKIG,JM),JM=1,NTM)
  CALCULATE DENOTEMPERATURE IP RELATIVE HUMIDITY READ IN TD
  IF(I08M=1)I35=I35+133
  IF(I08N=1)I34=I34+134
  TAN=TAN(IG,JM)
  DUM=(ALOG10(TO(IG,JM))-2.)/Z.5*(TAN-32.)/(TAN+395-14)
  TO(IG,JM)=627-14*(DUM/(1-DUM))+32.
CONTINUE
134 IF(I08PR=1)I36=I36+135
  READKR=500)ACD0,(ATPRIG,JM),JM=1,NTM)
  IF(IPRT-LT-2)WRITE(KM=500)ACD0,(ATPRIG,JM),JM=1,NTM)
  READKR=500)ACD0,(WVVELIG,JM),JM=1,NTM)
  IF(IPRT-LT-2)WRITE(KM=500)ACD0,(WVVELIG,JM),JM=1,NTM)
  READKR=502)ACD0,(ICSGIG,JM),JM=1,NTM)
  IF(IPRT-LT-2)WRITE(KM=502)ACD0,(ICSGIG,JM),JM=1,NTM)
  IF(I08L=1)I38=I38+137
  READKR=502)ACD0,(ICLIG,JM),JM=1,NTM)
  IF(IPRT-LT-2)WRITE(KM=502)ACD0,(ICLIG,JM),JM=1,NTM)
  IF(ITECH=2)I40=I40+139,139
  NTM1=NTM
  GOTO 1396
1393 NTM1=NT1
1396 READKR=500)ACD0,(COYSLCIG,JM),JM=1,NTM1)
  IF(IPRT-LT-2)WRITE(KM=500)ACD0,(COYSLCIG,JM),JM=1,NTM1)
  CONTINUE
140 C ** SET UP DUMMY VARIABLES
  D1=1-THETA
  D2=THETA/2.
  D3=01/2.
  D4=1./(RHO*CP)
  TIME(I)=FHR2
  IDAY(I)=IDAY2
C *****
C ** TIME LOOP *
C *****
  JM=1
  J=1
  GOTO 301
141 J1=J+1
  D5=1./(7200.*DT(J))
  D5A=2.*D5
  FHR1=FHR2
  IF(FHR1-24.)I43=I43+142,143
  FHR1=0.
  IDAY1=IDAY2+1
  GOTO 144
143 IDAY1=IDAY2
  DTHR=DT(J)
144

```

3. Program listing (continued).

```

FMR2=FHR1+DTHR
IF(FHR2-24.)147,147,145
145 FMR2=FHR2-24.
    IDAY2=IDAY1+1
    GOT0 148
147 IDAY2=IDAY1
148 IF(IDAY2-365)152,152,150
150 IDAY2=IDAY2-365
152 TIME(J1)=FMR2
IDAY(J1)=IDAY2
WRITE(NK,526)(TITLE(L),L=1,30),J,DT(J),IDAY(J),TIME(J),IDAY(J1),
* TIME(J1)
* WRITE(NK,527)
C *****
C ** STREAM LOOP (TRIBUTARIES FIRST, MAIN STREAM LAST) *
C *****
IF(NS-1)165,165,158
158 K=2
KI=K-1
GOT0 170
C ** SAVE TRIBUTARY STREAM TEMPERATURE FOR INFLOW TO MAIN STREAM
160 I=JUNCK)
K=K+1
TL(I,J1)=I+T
KI=K-1
KI=K-1
IF(K=NS)170,170,165
165 KI=1
KI=0
WRITE(NK,521)
WRITE(NK,524)KI
172 N1=NSK*1
C *****
C ** SUB-REACH LOOP *
C *****
DO 295 I=1, NK1
I1=I+1
C ** CALCULATE NON-ADVECTIVE HEAT FLUXES AS LINEAR FUNCTIONS OF STREAM
C TEMPERATURE
C ** DETERMINE MET GROUP FOR SUB-REACH
IG=MRG(I,K)
C ** DETERMINE MET DATA TIME STEP
JMDT=JMDT+JM
176 IF(I=JMDT)180,180,178
178 JM=JM+1
C ** SET UP DUMMY VARIABLES
C ** CONVERT OE & OR IN INCHES TO FEET/SEC
180 QEE=OE(IG,JM)/(43200.*DT(J))
QOR=OR(IG,JM)/(43200.*DT(J))
TAA=TAC(IG,JM)
IF(IOTR)185,185,190
185 TRB=TRC(IG,JM)
GOT0 191
190 TRR=TAA
191 TDD=TD(IG,JM)
ELV=02*(ELVTM(I,J,K)+ELVTM(I1,J,K))+03*(ELVTM(I,J,K)
* ELVTM(I1,J,K))
C ** ESTIMATE ATMOSPHERIC PRESSURE BASED ON ELEVATION IF ATPR NOT READ
IF(IDATPR)192,192,193
192 ATPR=29.92--0008*ELV
GOT0 194
193 ATPRR=ATPR(IG,JM)
194 MDWELL=MDVEL(IG,JM)
ICSS=ICSC(IG,JM)
ICLL=ICLC(IG,JM)
IF(IOCCL)195,196,196
195 ICLL=ICSC(IG,JM)
196 DAYSOL=DYSL(IG,J)
TIJ=TS(I,J,K)
TIJ=TS(I,J,K)
TIIJ=TS(I1,J,K)
TSAV=(TIIJ+TIJ+TIIJ+TIIJ)/3.
017=80C(I,J,K)
018=80C(I1,J,K)
019=80C(I,J,K)
020=80C(I1,J,K)
027=CSA(I,J,K)
028=CSA(I1,J,K)
029=CSA(I,J,K)
030=CSA(I1,J,K)
031=TK(I,K)
DPAY=02*(D27/D17+D28/D18)+03*(D29/D19+D30/D20)
06=DMETA/DX
D7=DL/DX
ALSS=ALSS(I,K)
ALSSR=ALSS(I,K)
C * OBTAIN NET NON-ADVECTIVE HEAT TRANSFER ACTING OVER SURFACE AREA
C ** IN LINEAR FORM
C1=0.
C2=0.
IF(IOMTC(1))198,198,197
197 ALL=OLC(1)CC(1)+CC(2)+CC(2)
198 IF(IOMTC(2))200,200,199
199 ALL=EG(2)CC(1)+CC(5)+CC(5)
200 IF(IOMTC(3))202,202,201
201 CALL ATRAD(C1(6)+C1(7)+CC(6)+CC(7))
202 IF(IOMTC(4))204,204,203
203 CALL BARRAD(C1(8)+CC(8))
204 IF(IOMTC(5))206,206,205
205 CALL EVLHW(C1(9)+CC(9))
206 IF(IOMTC(6))208,208,207
207 CALL CONO(C1(10)+CC(10))
208 IF(IOMTC(7))210,210,209
209 CALL SMLHF(C1(11)+CC(11))
210 IF(IOMTC(8))212,212,211
211 CALL SURLR(C1(12)+CC(12))
212 IF(IOMTC(9))214,214,213
213 CALL BEDSR(C1(13)+CC(13))
214 DO 215 IC=1,13
C1=C1+CC(1C)
C2=C2+CC(2C)
215 CONTINUE
C1=C1+D5A
C2=C2+D5A
C * OBTAIN NET HEAT TRANSFER ACTING OVER STREAM BED AND BANK *
C ** LINEAR FORM
C3=0.
C4=0.
IF(IOMTC(10))218,218,217
217 CALL BEDRO(C1(1)+CC(1))
218 IF(IOMTC(9))220,220,219
219 CALL BEDCOM(C1(2)+CC(2))
220 DO 221 IC=1,2
C3=C3+CC(3C)
C4=C4+CC(4C)

```


3. Program listing (continued).

```

221 CONTINUE
C3=C3+D5A
C ** SET UP DUMMY VARIABLES
D8=D8+CI
D9=D9+C2
D11=D11+C3
D21=PM(I,J,K)
D22=PM(I,J,K)
D23=PM(I,J,K)
D24=PM(I,J,K)
C * SEPARATE +VE & -VE VALUES OF OG & OL
OG=O-
OL=O+
OG6=OG(I,K)
OL6=OL(I,K)
IF(L0GT=4)235,223,222
222 OG6=OG6/CD2,OL6=OL6/CD2*(023+024)
06(I,K)=OG6
06(I,K)=OL6
C IF BED CONDUCTION MODELED, THEN STREAM TEMPERATURE IS USED FOR
C TEMPERATURE OF GROUNDWATER ENTERING STREAM, BECAUSE HEATING OF
C GROUNDWATER IS INCLUDED IN BED CONDUCTION, OTHERWISE USE
C TG AS INPUT FOR TEMPERATURE AT WHICH GROUNDWATER ENTERS STREAM
223 IF(L0MTC(9))224,224,228
224 IF(OG6)228,235,230
228 OG=OG6
230 GOTD 235
230 OG=OG6
235 DO 260 JJ=J,J1
II=JJ-J+1
OLP(II)=O-
OLM(II)=O+
OLL=OLL(I,J,K)
IF(OLL)245,260,250
245 OLM(II)=OLL
GOTD 260
250 OLP(II)=OLL
260 CONTINUE
D12=D10+OGP*031
D13=D11+OGM
D14=D9+GEE
D15=OLM(2)
D16=OLM(1)
D25=OS(I1,J1,K)
D26=D8+RRR*IRR
C ** CALCULATE COEFFICIENTS
A=D5+027-D6+QSKI,J1,K)-D2*(C014+017+D13+021+D15)
B=D5+028+06+D25-D2*(C014+018+013+022+015)
C=D5+029+07+QSKI,J,K)-D3*(C014+D14+D10+D13+023+016)
D=D5+030+07+QSKI,J,K)+D3*(C014+D20+D13+024+016)
E=D2*(C026*(017+018)+012*(C021+D22)+2*OLP(1)+OLL(I,J,K))
F=D3*(D26*(019+D20)+D12*(C023+D24)+2*OLP(1)+OLL(I,J,K))
C ** SOLVE FOR STREAM TEMPERATURE AT I+1,J+1
TSAV=4C+TIJD+TIIJVE-A*TIJJ/B
TSAV=D2*(TIJ+TIIJ)+D3*(TIJ+TIIJ)
C STORE GROUNDWATER TEMPERATURE IN TGI FOR PRINTING
IF(OG6)261,262,261
261 TGI(I,K)=TSAV
GOTD 266
262 IF(OG6)264,264,263
263 TGI(I,K)=D31
GOTD 266
264 TGI(I,K)=O-

```

```

C ** POINT LOAD
266 OPL=OP(I1,J1,K)
IF(OPL)270,270,264
268 T=C025*(TIIJ+OPL)*P(I1,J1,1)/(C025*OPL)
GOTD 275
270 T=TIIJ1
275 TSC(I1,J1,K,1)=T
TSC(I1,J1,K,2)=TIIJ1
C *****
C ** PRINT HEAT TRANSFER COMPONENTS *
C *****
DO 285 IC=1,13
CCL(IC)=CC1(IC)+CC2(IC)*TSAV
CONTINUE
285 DO 290 IC=1,2
CC3(IC)=CC3(IC)+CC4(IC)*TSAV
CONTINUE
290 C1=(C1+C2+TSAV)/D5A-CC1(13)
C3=(C3+C4+TSAV)/D5A+CC1(13)
C7OT(I1,J1,K)=C3+C3
CCL(3)=CC1(1)+CC1(2)+CC1(13)
WRITE(KM,520)(CCL(IC),IC=1,13),(CC3(IC),IC=1,2),C1,C3
CCL(3)=O-
295 CONTINUE
C END OF SUB-REACH LOOP
C IFK=I1297,297,160
END OF STREAM LOOP
297 WRITE(KM,529)
C *****
C ** PRINT SUB-REACH SUMMARY *
C *****
J=J+1
C ** TITLES
301 IF(J-1)302,302,303
GOTD 304
302 WRITE(KM,525)(TITLE(L),L=1,30),J,IDAY(J),TIME(J)
303 WRITE(KM,530)(TITLE(L),L=1,30),J,IDAY(J),TIME(J)
304 WRITE(KM,520)(UNIT(L),L=1,30)
DO 305 K=1,NS
KI=K-1
KPK=1
IF(K1)325,325,305
C ** TRIBUTARIES
305 WRITE(KM,524)KI
NXL=N8(K)-1
DO 315 I=1,NXL
LL=1
IF(OP(I,J,K))309,308,307
307 LL=2
308 WRITE(KM,523)(I,K,CCL(I,J,K),OC(I,J,K),DDXL(K),
* OLL(I,J,K),OLM(I,K),OPL(I,J,K),MRC(I,K),
* TSC(I1,J1,K,1),TSC(I1,J1,K,2),
* TSC(I1,J1,K,2)+L=1,LL)
INOT=INOT+(I,K)
IF(INOT)315,315,310
310 WRITE(KM,531)TSC(INOT,J)
315 CONTINUE
I=N8(K)
LL=1

```

3. Program listing (continued).

```

319 IF(OP(I,J,K)) 320=320+319
320 LL=2
321 WRITE(NH,522)I,X(I,K),CSA(I,J,K),BD(I,J,K),PM(I,J,K),OP(I,J,K)
C **
322 IF(INOT)325=325+322
323 WRITE(KH,531)TSOK(IMOT,J)
324 ** MAIN STREAM
325 WRITE(KH,521)
330 IF(NS-K)330=330+335
331 GOTO 340
335 MX1=NUN(KP)
340 IF(K1)345=345+350
345 MX0=1
350 GOTO 360
355 MX0=NUN(K)*1
360 DO 380 I=MX0-MX1
LL=1
IF(OP(I,J))363=363+362
362 LL=2
363 WRITE(KH,523)I,X(I,K),CSA(I,J,K),BD(I,J,K),PM(I,J,K),DDX(I,K)
C **
364 IF(INOT)380=380+365
365 WRITE(KH,531)TSOK(IMOT,J)
380 CONTINUE
385 CONTINUE
I=MX1+1
LL=1
IF(OP(I,J))395=395+390
390 LL=2
395 WRITE(KH,522)I,X(I,K),CSA(I,J,K),BD(I,J,K),PM(I,J,K),OP(I,J,K)
C **
397 IF(INOT)399=399+397
398 WRITE(KH,531)TSOK(IMOT,J)
399 WRITE(KH,529)
C **
400 IF(J-MTRUM)414=450+450
C **
401 END OF TIME LOOP
C **
402 *****
403 ** CALCULATE STATISTICS *
404 *****
450 STOP
END

```

```

SUBROUTINE SOLRAD(C1,C12,C21,C22)
C *****
C *** TO ESTIMATE INCIDENT AND REFLECTED SOLAR RADIATION OVER TIME *****
C INTERVAL DT(J)
C *****
COMMON/GEOM/ABC2,NJUNK2,XCI(4,2),DOK(14,2),CSA(14,300,2),
BD(14,300,2),PK(14,300,2),LAT,ELV(K,14,300,2),ELV,
ALSRC(14,2),ALSS(C(14,2)),ALSPR,ALSSS,GRDRF(14,2),
SMADECI(4,2),DPAV)
COMMON/TIME/DTIME(300),IDAY(300),DTSL,DTMR,FHRI,FHR2,
IDAT1-IDAT5,FMSR,FMS5,
COMMON/FLOW/OSK(14,300,2),OLC(14,300,2),OGC(14,2),OP(14,300,2),
GRK3,300,OE(3,300),ERR,OE,OLP(2),OLNK(2),OGP,OGM,
OGI(14,2),
COMMON/METL/MRG(14,300),CC1(13),CC2(13),CC3(13),CC4(2),MDVEL(3,300),
RGS(14,300),TGSS,IGL(3,300),ICLL,MDVELL,ATREF,SIGMA,
RUC,FHM,FMTG,SOLCST,DSDEP,ATPR(3,300),ATPRP,
OYSLC,300,DAYSO,ATEN,BOTREF,SURABS,SOLREF,
AAL(13,88(11)),TEC(3),ESL(4),ES2(4),COT(14,300,2),
COMMON/TEMP/TS(14,300,2),TSOK(2,300),INOTM(14,2),TG(14,2),
TL(14,300,2),TG(14,2),TR(3,300),TPR,TP(14,300,2),
TAL(3,300),TOK(3,300),TSA,TDO,TAA)
COMMON/STAT/
COMMON/GEUL/UNIT(30),TITL(30),I,J,K,IG,PI,PI2,DTOR,KW,
ETP,IDHTCC(10),ITECHM,COEF(6),D31)
C *****
C ** INITIALISE
C11=0,
C12=0,
C21=0,
C22=0,
IF(ITECH=2)5=125-175
C *****
C *** TECHNIQUE 1 - SOLAR RADIATION CALCULATED *
C *****
C ** CALCULATE RELATIVE DISTANCE EARTH - SUN, ANGULAR FRACTION OF
YEAR, AND EQUATION OF TIME
R=1+0.17*cos(.0172142063*(196-IDAY2))
ANFYR=1.72028E-2*(IDAY2-1)
ANFYR2=2.*ANFYR
ET=-.12357*SIN(ANFYR)+.004289*cos(ANFYR)-.153809*SIN(ANFYR2)
ET=DTSL-ET
DELTA=ARCSIN(.07868570945IN(4.995783951+ANFYR*3.342E-2+SIN(ANFYR)
-.153809*SIN(ANFYR2)+.004289*ANFYR)+.479837463E-4*SIN(ANFYR2)-
2-.82743333E-5*cos(ANFYR2))
C ** CALCULATE HOUR ANGLE AND STANDARD TIME OF SUN RISE
ANMSR=(SIN(CALSR))-SIN(FLAT)*SIN(DELTA)/COS(FLAT)+COS(DELTA)
IF(ANMSR)15=20+20
15 ANMSR=PI+ARCCOS(ABS(ANMSR))
GOTO 25
20 ANMSR=PI-ARCCOS(ABS(ANMSR))
FMSR=3.819718634*ANMSR*ET-12,
IF(FHR2-FMSR)20=200+28
C ** CALCULATE HOUR ANGLE AND STANDARD TIME OF SUN SET
ANMS5=(SIN(CALSR5))-SIN(FLAT)*SIN(DELTA)/COS(FLAT)+COS(DELTA)
IF(ANMS5)30=30+35
30 ANMS5=PI-ARCCOS(ABS(ANMS5))
GOTO 40
40 ANMS5=PI+ARCCOS(ABS(ANMS5))
FMS5=3.819718634*ANMS5*ET+12,
IF(FHRI-FMS5)43=200+200

```

3. Program listing (continued).

```

C ** ELIMINATE PARTS OF DT OUTSIDE SUNRISE - SUNSET PERIOD
43 IF(FMHR1-FMSR)45,50,50
45 FM1=FMSR
GOTO 65
50 FM1=FHR1
65 IF(FHR2-FHSS)70,75,75
70 FM2=FHR2
GOTO 80
75 FM2=FMS
C ** CALCULATE PRECIPITABLE WATER CONTENT OF THE ATMOSPHERE
80 PWC=EXP(-.03411+TDD-2-.076239566)
DUM1=C-.465+.34036*PWC)
C ** INTEGRATE SOLAR RADIATION OVER FHI-FH2
AS=SIM(FLAT)*SIN(DELTA)
AC=COS(FLAT)*COS(DELTA)
DUM2=(1.-6-.879166667E-6*ELV)*.5-.256
DUM2=.5*GRDRF(I,K)
DUM3=1.+DSTDEP
DUMA=(1.-.0065*TCSS**2)*(1.-SHADE(I,K))
FM=FH2-FHI
M=FIX(FH)
N=N+1
82 N=N+1
85 IF(N-4)86,87,87
86 N=N
87 DEL=FM/M
DFH1=FHI
DFH2=FHI+DEL/2.
DFH3=FHI+DEL
DO 120 L=1,M
CALL HRANGL(DFH1,DAWH1)
CALL HRANGL(DFH2,DAWH2)
CALL HRANGL(DFH3,DAWH3)
DCL1=SOLEST*(AS+CFH3-DFH1)*3.-81971.8634*AC*(SIN(DAWH3)
- SIN(L-AS)*COS(DAWH2)
+ SIN(L+AS)*COS(DAWH2)
IF(ETAL=0)DUM1=DUM1*.95+.90
90 ALDEG=ATORB*BSI*(SIN(L)
+ RE-18/ALDEG**(.77)
GOTO 180
95 SVAL=8.-
ALDEG=8.-
RE=18/ALDEG.-
C ** CALCULATE OPTICAL AIR MASS
100 OAW=OAWCT/(SIN(ALPHA)+.001465*(ALDEG+.885))*(.1-253)
C ** CALCULATE MEAN TROPOSPHERIC TRANSMISSION COEFFICIENTS
ATC1=EXP(DUM1*.179*.121+RE*(.772+DAWH))
ATC2=EXP(DUM1*.179*.121+RE*(.772+DAWH))
DCL1=DCL1*(ATC2+.5*(DUM1-ATC1))/(.1.-DUM2*(DUM3-ATC1))-DUM4
C11=C11+801
C12=C12-DCL1*RF
DFN1=DFH1+DEL
DFN2=DFH2+DEL
DFN3=DFH3+DEL
120 CONTINUE
GOTO 200

C *****
C ** TECHNIQUE 2 - OBSERVED TOTAL DAILY SOLAR RADIATION DISTRIBUTED *
C ** BETWEEN SUNRISE AND SUNSET *****
C *****

C ** ELIMINATE PARTS OF DT OUTSIDE SUNRISE - SUNSET PERIOD
125 IF(FHR2-FMSR)200,200,130
130 IF(FMHR1-FMSS)135,200,200
135 IF(FMHR1-FMSR)140,145,145
140 FM1=FMSR
GOTO 150
145 FM1=FHR1
150 IF(FHR2-FHSS)155,160,160
155 FM2=FHR2
GOTO 165
160 FM2=FMS
C ** INTEGRATE SOLAR RADIATION OVER FHI-FH2
N=12.+DAYSOL/(FHSS-FMSR)**3
165 XX1=FHI-FMSR
XX2=FH2-FMSR
XX12=XX1*XX1
XX22=XX2*XX2
C11=(M*(FHSS-FMSR))*(XX22-XX12)/4.-M*(XX22-XX2-XX12*(XX11/6.-)
* (1.-SHADE(I,K)))
C12=C11+DAYSOL
GOTO 200

C *****
C ** TECHNIQUE 3 - USE OBSERVED SOLAR RADIATION DATA *
C *****
175 C11=DAYSOL*(1.-SHADE(I,K))
200 RETURN
END

SUBROUTINE HRANGL(F,A)
C ** D CONVERT STANDARD TIME IN HOURS TO HOUR ANGLE *
C ** COMMON/GENL/UMIT(30),ITL(30),I,J,K,LG,PI,PI2,DTORAW,
ET,IJMT(10),ITECH,COEF(6),C31
IFCF=12.)5,5,10
A=(F*12.-ET)*-.2617993878
GOTO 15
10 A=(F-12.-ET)*-.2617993878
15 IF(A)20,35,25
20 A=A*PI2
GOTO 35
25 IF(A-PI)35,35,30
30 A=A-PI2
35 RETURN
END

```


3. Program listing (continued).

```

SUBROUTINE VEGRAD(C14,C15,C24,C25)
RETURN
END

SUBROUTINE ATRAD(C16,C17,C26,C27)
C..... TO ESTIMATE INCIDENT AND REFLECTED ATMOSPHERIC RADIATION OVER *
C TIME INTERVAL DT(J)
C.....
COMMON/GEOM/NBK(2),NJK(2),X(1,2),DDX(1,2),CSA(14,300,2),
BDK(14,300,2),PH(1,2),PH(1,2),FLAT,ELVTM(14,300,2),ELV,
ALSR(14,2),ALSS(1,2),ALSRR,ALSSS,GRDRF(14,2),
SHADE(1,2),DPAV
COMMON/TIME/DT(300),TIME(300),IDAY(300),DTSL,DTHR,FHRL,FHRZ,
IDAY1,IDA2,FHSR,FHSS
COMMON/FLOW/QSC(14,300,2),QL(1,2),Q(1,2),Q(1,2),OP(1,2),OP(1,2),OP(1,2),
GR(3,300),QEL(3,300),QRR,QEE,QLP(2),QLM(2),QGP,QGM,
QG(1,2)
COMMON/METL/NRG(1,2),CCI(1,2),CC2(1,2),CC3(2),CC4(2),MDVEL(3,300),
ICS(3,300),ICSS,ICL(3,300),ICLL,MDVELL,ATREF,SIGMA,
RHO,FLW,FMT,SQLCS,DSDEP,ATPR(3,300),ATPRP,
DYSL(3,300),DAYSOL,ATEN,BOTREF,SURABS,SOLREF,
AAC(1,2),BB(1,2),TEC(3),ESI(4),ES2(4),COT(14,300,2),
COMMON/TEMP/TSC(14,300,2),TSC(2,300),INDTN(14,2),TGL(1,2),
TL(1,300,2),TG(1,2),TR(3,300),TSAV,TDD,TAA
COMMON/STAT/
COMMON/GENL/JUNIT(30),I,J,K,IG,PI,PIZ,DTOR,KM,
ET,IOHTCC(10),ITECH,CDEF(6),DS1
C
C26=0-
C27=0-
ICL1=ICLL*1
EA=EXP(C8.642*T00-6.83)/(C-555.6*T00+219.5)
BETA=AA*ICL1+BB*(ICL1+EA)
C16=BETA*SIGMA*(TAA+459.67)**4*DTHR
C17=-ATREF*C16
RETURN
END

SUBROUTINE BAKRAD(C18,C28)
C..... TO ESTIMATE BACK RADIATION FROM WATER SURFACE OVER TIME *
C INTERVAL DT(J)
C.....
COMMON/GEOM/NBK(2),NJK(2),X(1,2),DDX(1,2),CSA(14,300,2),
BDK(14,300,2),PH(1,2),PH(1,2),FLAT,ELVTM(14,300,2),ELV,
ALSR(14,2),ALSS(1,2),ALSRR,ALSSS,GRDRF(14,2),
SHADE(1,2),DPAV
COMMON/TIME/DT(300),TIME(300),IDAY(300),DTSL,DTHR,FHRL,FHRZ,
IDAY1,IDA2,FHSR,FHSS
COMMON/FLOW/QSC(14,300,2),QL(1,2),Q(1,2),Q(1,2),OP(1,2),OP(1,2),OP(1,2),
GR(3,300),QEL(3,300),QRR,QEE,QLP(2),QLM(2),QGP,QGM,
QG(1,2)
COMMON/METL/NRG(1,2),CCI(1,2),CC2(1,2),CC3(2),CC4(2),MDVEL(3,300),
ICS(3,300),ICSS,ICL(3,300),ICLL,MDVELL,ATREF,SIGMA,
RHO,FLW,FMT,SQLCS,DSDEP,ATPR(3,300),ATPRP,
DYSL(3,300),DAYSOL,ATEN,BOTREF,SURABS,SOLREF,
AAC(1,2),BB(1,2),TEC(3),ESI(4),ES2(4),COT(14,300,2),
COMMON/TEMP/TSC(14,300,2),TSC(2,300),INDTN(14,2),TGL(1,2),
TL(1,300,2),TG(1,2),TR(3,300),TSAV,TDD,TAA
COMMON/STAT/
COMMON/GENL/JUNIT(30),I,J,K,IG,PI,PIZ,DTOR,KM,
ET,IOHTCC(10),ITECH,CDEF(6),DS1
C
C26=0-
C28=-.0815*DTHR
RETURN
C18=-.54-.25*DTHR
C28=-1-.084*DTHR
RETURN
END

SUBROUTINE SMLNF(C11,C21)
RETURN
END

IF(TSAV-68.)10=10+20
C18=-68-27*DTHR
C28=-.0815*DTHR
RETURN
C18=-.54-.25*DTHR
C28=-1-.084*DTHR
RETURN
END
    
```


3. Program listing (continued).

```

SUBROUTINE SURLRL(C112,C212)
RETURN
END

SUBROUTINE EVLHVC19(C29)
C *****
C *** TO ESTIMATE LATEL HEAT OF VAPORISATION SUPPLIED BY STREAM TO ***
C *** EVAPORATING WATER OVER TIME INTERVAL DT(J) ***
C *****
COMMON/GEOM/NBK(2),NJK(2),X(14,2),DDX(14,2),CSA(14,300,2),ELV,
BD(14,300,2),PH(14,300,2),FLAT,ELVTM(14,300,2),ELV,
SHADE(14,2),DPAV
COMMON/TIME/DT(300),TIME(300),IDAY(300),DTSL,DTHR,FHR1,FHR2,
OR(3,300),OE(3,300),ORR,OE,OLP(2),OLMC(2),OGP,OGM,
OGI(14,2)
COMMON/METL/MRG(14,2),CC(13),CC2(13),CC3(2),CC4(2),MDVEL(3,300),
ICS(3,300),ICSS,I(1,3,300),ICLL,MDVELL,ATREF,SIGMA,
RHO,FLHV,FHTC,SOLCST,DSDEP,ATPRC(3,300),ATPRR,
DYSL(3,300),DAYSOL,ATEM,BOTREF,SURABS,SOLREF,
AA(11),BB(11),TEC(3),ESI(4),ESI2(4),CTOT(14,300,2),
TL(14,300,2),IG(14,2),TSC(2,300),FMOTM(14,2),TGI(14,2),
TAC(3,300),TDC(3,300),TSAV,TDD,TAA
COMMON/STAT/
COMMON/GENL/JUMITTC(30),TITLCC(30),I,J,K,IG,PI,PI2,DTOR,KW,
ET,DTMTC(10),ITECH,COEF(6),DS1
C *****
C210=-3.362714687E-4=ATPRR-RHO*FLHV+FHTC*MDVELL-DTHR
C110=-C210*TAA
RETURN
END

SUBROUTINE SURLRL(C112,C212)
RETURN
END

SUBROUTINE EVLHVC19(C29)
C *****
C *** TO ESTIMATE LATEL HEAT OF VAPORISATION SUPPLIED BY STREAM TO ***
C *** EVAPORATING WATER OVER TIME INTERVAL DT(J) ***
C *****
COMMON/GEOM/NBK(2),NJK(2),X(14,2),DDX(14,2),CSA(14,300,2),ELV,
BD(14,300,2),PH(14,300,2),FLAT,ELVTM(14,300,2),ELV,
SHADE(14,2),DPAV
COMMON/TIME/DT(300),TIME(300),IDAY(300),DTSL,DTHR,FHR1,FHR2,
OR(3,300),OE(3,300),ORR,OE,OLP(2),OLMC(2),OGP,OGM,
OGI(14,2)
COMMON/METL/MRG(14,2),CC(13),CC2(13),CC3(2),CC4(2),MDVEL(3,300),
ICS(3,300),ICSS,I(1,3,300),ICLL,MDVELL,ATREF,SIGMA,
RHO,FLHV,FHTC,SOLCST,DSDEP,ATPRC(3,300),ATPRR,
DYSL(3,300),DAYSOL,ATEM,BOTREF,SURABS,SOLREF,
AA(11),BB(11),TEC(3),ESI(4),ESI2(4),CTOT(14,300,2),
TL(14,300,2),IG(14,2),TSC(2,300),FMOTM(14,2),TGI(14,2),
TAC(3,300),TDC(3,300),TSAV,TDD,TAA
COMMON/STAT/
COMMON/GENL/JUMITTC(30),TITLCC(30),I,J,K,IG,PI,PI2,DTOR,KW,
ET,DTMTC(10),ITECH,COEF(6),DS1
C *****
EA=EXP(0.842-TDD-68.3/6.555*6*TDD+219.5)
DUM=RHO*FLHV+FHTC*MDVELL-DTHR
DU TO I=1,3
IF(TSAV=TEC(IE))I5=15*10
CONTINUE
10
15
IE=6
C19=DUM*(ESI(IE)-EA)
C29=-DUM*ESI(IE)
RETURN
END

```

3. Program listing (continued).

```

C *****
C ***** SUBROUTINE BEDSRD(C113,C213)
C ***** TO ESTIMATE SOLAR RADIATION ABSORBED BY STREAM BED OVER TIME *****
C ***** INTERVAL DT(J) *****
C *****
C ***** COMMON/GEOM/ABSC(2),NUN(2),X(14,2),DDX(14,2),CSA(14,300,2),
C ***** BD(14,300,2),PH(14,300,2),FLAT,ELVFN(14,300,2),ELV,
C ***** ALSRC(14,2),ALSSC(14,2),ALSR,ALSS,GRDRF(14,2),
C ***** SHADE(14,2),DPAV
C ***** COMMON/TIME/DT(300),TIME(300),IDAY(300),DTSL,DTHR,FHR1,FHR2,
C ***** IDAT1,IDA2,FHSP,FHSS
C ***** COMMON/FLOW/QSC(14,300,2),QL(14,300,2),QG(14,2),QP(14,300,2),
C ***** QR(3,300),QEC(3,300),QRR,QEE,QLP(2),QLM(2),QGP,QGM,
C ***** QG1(14,2)
C ***** COMMON/METL/MRG(14,2),CC1(13),CC2(13),CC3(2),CC4(2),MDVEL(3,300),
C ***** ICS(3,300),ICSS,ICL(3,300),ICLL,MDVELL,ATREF,SIGMA,
C ***** RHO,FLH,FMTG,SOLCST,DSDEP,ATPR(3,300),ATPRR,
C ***** DTSL(3,300),DAYSQL,ATEN,BOTREF,SURABS,SOLREF,
C ***** AAC(11),BR(11),TEC(1),ESI(4),ES2(4),CTOT(14,300,2),
C ***** COMMON/TEMP/TSC(14,300,2),TSOK(2,300),INOTM(14,2),TGI(14,2),
C ***** TLL(14,300,2),TGC(14,2),TR(3,300),TRR,TP(14,300,2),
C ***** TAC(3,300),TDC(3,300),TSAV,TDD,TA
C ***** COMMON/STAT/
C ***** COMMON/GENL/UNIT(30),TITLE(30),I,J,K,LG,PI,PI2,DYOR,KW,
C ***** ET,IOHTCC(10),ITECH,COEF(6),D31
C *****
C ***** C113=(1-BOTREF)*C1-C2-SURABS*(CC1(1)+CC1(2))*EXP(-ATEN-DPAV)
C ***** C213=0.
C ***** RETURN
C ***** END

```

```

SUBROUTINE BEDBRD(C31,C41)
RETURN
END

```

```

C *****
C ***** SUBROUTINE BEDCON(C32,C42)
C ***** TO ESTIMATE HEAT TRANSFER BY CONDUCTION AT STREAM BED-WATER *****
C ***** INTERFACE OVER TIME INTERVAL DT(J) *****
C *****
C ***** COMMON/GEOM/ABSC(2),NUN(2),X(14,2),DDX(14,2),CSA(14,300,2),
C ***** BD(14,300,2),PH(14,300,2),FLAT,ELVFN(14,300,2),ELV,
C ***** ALSRC(14,2),ALSSC(14,2),ALSR,ALSS,GRDRF(14,2),
C ***** SHADE(14,2),DPAV
C ***** COMMON/TIME/DT(300),TIME(300),IDAY(300),DTSL,DTHR,FHR1,FHR2,
C ***** IDAT1,IDA2,FHSP,FHSS
C ***** COMMON/FLOW/QSC(14,300,2),QL(14,300,2),QG(14,2),QP(14,300,2),
C ***** QR(3,300),QEC(3,300),QRR,QEE,QLP(2),QLM(2),QGP,QGM,
C ***** QG1(14,2)
C ***** COMMON/METL/MRG(14,2),CC1(13),CC2(13),CC3(2),CC4(2),MDVEL(3,300),
C ***** ICS(3,300),ICSS,ICL(3,300),ICLL,MDVELL,ATREF,SIGMA,
C ***** RHO,FLH,FMTG,SOLCST,DSDEP,ATPR(3,300),ATPRR,
C ***** DTSL(3,300),DAYSQL,ATEN,BOTREF,SURABS,SOLREF,
C ***** AAC(11),BR(11),TEC(1),ESI(4),ES2(4),CTOT(14,300,2),
C ***** COMMON/TEMP/TSC(14,300,2),TSOK(2,300),INOTM(14,2),TGI(14,2),
C ***** TLL(14,300,2),TGC(14,2),TR(3,300),TRR,TP(14,300,2),
C ***** TAC(3,300),TDC(3,300),TSAV,TDD,TA
C ***** COMMON/STAT/
C ***** COMMON/GENL/UNIT(30),TITLE(30),I,J,K,LG,PI,PI2,DYOR,KW,
C ***** ET,IOHTCC(10),ITECH,COEF(6),D31
C *****
C ***** C32=(COEF(1)-CC1(13))*COEF(2)/DTHR+COEF(3)*D31+DTHR
C ***** C42=COEF(4)*DTHR
C ***** RETURN
C ***** END

```

4. Examples of input and output (a) main stream only (Spawn Creek, see Comer et al., 1975).

LISTING EF DATA

KRF	NTAS	DI	NI	5	1	1	1	0	ES2	0-0098	0-0120	0-0312	0-0509	0-0000	0-0000	0-0000	0-0000	0-0000	
NIAS	DI	NI	5	1	1	1	0	ES2	0-0098	0-0120	0-0312	0-0509	0-0000	0-0000	0-0000	0-0000	0-0000	0-0000	
NI	DI	NI	5	1	1	1	0	ES2	0-0098	0-0120	0-0312	0-0509	0-0000	0-0000	0-0000	0-0000	0-0000	0-0000	
NI	DI	NI	5	1	1	1	0	ES2	0-0098	0-0120	0-0312	0-0509	0-0000	0-0000	0-0000	0-0000	0-0000	0-0000	
2413-0000	2015-0000	100-0000	3-7500	0-8000	1-2300	1-6500													
3-1700	4-5800	3-2900	3-2100	2240-0000	2240-0000	6-2100													
7-0000	6-5000	4-2000	4-2000	5-5000	9-4000														
8-0000	7-0000	5-2000	5-2000	6-7000	10-0000														
4-3100	4-3700	4-3700	6-3400	6-5000	10-6600														
6463-0000	5275-0000	6127-0000	6120-0000	6035-0000	5950-0000														
3-0000	0-0000	0-0000	0-0000	0-0000	0-0000														
DSTEMP RUN 1 SPAWN CREEK AUGUST 29-30, 1974 DIURNAL **CALCULATION**																			
FOURLY INTERVALS																			
CF	DF	FT2	FT	DF	CF	FT	FT2S-1	FTS-1	CF	CF	CF	CF	CF	CF	CF	CF	CF	CF	CF
10FT	1	1	1	1	1	1	1	1	1	1	1	1	1	1	1	1	1	1	1
PRECIP	1	62-3170	0-9984	1053-0000	143-5000	0-0300	0-0152	0-6000											
TIME	1	13-0000	0-4667	8-2500	18-5000														
COEF 1	241	429-000	0-020-10300E-02	17400E-02	0-3000														
COEF 2	-3573-6000	0-3600	78-6600	-4-9520															
CG	0-0002	0-0002	0-0002	0-0002	0-0002														
IG	48-7000	48-7000	48-7000	48-7000	48-7000														
TL	1 3	50-0000	50-5000	50-5000	49-0000	48-5000	47-0000	47-0000	47-0000	47-0000	47-0000	47-0000	47-0000	47-0000	47-0000	47-0000	47-0000	47-0000	47-0000
TL	1 4	44-0000	44-0000	44-0000	44-0000	44-0000	44-0000	44-0000	44-0000	44-0000	44-0000	44-0000	44-0000	44-0000	44-0000	44-0000	44-0000	44-0000	44-0000
TL	1 5	56-7000	57-2000	57-6000	56-6000	55-4000	53-7000	52-4000	52-4000	52-4000	52-4000	52-4000	52-4000	52-4000	52-4000	52-4000	52-4000	52-4000	52-4000
TS1E11	1	44-8000	47-5000	47-5000	45-6000	44-6000	43-7000	42-8000	42-5000	42-5000	42-5000	42-5000	42-5000	42-5000	42-5000	42-5000	42-5000	42-5000	42-5000
TS1S	1	46-0000	46-0000	46-0000	46-0000	46-0000	46-0000	46-0000	46-0000	46-0000	46-0000	46-0000	46-0000	46-0000	46-0000	46-0000	46-0000	46-0000	46-0000
NOI	2	43-5000	44-5000	44-5000	44-5000	44-5000	44-5000	44-5000	44-5000	44-5000	44-5000	44-5000	44-5000	44-5000	44-5000	44-5000	44-5000	44-5000	44-5000
TS1C1 1 4	46-0000	45-5000	45-5000	45-5000	45-5000	45-5000	45-5000	45-5000	45-5000	45-5000	45-5000	45-5000	45-5000	45-5000	45-5000	45-5000	45-5000	45-5000	45-5000
TS2 1 6	44-0000	44-0000	44-0000	44-0000	44-0000	44-0000	44-0000	44-0000	44-0000	44-0000	44-0000	44-0000	44-0000	44-0000	44-0000	44-0000	44-0000	44-0000	44-0000
AA	1	48-0000	48-0000	48-0000	48-0000	48-0000	48-0000	48-0000	48-0000	48-0000	48-0000	48-0000	48-0000	48-0000	48-0000	48-0000	48-0000	48-0000	48-0000
BB	1	0-1500	0-1500	0-1500	0-1500	0-1500	0-1500	0-1500	0-1500	0-1500	0-1500	0-1500	0-1500	0-1500	0-1500	0-1500	0-1500	0-1500	0-1500
EE	1	0-1300	0-1200	0-1050	0-0900	0-0800	0-0730	0-0600	0-0500	0-0400	0-0300	0-0200	0-0100	0-0000	0-0000	0-0000	0-0000	0-0000	0-0000
ESI	1	50-0000	68-0000	86-0000	104-0000	122-0000	140-0000	158-0000	176-0000	194-0000	212-0000	230-0000	248-0000	266-0000	284-0000	302-0000	320-0000	338-0000	356-0000

DSTEMP RUN 1 SPAWN CREEK AUGUST 29-30, 1974 DIURNAL **CALIBRATION** HOURLY INTERVALS

STREAM TEMPERATURES, ADVECTIVE HEAT SOURCES, AND HYDRAULIC DATA

INITIAL CONDITIONS TIME PT NO 1 DAY 241 HOUR 13.00

COPP PT NO	RIVER DISTANCE	X-SECTN AREA	TOP WIDTH	WETTED PERIM	HYDRAULIC				POINT LOAD	MET STREAM -FLOW	INFLW CP	INFLW TEMPS			HEATEX /FT2	STREAM TEMPS		
					SUB-RCH LENGTH	LATINF*	GRD+TR INFLOW	SO+RCH LENGTH				LATINF*	TRIBINF	TEMP		TEMP	TEMP	DF
		MILES	FT2	FT	FT	FT	FT	FT	FT	CFS	CFS	DF	DF	DF	BTU	DF	DF	DF
MAIN																		
1	0.00	3.17	7.00	8.00	2415.00	0.0000	.0000	0.00	4.01	1	0.00	0.00	0.00	0.00	46.00			
2	0.40	4.58	6.50	7.00	2015.00	0.0000	.0000	0.00	4.37	1	0.00	0.00	0.00	0.00	48.00			
3	0.75	2.39	4.20	5.20	100.00	0.0162	.0000	0.00	4.72	1	50.00	0.00	0.00	0.00	50.00			
4	0.80	3.21	4.20	5.20	2240.00	0.0000	.0000	0.00	6.34	2	56.70	0.00	0.00	0.00	50.00			50.00
5	1.23	3.29	5.50	6.70	2240.00	0.0000	.0000	0.00	8.50	2	56.70	0.00	0.00	0.00	52.00			
6	1.65	6.21	9.40	10.00				0.00	10.66				0.00	54.00			54.00	

DSTEMP RUN 1 SPAWN CREEK AUGUST 29-30, 1974 DIURNAL **CALIBRATION**

HOURLY INTERVALS

COMPONENTS OF HEAT EXCHANGE AT STREAM SURFACE AND BED

TIME INTERVAL NO 1 SIZE DT= 1. HRS (DAY 241 HOUR 13.00 TO DAY 241 HOUR 14.00)

ALL UNITS ARE BTUFT-2 PER DT IN HRS

REACH NO	SOLAR RADIATION			SURFACE COMPONENTS				BED COMPONENTS				TOTALS					
	INCIDT	REFLEC	ABSORP	VEGTN INCIDT	RADTN REFLEC	ATMOS INCIDT	RADTN REFLEC	BACK RADTN	EVAP LHVAP	COND	SNOW LHFLS	SURF RENEW	BEDAB SOLRD	BACK BEDRD	BED COND	SURF EXCHGE	BED EXCHGE
MAIN																	
1	140.	-11.	129.	0.	0.	116.	-3.	-110.	-71.	100.	0.	0.	0.	0.	0.	160.	0.
2	168.	-13.	155.	0.	0.	116.	-3.	-112.	-78.	95.	0.	0.	0.	0.	0.	172.	0.
3	266.	-21.	245.	0.	0.	116.	-3.	-112.	-81.	93.	0.	0.	0.	0.	0.	257.	0.
4	280.	-22.	258.	0.	0.	110.	-3.	-114.	-96.	71.	0.	0.	0.	0.	0.	224.	0.
5	280.	-22.	258.	0.	0.	110.	-3.	-115.	-112.	65.	0.	0.	0.	0.	0.	202.	0.

DSTEMP RUN 1 SPAWN CREEK AUGUST 29-30, 1974 DIURNAL **CALIBRATION**

HOURLY INTERVALS

STREAM TEMPERATURES, ADVECTIVE HEAT SOURCES, AND HYDRAULIC DATA

TIME PT NO 2 DAY 241 HOUR 14.00

COPP PT NO	RIVER DISTANCE	X-SECTN AREA	TOP WIDTH	WETTED PERIM	HYDRAULIC				POINT LOAD	MET STREAM -FLOW	INFLW CP	INFLW TEMPS			HEATEX /FT2	STREAM TEMPS		
					SUB-RCH LENGTH	LATINF*	GRD+TR INFLOW	SO+RCH LENGTH				LATINF*	TRIBINF	TEMP		TEMP	TEMP	DF
		MILES	FT2	FT	FT	FT	FT	FT	FT	CFS	CFS	DF	DF	DF	BTU	DF	DF	DF
MAIN																		
1	0.00	3.17	7.00	8.00	2415.00	0.0000	.0000	0.00	4.01	1	0.00	48.70	0.00	160.	46.00			
2	0.40	4.58	6.50	7.00	2015.00	0.0000	.0000	0.00	4.37	1	0.00	48.70	0.00	172.	49.23			
3	0.75	2.39	4.20	5.20	100.00	0.0162	.0000	0.00	4.72	1	50.50	48.70	0.00	257.	49.66			
4	0.80	3.21	4.20	5.20	2240.00	0.0000	.0000	0.00	6.34	2	57.20	48.70	0.00	224.	50.23			50.50
5	1.23	3.29	5.50	6.70	2240.00	0.0000	.0000	0.00	8.50	2	57.20	48.70	0.00	202.	53.13			
6	1.65	6.21	9.40	10.00				0.00	10.66				0.00	54.70			54.50	

DSTEMP RUN 1 SPAWN CREEK AUGUST 29-30, 1974 DIURNAL **CALIBRATION** HOURLY INTERVALS

COMPONENTS OF HEAT EXCHANGE AT STREAM SURFACE AND BED

TIME INTERVAL NO 2 SIZE DT= 1.0 HRS (DAY 241 HOUR 14.00 TO DAY 241 HOUR 15.00)

ALL UNITS ARE BTUFT-2 PER DT IN HRS

REACH NO	SOLAR RADIATION			SURFACE VEGTN RADTN		ATMOS RADTN		BACK RADTN	EVAP LHVAP	COND	SNOW LHFUS	SURF RENEW	BED COMPONENTS			TOTALS		
	INCIDT	REFLEC	ABSORP	INCIDT	REFLEC	INCIDT	REFLEC						BEDAB	BACK	BED	COND	EXCHGE	BED
1	127.	-10.	117.	0.	0.	115.	-3.	-110.	-67.	88.	0.	0.	0.	0.	0.	0.	139.	0.
2	153.	-12.	140.	0.	0.	115.	-3.	-112.	-74.	83.	0.	0.	0.	0.	0.	0.	149.	0.
3	242.	-19.	222.	0.	0.	115.	-3.	-113.	-77.	81.	0.	0.	0.	0.	0.	0.	226.	0.
4	255.	-20.	234.	0.	0.	110.	-3.	-114.	-91.	64.	0.	0.	0.	0.	0.	0.	200.	0.
5	255.	-20.	234.	0.	0.	110.	-3.	-116.	-104.	58.	0.	0.	0.	0.	0.	0.	179.	0.

DSTEMP RUN 1 SPAWN CREEK AUGUST 29-30, 1974 DIURNAL **CALIBRATION** HOURLY INTERVALS

STREAM TEMPERATURES, ADVECTIVE HEAT FLUXES, AND HYDRAULIC DATA

TIME POINT NO 3 DAY 241 HOUR 15.00

COPP PT NO	RIVER DISTANCE	X-SECTN AREA	TOP WETTED			HYDRAULIC			POINT LOAD	STREAM GP -FLCW NO	INFLOW TEMPS			HEATEX /FT2	STREAM TEMPS		
			WIDTH	PERIM	LENGTH	TRN-VE	LATIN-VE	GRNTR INFLCW			TEMP	TEMP	TEMP		DF	DF	DF
1	0.00	3.17	7.00	8.00	2415.00	0.0000	0.0002	0.00	4.01	1	0.00	48.70	0.00	139.	46.50		
2	0.40	4.58	5.50	7.00	2015.00	0.0000	0.0003	0.00	4.37	1	0.00	48.70	0.00	149.	48.84		
3	0.78	2.39	4.20	5.20	100.00	0.0162	0.0003	0.00	4.72	1	50.50	48.70	0.00	226.	50.56		
4	0.80	3.21	4.20	5.20	2240.00	0.0000	0.0003	0.00	6.34	2	57.60	48.70	0.00	200.	50.58	50.50	
5	1.23	3.29	5.50	6.70	2240.00	0.0000	0.0002	0.00	8.50	2	57.60	48.70	0.00	179.	52.82		
6	1.65	6.21	9.40	10.00				3.00	10.66				0.00	54.89		55.00	

Note: These output tables continue through time point No. 25, day 242, hour 13:00.

MAIN & TRIBUTARY DUMMY DEBUGGING DATA

STREAM TEMPERATURES, ADVECTIVE HEAT SOURCES, AND HYDRAULIC DATA

INITIAL CONDITIONS TIME PT NO 1 DAY 222 HOUR 21:00

COMP PT NO	RIVER DISTANCE	X-SECTN AREA	TOP WIDTH	ADTTD PERIM	HYDRAULIC			POINT LNAD	STREAM FLOW NO	WET TEMP			HEATFX /DT	STREAM TEMPS		
					SUR-RECH LENGTH	LATINF*	INFLW*			CP	LATIN*	PT LD		CF	CF	CF

MAIN																
1	50.00	100.00	25.00	33.00	1000.00	0.0000	0.0000	0.00	500.00	1	0.00	0.00	0.00	0.	77.00	
2	49.81	100.00	25.00	33.00	2000.00	0.0000	0.0000	0.00	500.00	2	0.00	0.00	0.00	0.	77.00	
3	49.43	100.00	25.00	33.00	10.00	10.0000	0.0000	0.00	500.00	2	77.00	0.00	0.00	0.	77.00	
TRIB1																
1	0.76	19.20	9.60	13.60	2500.00	0.0009	0.0000	0.00	96.00	1	70.00	0.00	0.00	0.	77.00	
2	0.28	19.60	9.80	13.80	1500.00	0.0013	0.0000	0.00	98.00	2	70.00	0.00	0.00	0.	77.00	
3	0.00	20.00	10.00	14.00				0.00	100.00				0.00		77.00	
MAIN																
4	49.43	120.00	26.00	35.23	2000.00	0.0000	0.0000	0.00	600.00	2	0.00	0.00	0.00	0.	77.00	
5	49.05	120.00	26.00	35.23				100.00	600.00				100.00		77.00 77.00	

MAIN & TRIBUTARY DUMMY DEBUGGING DATA

COMPONENTS OF HEAT EXCHANGE AT STREAM SURFACE AND BED

TIME INTERVAL NO 1 SIZE DT= 3. HRS (DAY 222 HOUR 21:00 TO DAY 222 HOUR 24:00)

ALL UNITS ARE STUFT-2 PER DT IN HRS

REACH NO	SOLAR RADIATION		SURFACE		COMPONENTS				BED COMPONENTS				TOTALS		
	INCIDT	REFLEC	VEGTR	INCIDT	ATMOS	BACK	EVAP	COND	SNDW	SURF	BEDAB	EACK	BED	SURF	BED

TRIB1															
1	0.	0.	0.	0.	312.	-9.	-409.	-307.	-85.	0.	0.	0.	0.	0.	-502.
2	0.	0.	0.	0.	300.	-9.	-409.	-340.	-112.	0.	0.	0.	0.	0.	-570.
MAIN															
1	0.	0.	0.	0.	312.	-9.	-410.	-311.	-97.	0.	0.	0.	0.	0.	-505.
2	0.	0.	0.	0.	300.	-9.	-410.	-345.	-114.	0.	0.	0.	0.	0.	-577.
3	0.	0.	0.	0.	300.	-9.	-409.	-344.	-114.	0.	0.	0.	0.	0.	-576.
4	0.	0.	0.	0.	300.	-9.	-409.	-344.	-113.	0.	0.	0.	0.	0.	-575.

MAIN & TRIBUTARY DUMMY DEBUGGING DATA

STREAM TEMPERATURES, ADVECTIVE HEAT SOURCES, AND HYDRAULIC DATA

TIME PT NO 2 DAY 222 HOUR 24:00

COMP PT NO	RIVER DISTANCE	X-SECTN AREA	TOP WIDTH	ADTTD PERIM	HYDRAULIC			POINT LNAD	STREAM FLOW NO	WET TEMP			HEATFX /DT	STREAM TEMPS		
					SUR-RECH LENGTH	LATINF*	INFLW*			CP	LATIN*	PT LD		CF	CF	CF

MAIN																
1	50.00	100.00	25.00	33.00	1000.00	0.0000	0.0000	0.00	500.00	1	0.00	0.00	0.00	-505.	75.00	
2	49.81	100.00	25.00	33.00	2000.00	0.0000	0.0000	0.00	500.00	2	0.00	0.00	0.00	-577.	75.00	
3	49.43	100.00	25.00	33.00	10.00	10.0000	0.0000	0.00	500.00	2	74.32	0.00	0.00	-576.	74.98	
TRIB1																
1	0.76	19.20	9.60	13.60	2500.00	0.0009	0.0000	0.00	96.00	1	70.00	0.00	0.00	-502.	75.00	
2	0.28	19.60	9.80	13.80	1500.00	0.0013	0.0000	0.00	98.00	2	70.00	0.00	0.00	-570.	74.63	
3	0.00	20.00	10.00	14.00				0.00	100.00				0.00		74.32	
MAIN																
4	49.43	120.00	26.00	35.23	2000.00	0.0000	0.0000	0.00	600.00	2	0.00	0.00	0.00	-575.	74.87	
5	49.05	120.00	26.00	35.23				100.00	600.00				100.00		78.47 74.88	

MAIN & TRIBUTARY DUMMY DEBUGGING DATA

COMPONENTS OF HEAT EXCHANGE AT STREAM SURFACE AND BED

TIME INTERVAL NO 2 SIZE DT= 24. HRS (DAY 222 HOUR 24.00 TO DAY 223 HOUR 24.00)

ALL UNITS ARE BTUFT-2 PER DT IN HRS

REACH NO	SOLAR RADIATION			SURFACE		COMPONENTS			EVAP	COND	SAGW LHFUS	BED COMPONENTS				TOTALS	
	INCIDT	REFLEC	ABSORP	VEGTA INCIDT	RADTN REFLEC	ATMOS INCIDT	RADTN REFLEC	BACK RADTN				COND	SURF BEDAR	EACH BEDRD	COND	BED EXCHGE	SURF EXCHGE
TRIB1																	
1	1412.	-90.	1322.	0.	0.	3032.	-91.	-3309.	-499.	63.	0.	0.	0.	0.	0.	518.	0.
2	1384.	-92.	1293.	0.	0.	2884.	-87.	-3305.	-746.	-43.	0.	0.	0.	0.	0.	-3.	0.
MAIN																	
1	1247.	-88.	1157.	0.	0.	3032.	-91.	-3310.	-504.	61.	0.	0.	0.	0.	0.	347.	0.
2	1140.	-74.	1066.	0.	0.	2884.	-87.	-3310.	-763.	-42.	0.	0.	0.	0.	0.	-254.	0.
3	1140.	-74.	1066.	0.	0.	2884.	-87.	-3309.	-757.	-47.	0.	0.	0.	0.	0.	-250.	0.
4	1140.	-74.	1066.	0.	0.	2884.	-87.	-3308.	-755.	-46.	0.	0.	0.	0.	0.	-246.	0.

MAIN & TRIBUTARY DUMMY DEBUGGING DATA

STREAM TEMPERATURES, ADVECTIVE HEAT SOURCES, AND HYDRAULIC DATA

TIME PT NO 3 DAY 223 HOUR 24.00

COPP PT NO	RIVER DISTANCE	X-SECTN AREA	TOP WIDTH	WETTED PERIM	HYDRAULIC			POINT LOAD	STREAM GP	MET FLOW	INFLOW TEMPS			HEATEX /DT	STREAM TEMPS		
					SUB-RCH LENGTH	LATINF TRIBINF	GRDWTR INFLOW				LATIN	GWINF	PT LD		DF	DF	DF
MAIN																	
1	50.00	100.00	25.00	33.00	1000.00	0.0000	0.0000	0.00	500.00	1	0.00	0.00	0.00	347.	79.00		
2	49.81	100.00	25.00	33.00	2000.00	0.0000	0.0000	0.00	500.00	2	0.00	0.00	0.00	-254.	78.99		
3	49.43	100.00	25.00	33.00	10.00	10.0000	0.0000	0.00	500.00	2	79.01	0.00	0.00	-250.	78.96		
TRIB1																	
1	0.76	19.20	9.60	13.60	2500.00	0.0009	0.0000	0.00	96.00	1	70.00	0.00	0.00	518.	79.00		
2	0.28	19.60	9.80	13.80	1500.00	0.0013	0.0000	0.00	98.00	2	70.00	0.00	0.00	-3.	79.04		
3	0.00	20.00	10.00	14.00				0.00	100.00				0.00		79.01		
MAIN																	
4	49.43	120.00	26.00	35.23	2000.00	0.0000	0.0000	0.00	600.00	2	0.00	0.00	0.00	-246.	78.97		
5	49.05	120.00	26.00	35.23				100.00	600.00				100.00		81.93	78.92	